

12-14-2015

## Supported Group IB-PD Bimetallic Catalysts Prepared by Electroless Deposition and Galvanic Displacement for Selective Hydrogenation of Acetylene

Yunya Zhang  
*University of South Carolina - Columbia*

Follow this and additional works at: <https://scholarcommons.sc.edu/etd>

 Part of the [Chemical Engineering Commons](#)

---

### Recommended Citation

Zhang, Y.(2015). *Supported Group IB-PD Bimetallic Catalysts Prepared by Electroless Deposition and Galvanic Displacement for Selective Hydrogenation of Acetylene*. (Doctoral dissertation). Retrieved from <https://scholarcommons.sc.edu/etd/3238>

This Open Access Dissertation is brought to you by Scholar Commons. It has been accepted for inclusion in Theses and Dissertations by an authorized administrator of Scholar Commons. For more information, please contact [digres@mailbox.sc.edu](mailto:digres@mailbox.sc.edu).

SUPPORTED GROUP IB-Pd BIMETALLIC CATALYSTS PREPARED BY  
ELECTROLESS DEPOSITION AND GALVANIC DISPLACEMENT FOR SELECTIVE  
HYDROGENATION OF ACETYLENE

by

Yunya Zhang

Bachelor of Science  
Dalian University of Technology, 2010

---

Submitted in Partial Fulfillment of the Requirements

For the Degree of Doctor of Philosophy in

Chemical Engineering

College of Engineering and Computing

University of South Carolina

2015

Accepted by:

John R. Monnier, Major Professor

Christopher T. Williams, Major Professor

Donna A. Chen, Committee Member

John R. Regalbuto, Committee Member

Miao Yu, Committee Member

John W. Weidner, Committee Member

Lacy Ford, Senior Vice Provost and Dean of Graduate Studies

© Copyright by Yunya Zhang, 2015  
All Rights Reserved.

## DEDICATION

I dedicate this work to my husband Weijian Diao, for his love and company through my graduate studies. I would not reach this far without his daily help, support and encouragement. His optimism and sense of humor inspires me every day.

I dedicate this work to my parents Zongliang Zhang and Shufang Wang as a small token of my gratitude for their unconditional love and support.

## ACKNOWLEDGEMENTS

I would like to express my greatest gratitude to my advisors, Dr. John R. Monnier and Dr. Christopher T. Williams. Thank you for taking me in the group and teaching me catalysis. I really appreciate your guidance, encouragement and patience giving me strength to keep forward on the path of research. Thank you for funding me to attend a lot of important conferences.

I would like to acknowledge my committee members, Dr. Donna A. Chen, Dr. John R. Regalbuto and Dr. Miao Yu, for taking precious time to guide me and teach me.

I would also like to thank the chemical engineering department staffs, Marcia Rowen, Loretta Hardcastle, Vernon Dorrell and Brian Loggans, for their assistance in a variety of ways. I would like to give the special thanks to Carol Stork for her generous help on experimental work and to Dr. Shuguo Ma for his assistance on XPS.

I would like to thank all my group members and colleagues. Especially thanks to Dr. Jayakiran Rebelli, Dr. Shuai Tan, Dr. Xiaojing Sun, Dr. Hyeran Cho, Dr. Abraham Rodriguez, Dr. Akkarat Wongkaew and John Tengco, who taught me and helped me a lot on experiments.

Thanks to my dearest friends, Long Cai, Xiaojing Sun, Fan Wu, Shuai Tan, Qiang Gao, Jingyi Huo, Tingting Yang, Hong Liu, Yiling Dai, Zhiyong Wang, Tianyuan Xie, Yating Mao, Kangmin Xie, Shuo Cao, Qiuli Liu, Zhuonan Song, and Marjorie Nicholson, who made this tough journey interesting and joyous.

## ABSTRACT

Ethylene is the building block for many chemical intermediates in the petrochemical industry. The current worldwide ethylene production is over 150 million tons per year and demand increases by 3-5% annually. However, ethylene produced from steam cracking of light naphtha contains up to 2% acetylene which acts as a poison for the downstream ethylene polymerization catalysts. Selective hydrogenation of acetylene in the ethylene stream using supported Pd catalysts is the industrially preferred method of lowering acetylene to acceptable ppm levels (< 5 ppm). Due to inferior selectivity at high acetylene conversion and the formation of “green oil”, or ethylene/acetylene oligomers, during reaction, small amounts of Group IB metals have been added to improve the performance of current generation catalysts. However, the bimetallic effects of the above additives have not been experimentally confirmed, possibly because the conventional methods of catalyst preparation result in both monometallic and bimetallic particles with varying compositions. This in turn makes it difficult to determine the position of the two metallic components, and bimetallic interactions typically occur only when the two metals form proximal contact instead of separate particles.

In this study, a series of Ag- and Au-Pd/SiO<sub>2</sub> bimetallic catalysts were prepared by electroless deposition (ED) with incremental and controlled coverages of Ag and Au on Pd. The selectivity of acetylene to ethylene and turnover frequencies of acetylene conversion were enhanced at high coverages of Ag and Au on Pd surfaces due to the

transition of acetylene adsorption modes, which was further confirmed by the kinetics of acetylene hydrogenation. The similar performance trends for Ag- and Au-Pd/SiO<sub>2</sub> suggest that the bimetallic effect for these catalysts was likely geometric and not electronic in nature. For comparison, a series of reverse Pd-Ag/SiO<sub>2</sub> bimetallic catalysts where variable coverages of Pd were deposited onto Ag surfaces was prepared using galvanic displacement (GD) of Ag<sup>0</sup> by Pd<sup>2+</sup> to further explore the nature of bimetallic effects for selective acetylene hydrogenation. Unlike for the earlier case for Ag on Pd surfaces using ED, for samples prepared by GD there was considerable diffusion of Pd into the Ag lattice to give greater electronic interactions between these two metals, which limited selectivity of acetylene hydrogenation to form ethylene.

## TABLE OF CONTENTS

DEDICATION .....	iii
ACKNOWLEDGEMENTS.....	iv
ABSTRACT .....	v
LIST OF TABLES .....	ix
LIST OF FIGURES .....	x
LIST OF SYMBOLS .....	xii
LIST OF ABBREVIATIONS.....	xiii
CHAPTER 1 INTRODUCTION AND LITERATURE REVIEW.....	1
1.1 OVERVIEW AND BACKGROUND .....	2
1.2 SELECTIVE HYDROGENATION OF ACETYLENE.....	5
1.3 PREPARATION METHODS OF BIMETALLIC CATALYSTS .....	10
1.4 ELECTROLESS DEPOSITION.....	19
1.5 GALVANIC DISPLACEMENT.....	29
CHAPTER 2 EXPERIMENTAL PROCEDURES .....	32
2.1 LIST OF CHEMICAL MATERIALS.....	33
2.2 CATALYST PREPARATION.....	33
2.3 CATALYST CHARACTERIZATION.....	40
2.4 CATALYST EVALUATION .....	44
CHAPTER 3 SELECTIVE HYDROGENATION OF ACETYLENE IN EXCESS ETHYLENE USING AG- AND AU-PD/SiO <sub>2</sub> BIMETALLIC CATALYSTS PREPARED BY ELECTROLESS DEPOSITION.....	48

3.1 ABSTRACT .....	49
3.2 INTRODUCTION.....	49
3.3 RESULTS AND DISCUSSION .....	52
3.4 CONCLUSIONS .....	66
CHAPTER 4 Pd-Ag/SiO <sub>2</sub> BIMETALLIC CATALYSTS PREPARED BY GALVANIC DISPLACEMENT FOR SELECTIVE HYDROGENATION OF ACETYLENE IN EXCESS ETHYLENE.	68
4.1 ABSTRACT .....	69
4.2 INTRODUCTION.....	69
4.3 RESULTS AND DISCUSSION .....	72
4.3 CONCLUSIONS .....	90
CHAPTER 5 CONCLUSIONS .....	91
REFERENCES .....	94
APPENDIX A – LIST OF PUBLICATIONS.....	102
APPENDIX B – PERMISSION TO REPRINT.....	103

## LIST OF TABLES

Table 1.1 Common metal ion sources for electroless deposition. ....	22
Table 1.2 Complexing agents used in the electroless deposition for common metals. ....	25
Table 1.3 Stabilizing agents used in the electroless deposition for common metals. ....	26
Table 2.1 Standard reduction potentials for different Pd salts. ....	38
Table 3.1 Ag-Pd/SiO <sub>2</sub> and Au-Pd/SiO <sub>2</sub> bimetallic catalysts that were evaluated for acetylene hydrogenation. Base catalyst is 1.85 wt% Pd/SiO <sub>2</sub> . Theoretical coverage in monolayers (ML) represents monodisperse coverage of Ag or Au on Pd surface, assuming 1:1 adsorption stoichiometry. ....	53
Table 4.1 Composition of Pd-Ag catalysts after galvanic displacement experiments. Actual catalyst compositions based on analyzed Ag and Pd loadings, not predictive stoichiometries. ....	77

## LIST OF FIGURES

Figure 1.1 Network of the main reactions that may occur during acetylene hydrogenation in excess ethylene. ....	6
Figure 1.2 Scheme of acetylene and ethylene adsorbed states identified on palladium surface during acetylene and ethylene chemisorption, decomposition, and hydrogenation. ....	7
Figure 1.3 Electrostatic adsorption mechanism. ....	15
Figure 1.4 Electroless deposition mechanism.....	21
Figure 1.5 Catalytic activities of metals for anodic oxidation of different reducing agents. ....	24
Figure 1.6 Schematic diagram of mixed potential concept.....	27
Figure 3.1 Adsorption modes of acetylene on Pd surface. ....	51
Figure 3.2 Actual coverage of Ag or Au on Pd/SiO <sub>2</sub> as a function of moles of Ag or Au deposited. Black line is the theoretical coverage of Ag or Au metal on Pd surface at a 1:1 deposition stoichiometry. Dashed lines show coverage based on chemisorption of Pd sites. ....	54
Figure 3.3 (A) Conversion of acetylene and selectivity of acetylene to ethylene and (B) selectivity of acetylene to ethane and C <sub>4</sub> s as a function of Ag coverage on Pd/SiO <sub>2</sub> . Reaction conditions: 65 °C and feed composition of 1% C <sub>2</sub> H <sub>2</sub> , 5% H <sub>2</sub> , 20% C <sub>2</sub> H <sub>4</sub> , and balance He at GHSV = 6.0 × 10 <sup>5</sup> . Representative error bars for all data are shown for samples having $\theta_{Ag} = 0.92$ . ....	55
Figure 3.4 (A) Conversion of acetylene and selectivity of acetylene to ethylene and (B) selectivity of acetylene to ethane and C <sub>4</sub> s as a function of Au coverage on Pd/SiO <sub>2</sub> . ....	56
Figure 3.5 Effect of (A) Ag and (B) Au coverage on Pd for TOF of acetylene hydrogenation. ....	61
Figure 3.6 The C <sub>2</sub> H <sub>2</sub> pressure dependencies for Pd/SiO <sub>2</sub> and Ag-Pd/SiO <sub>2</sub> ( $\theta_{Ag} = 0.92$ ) at 50 °C and H <sub>2</sub> pressure of 0.05 atm.....	63

Figure 3.7 The H <sub>2</sub> pressure dependencies for Pd/SiO <sub>2</sub> and Ag-Pd/SiO <sub>2</sub> ( $\theta_{\text{Ag}} = 0.92$ ) at 50 °C and C <sub>2</sub> H <sub>2</sub> pressure of 0.01 atm.....	64
Figure 3.8 Arrhenius plots for the temperature dependencies of C <sub>2</sub> H <sub>2</sub> conversion for (A) Pd/SiO <sub>2</sub> and (B) Ag-Pd/SiO <sub>2</sub> ( $\theta_{\text{Ag}} = 0.92$ ) at C <sub>2</sub> H <sub>2</sub> pressure of 0.01 atm and H <sub>2</sub> pressure of 0.05 atm. ....	65
Figure 4.1 Uptake curves for H <sub>2</sub> titration of O-precovered Ag sites at 170 °C for 2 wt% Ag/SiO <sub>2</sub> .....	73
Figure 4.2 XRD pattern of 2 wt% Ag/SiO <sub>2</sub> . ....	73
Figure 4.3 Ag dissolution from 2 wt% Ag/SiO <sub>2</sub> in pH 2 HNO <sub>3</sub> solution at room temperature. ....	75
Figure 4.4 Time-dependent galvanic displacement profiles of (A) deposited Pd <sup>2+</sup> from bath solution and (B) galvanically displaced Ag <sup>+</sup> from 2 wt% Ag/SiO <sub>2</sub> at room temperature with different initial Pd <sup>2+</sup> concentrations.....	76
Figure 4.5 First order plots for Pd <sup>2+</sup> disappearance vs. time for (A) 0.09, (B) 0.28, (C) 0.32 wt% Pd on Ag/SiO <sub>2</sub> . A straight line correlation confirms first order dependency. ....	79
Figure 4.6 Time-dependent galvanic displacement profiles of (A) deposited Pd <sup>2+</sup> from bath solution and (B) galvanically displaced Ag <sup>+</sup> from 2 wt% Ag/SiO <sub>2</sub> at 25, 50 and 75 °C with same initial Pd <sup>2+</sup> concentration.....	80
Figure 4.7 FTIR spectra for CO adsorption on various Pd-Ag/SiO <sub>2</sub> bimetallic catalysts. ....	82
Figure 4.8 XPS spectra of (A) Pd 3d on 2 wt% Pd/SiO <sub>2</sub> and Pd-Ag/SiO <sub>2</sub> and (B) Ag 3d on 2 wt% Ag/SiO <sub>2</sub> and Pd-Ag/SiO <sub>2</sub> . All samples were reduced <i>in situ</i> at 200 °C in 100% H <sub>2</sub> for 2 h. ....	85
Figure 4.9 Ag 3d spectra of 2 wt% Ag/SiO <sub>2</sub> for (1) <i>ex situ</i> pretreatment in air at 300 °C for 2 h and in 10% H <sub>2</sub> /He at 300 °C for 2 h, (2) <i>in situ</i> pretreatment in 100% H <sub>2</sub> at 200 °C for 2 h, and (3) <i>in situ</i> pretreatment in 100% O <sub>2</sub> at 200 °C for 2 h.....	86
Figure 4.10 (A) Conversion of acetylene and selectivity of acetylene to ethylene and (B) selectivity of acetylene to ethane and C <sub>4</sub> s as a function of Pd weight loadings on Ag/SiO <sub>2</sub> . Reaction conditions: 65 °C and feed composition of 1% C <sub>2</sub> H <sub>2</sub> , 5% H <sub>2</sub> , 20% C <sub>2</sub> H <sub>4</sub> , and balance He at GHSV = 6.0 × 10 <sup>5</sup> h <sup>-1</sup> . Error bars represent maximum and minimum values for each data point; data point is average value.....	88

## LIST OF SYMBOLS

$\Delta E^\circ$	Total cell potential
$E^\circ_{\text{ox}}$	Oxidation potential
$E^\circ_{\text{red}}$	Reduction potential
$i_a$	Partial anodic current
$i_c$	Partial cathodic current
$\theta$	Coverage of secondary metal on primary metal
$K$	Adsorption rate
$P_{\text{C}_2\text{H}_2}$	Partial pressure of $\text{C}_2\text{H}_2$
$P_{\text{H}_2}$	Partial pressure of $\text{H}_2$
$K$	Reaction rate constant
wt%	Percentage of metal weight

## LIST OF ABBREVIATIONS

AA.....	Atomic absorption
BE .....	Binding energy
BET .....	Brunauer, Emmett and Teller
DMAB.....	Dimethyl amine borane
ED .....	Electroless deposition
FTIR.....	Fourier transform infrared
GD.....	Galvanic displacement
GHSV .....	Gas hourly space velocity
ID .....	Inside diameter
MCT-B.....	Mercury-cadmium-telluride B
ML.....	Monolayer
OD.....	Outside diameter
PZC .....	Point of zero charge
Redox .....	Reduction-oxidation
RT .....	Room temperature
SEA.....	Strong electrostatic adsorption
SFE.....	Surface free energy
TCD.....	Thermal conductivity detector
TOF.....	Turnover frequency
UHV .....	Ultra high vacuum

XPS ..... X-ray photoelectron spectroscopy  
XRD ..... X-ray diffraction

## CHAPTER 1:

### INTRODUCTION AND LITERATURE REVIEW

## 1.1 Overview and background

Ethylene, the simplest olefin, is used as a starting point for many syntheses in the petrochemical industry. Ethylene is highly reactive, due to its double bond, allowing it to be converted to a large assortment of products by addition [1], oxidation [2], and polymerization [3]. It is the building block for the production of plastics, solvents, cosmetics, fibers, films, adhesives, paints and packaging [4]. Today, the yearly worldwide ethylene capacity is over 150 million tonnes with a growth rate of 3.5% per year [5]. Ethylene is produced commercially through steam or catalytic cracking of a wide range of light naphtha feedstocks. In the cracking process, impurities such as 1-3% acetylene are also introduced in addition to the desirable ethylene [6]. Acetylene acts as a severe poison for downstream ethylene polymerization catalysts in even ppm concentrations and can actually degrade the quality of polyethylene. Industrial feedstocks for the production of ethylene polymers must contain no more than 5 ppm of acetylene [7]. However, conventional distillation cannot reduce acetylene concentration to the necessary level. Therefore, selective hydrogenation of acetylene in these cracking feedstocks is a critical industrial process for the purification of ethylene.

Although all Group VIII catalysts can be used to hydrogenate a double bond, palladium is superior to all of the others for promoting this reaction at low temperatures and pressures [8]. Industrially, low weight loading-supported palladium catalysts are used in selective hydrogenation of acetylene in high concentration ethylene streams to improve the quality of raw ethylene produced in steam crackers [9]. Acetylene is converted to ethylene, but it is important to prevent over hydrogenation to ethane, since ethane is itself the primary feedstock used for the formation of ethylene by cracking. In addition to

unwanted ethane, the accumulation of oligomers (known as “green oil”) produced from strongly adsorbed ethylene and acetylene moieties, and C<sub>4</sub>s and C<sub>6</sub>s on the surfaces of catalysts shorten the lifetime of these catalysts as the catalyst becomes fouled [6,10]. Therefore, selectivity of acetylene to ethylene rather than ethane, C<sub>4</sub>s and C<sub>6</sub>s, is a key objective. Since the 1940s, addition of various metals to Group VIII-based systems has attracted considerable attention from scientists to improve the activity and selectivity of these catalysts [11-13]. Multi-metallic catalysts were initially industrially applied in the 1960s and 1970s for hydrocarbon reforming. Nowadays, it is well known that bimetallic catalysts can exhibit catalytic properties different from their corresponding monometallic components. Such bimetallic catalysts can provide enhanced stability, activity and selectivity because of interactions between the two metals [14,15]. Therefore, bimetallic and, in some cases, multimetallic catalysts have replaced many monometallic catalysts in industrial catalytic processes. Various additives, such as Ag, Cu, Au, Ga, Pb, Zn and K have been reported to improve the performance of Pd catalysts for high selectivity of acetylene hydrogenation to ethylene [7,16-21]. Currently, Pd catalysts promoted by Ag are used industrially for the selective hydrogenation of acetylene.

The structural and mechanistic effects of the above additives are not yet well understood, possibly due to the conventional methods of catalyst preparation. Co-impregnation and successive impregnation are the two commonly used industrial procedures [22-24]. Both metal salts can be simultaneously deposited on the support through co-impregnation or successively deposited following stabilization of the first metal component. However, these two methods typically produce both monometallic and bimetallic catalyst particles with varying compositions. This complex mixture of

monometallic and bimetallic particles results in poor control of the final catalyst performance, and makes it difficult to characterize these catalysts to determine the position of the two metallic components and impossible to correlate catalyst performance with bimetallic catalyst composition. Because bimetallic interaction occurs only when the two metallic components form bimetallic compositions instead of separate particles, it is desirable to develop a preparation method in which the second metal only deposits on the surface of the first metal particles.

Electroless deposition (ED) and galvanic displacement (GD) are alternative, industrially feasible methods to produce true bimetallic catalysts. Electroless deposition deposits a secondary metal onto a pre-existing monometallic catalyst surface from a solution containing a reducible metal salt and a reducing agent [25-27]. Because the reducing agent is catalytically activated by the pre-existing metallic surface to produce an active hydrogen species, the secondary metal is only deposited on the primary metal. Galvanic displacement occurs when the base monometallic catalyst is displaced by a metallic ion in solution that has a higher reduction potential than the base metal [28-30]. The base material dissolves into solution while the metallic ions in the solution are reduced on the surface of the base material. Unlike ED, GD does not require chemical reducing agents since the base metal itself already serves as the reducing agent. However, GD is usually limited by the accessibility of the base metal, resulting in passivation of the reaction when a critical fraction of the base metal is covered. In contrast, ED can deposit multilayers of secondary metal over the base material. Since both methods are kinetically controlled, the final composition of a particular bimetallic catalyst can be controlled to

give rather precise combinations of the two metallic components. Consequently, both ED and GD can provide many potential advantages over conventional preparation methods.

ED has been well studied and used in our laboratory for the preparation of different bimetallic catalysts systems, and these catalysts showed improved catalytic performance for various applications compared to the monometallic catalysts or bimetallic catalysts prepared by conventional methods, such as Cu-Pd and Ag-Pt catalysts for the selective hydrogenation of 3,4-epoxy-1-butene [31,32], Pt-Rh, Pt-Pd, Co-Pt, and Pt-Ru electrocatalysts for fuel cell applications [33-38], Au-Pd catalysts for propylene hydrogenation and liquid phase oxidation of glycerol [39,40], and Ag-Ir catalysts for CO oxidation [41]. The primary goals of the current study is to use ED and GD to prepare truly bimetallic Group IB-Pd catalysts, and to investigate the nature of bimetallic effects of these catalysts for the selective hydrogenation of acetylene in excess ethylene [42,43]. The current literatures related to the preparation of bimetallic catalysts and selective hydrogenation of acetylene will be reviewed before the experimental procedures and the discussion of current results.

## 1.2 Selective Hydrogenation of Acetylene

### 1.2.1 Background

Studies of the selective hydrogenation of acetylene to ethylene in the presence of high excess of ethylene have continued during the past few decades for not only industrial interest but also fundamental importance where acetylene hydrogenation serves as a model reaction for selective hydrogenation of alkynes and conjugated dienes in both practical and theoretical studies. Since this catalytic process may proceed through several

parallel and sequential steps on different types of active metal sites, it remains to be a widely studied topic in catalysis.

### 1.2.2 Reaction Mechanism

The network of the main reactions that take place during acetylene hydrogenation in excess ethylene is shown in Figure 1.1 [44-47]. The only desired reaction is reaction ①, the half hydrogenation of acetylene to ethylene. At steady state conditions, the rates of reactions ③-⑥ are typically small compared to the rates of reaction ① and ②. However, reactions ④-⑥ are also important, since reaction ④ produces C<sub>4</sub> hydrocarbons which are the precursors of C<sub>6+</sub> hydrocarbon oligomers and carbonaceous residues. The liquid part of the hydrocarbons denoted as “green oil” accumulates on the catalyst surface and in the pores of catalysts, resulting in catalyst deactivation.

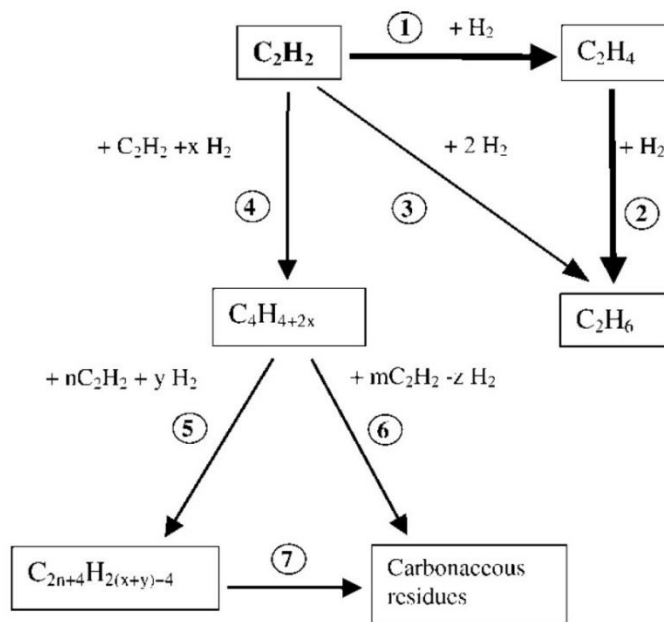


Figure 1.1 Network of the main reactions that may occur during acetylene hydrogenation in excess ethylene [44].

During acetylene and ethylene hydrogenation, adsorbed  $C_2$  species and carbonaceous deposits are present in different forms on the surface of Pd, depending on temperature, hydrogen surface coverage and the morphology of the Pd surface [44]. Figure 1.2 shows some of the identified adsorbed states of acetylene and ethylene on Pd [10,47-49]. The adsorption modes such as ethylidyne and ethylidene favor the formation of ethane, while the other adsorption can give rise to ethylene formation. When the adsorption temperature increases, hydrogen atoms will be lost from adsorbed  $C_2$  species, leading to formation of multiply-bonded species on the metal surface. As temperatures increase further, the strongly bonded species can condense to form  $C_nH_m$  oligomers and/or undergo C-C bond breaking to form amorphous carbon or a graphitic layer [E1,E5]. If the coverage of hydrogen on the surface is increased, the carbonaceous deposits can be partially hydrogenated to form additional and strongly-bonded oligomeric

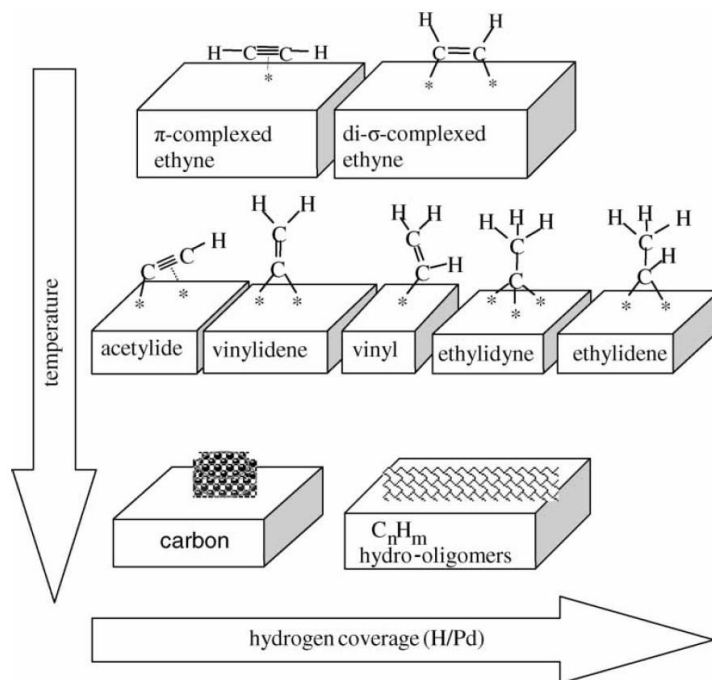


Figure 1.2 Scheme of acetylene and ethylene adsorption states identified on Pd surfaces during acetylene and ethylene chemisorption, decomposition, and hydrogenation [44].

species. Interestingly these carbonaceous deposits can play an important role for hydrogenation of acetylene in the absence of ethylene [48,50,51]. Ponec et al. proposed [50,51] that the formation of carbonaceous deposits as well as alloying of Pd with Cu and Au can decrease the size of large Pd ensembles that account for formation of non-selective ethane, but not adversely affect the small ensembles of Pd required for hydrogenation to ethylene. Therefore, selectivity of acetylene to ethylene is increased.

Borodziński et al. [52-54] developed a kinetic model that was in agreement with the above idea that carbonaceous deposits can increase selectivity by covering parts of a Pd surface to create small arrays of contiguous Pd sites for acetylene hydrogenation to ethylene. They proposed that the formation of a hydrocarbonaceous layer produces two types of catalytic sites: **A** and **E** sites which account for the conversion of **A**cetylene and **E**thylene, respectively. The active sites are the small (**A** site) and large (**E** site) exposed Pd ensembles on the surface of Pd among the carbonaceous species. During acetylene hydrogenation in the presence of ethylene, **A** sites are inactive for ethylene hydrogenation because while these sites are large enough to adsorb  $\pi$ -bonded ethyne, acetylide, vinylidene, vinyl and hydrogen, they are too small to adsorb ethylidyne and ethylidene based on small steric differences between ethylene and acetylene. On the other hand, **E** sites adsorb all reactants, which leads to both acetylene hydrogenation and ethylene hydrogenation. Thus, selectivity of the catalyst depends on the proportions and specific activities of **A** and **E** sites.

The above statement can be considered as kind of geometric (ensemble) effect caused by the formation of carbonaceous deposits but not by a bimetallic component. To achieve the same effect as the carbonaceous deposits, monometallic Pd catalysts can be

modified to change the Pd ensemble size to restrict ethylene adsorption. The use of a second metallic component, such as Ag or Au, is preferable to deposition of carbonaceous deposits since the latter choice is essentially uncontrollable in both extent and position of placement of the carbonaceous component. There are also many other proposed mechanisms [47,55] which are still controversial, since the reaction processes and various transformations undergone by the catalyst are complicated.

### 1.2.3 Modifiers

There are usually two kinds of modifiers used in acetylene hydrogenation in the presence of ethylene. One is a process modifier, such as gas co-feeds of carbon monoxide, amines, or sulfur compounds [56-58]. For instance, ppm amounts of CO can be added to the feed stream to act as a selective, reversibly-adsorbed inhibitor since it competes with ethylene but not acetylene for adsorption sites. Addition of CO is complex since it is a transient poison and the addition of too much can reduce catalyst activity. Thus, the effect of CO on catalyst performance depends on the reaction conditions and catalyst type, as well as its content in the inlet reaction mixture. More detail discussions on the effect of CO addition can be referred to other literature and reviews [44,57,59]. The other type of modifier is called a promoter, which is a solid phase component of a catalyst system that improves the performance of the active substance without having any significant activity of its own [44]. This kind of modifier is used in our study, such as Ag, Cu, Au, and even TiO<sub>2</sub> to control Pd ensemble sizes, particle shapes or morphologies, alter the electronic properties of Pd, and affect the formation of  $\beta$ -PdH [44,45,60]. Classical examples of the promoters for acetylene selective hydrogenation are the Group

IB metals (Ag, Au, and Cu). Almost all industrial Pd catalysts for this reaction are modified with Ag or Au, although there is still active discussion about their function. They may act as site blocking promoters by changing Pd ensembles size to create smaller groups of Pd atoms which are responsible for acetylene hydrogenation to ethylene [21,42]. This kind of function is similar to the effect caused by carbonaceous deposits discussed in the previous section. These promoters may also act as electronic promoters by interacting with adjacent Pd surface sites to change the electronic properties of Pd which can alter bond strengths between adsorbed reactants and Pd atoms [16,43]. Some have argued the IB promoters can also hinder the formation of the presumed, non-selective  $\beta$ -PdH phase by decreasing hydrogen solubility in the Pd lattice [60]. However, whether these promoters have one or more simultaneous function is not well studied, since the structure of the working catalyst is generally unknown or not well-enough defined due to uncontrolled, conventional preparation methods. Thus, it is critical to develop preparation methods that control the extent of and sites of promoter deposition (on Pd) to better determine the reaction mechanism for the selective acetylene hydrogenation reaction.

### 1.3 Preparation Methods of Bimetallic Catalysts

Bimetallic catalysts can be prepared by various methods. Each method includes a series of certain steps, and every step contains several parameters which can control the catalytic properties of the final heterogeneous catalysts. A slight change of any parameter can dramatically alter the catalyst properties and its performance for a given reaction. The choice of preparation method is based on the physical and chemical characteristics required for the final composition. Although many different preparation methods have

been developed over the decades, only few are used at the industrial scale because of scale-up issues, cost of raw material, and performance of the catalysts. The most widely used methods involve ion exchange [61], impregnation [23], homogeneous deposition precipitation [22], strong electrostatic adsorption [62], and redox reactions [63].

### 1.3.1 Ion Exchange

This method involves the displacement of an ion from an electrostatic interaction with the surface of a support by another ion species of the same positive or negative charge [22,61,64,65]. In practice, the support containing ions A is immersed in an excess volume (compared to the pore volume) of solution containing ions B which are to be introduced. Ions B gradually penetrate into the pores of the support and exchange with ions A which dissolve into the solution. This exchange will continue until equilibrium is obtained to give a distribution of the two ions between the solid and the solution. The exchange rate of ions depends on the properties of the support and the concentration of ions B in solution. This method provides especially good control of deposition of small amounts of metal on supports with large surface areas. Almost all solid mineral supports are oxides and exhibit ion exchange ability when the surface bears electrostatic charge. Zeolites, composed of trivalent cations  $\text{Al}^{3+}$  and quadrivalent cations  $\text{Si}^{4+}$  located in tetrahedral building blocks, are the most commonly used support in ion exchange methods. This framework exhibits a negative charge distributed on bridging oxygen atoms, and this charge is typically neutralized by cations including  $\text{H}^+$  and alkali ions. These cations are often accessible to ion exchange through the zeolite pore system. Cationic species such as  $[\text{Pd}(\text{EN})]^{2+}$ ,  $[\text{Pt}(\text{NH}_3)_4]^{2+}$  and  $[\text{Ru}(\text{NH}_3)_6]^{3+}$  etc. can be added to

exchange with the pre-existing cations on a zeolite until cations in the aqueous solution and cations on the zeolite reach equilibrium. This material can then be calcined to remove the ligands and reduced to the metallic state. To prepare bimetallic catalysts, a solution containing the second metal salt is added to further exchange with the excess cations. Thus, this method cannot produce catalysts with high metal weight loadings and does not guarantee proximal contact of the two metals.

### 1.3.2 Impregnation

By far the most widely used preparation route is impregnation, which is often referred to as impregnation and drying [22-24,64-66]. From an industrial point of view, impregnation is extremely important in the preparation of supported catalysts. The most attractive advantage of this method is its simplicity in practical operation on both the laboratory and industry levels. Many types of catalysts are produced by impregnation of porous supports with a solution containing a precursor of the active components, followed by the drying and calcination and /or reduction of the impregnated support. There are two different procedures of contacting depending on the volume of solution, which can be employed with impregnation of supports with active components. The first procedure, known as incipient wetness or dry impregnation, restricts the volume of the impregnation solution to be equivalent to or slightly less than the pore volume of the support. The procedure occurs rapidly, and the active components are transported by convection into the pores of the support. The operation must be controlled rather precisely, and the solution needs to be added gradually. The other procedure is wet impregnation, where the support is immersed in a solution containing the catalyst

precursor with a volume larger than the pore volume of the support. After a certain time, the excess solution can be removed either by decanting or evaporating the excess liquid. In this way, the active components in the excess solution diffuse into the pores of the support, taking several hours to obtain uniform concentration in the pores of the support. In most cases, the composition of the batch solution changes during the process and the release of debris can form a “mud” which makes it difficult to completely use the complete solution. In addition to variations of impregnation, drying also plays an important part in this preparation method. Geus [23,24] gives a complete illustration of the effect of redistribution during the drying step. For the preparation of bimetallic catalysts, the precursors for two metals can be added to the support by co-impregnation (two metal salts are simultaneously deposited) or successive impregnation (two metal salts are successively deposited) using the basic procedures described above. However, neither of these two ways can provide truly bimetallic catalysts with close contact of two metals, but instead results in the formation of both monometallic and bimetallic particles with variable compositions.

### 1.3.3 Deposition Precipitation

The limits of impregnation and drying as well as ion exchange often relates to poor reproducibility, a very broad distribution of particle size, and low to medium loadings of the active phase. For that reason, homogeneous deposition precipitation has become as an attractive alternative. This method involves the conversion of a soluble metal precursor into a precipitate on a support [22,23,64,65,67-69]. Typically, change of solution pH, addition of a precipitation agent or a reducing agent, or change in the

concentration of a complexing agent can achieve the above phase change. There are two processes involved: (1) precipitation from bulk solutions or from filled pores; (2) interaction with the support surface. To ensure that the precipitation takes place only on the surface of the support and not in the bulk solution, two conditions must be met. There must be an interaction between the soluble metal precursor and the surface of the support, and the concentration of the precursor must be maintained at a value to avoid the precipitation in solution. In practice, the support is slurried in the solution containing the soluble precursor in amounts sufficient to give the desired loading. The suspension is thoroughly stirred, and the precipitating agent is added. To achieve a successful deposition precipitation, the precipitating agent needs to be added gradually to avoid a rapid nucleation of the precipitation in solution. In principle, this strong precursor-support interaction increases the concentration of the metal precursor at the surface of the support, so that precipitation occurs initially on the surface. Once nucleation has occurred, precipitation continues to occur at the surface. Thermal/chemical treatment of the precipitate leads to the formation of a highly-dispersed metallic phase. To form bimetallic catalysts, two metal precursors can be precipitated simultaneously or sequentially, based on the desired catalytic composition.

#### 1.3.4 Strong electrostatic adsorption

The main consideration for the preparation of bimetallic catalysts is to create close interaction between the two metals since bimetallic interaction appears only when the two metal components form bimetallic clusters instead of separate particles. The above preparation methods, impregnation, deposition-precipitation and ion exchange, are

often proven to be unsatisfactory. Thus, methods based on strong electrostatic adsorption between the charged metal precursor and support and reduction-oxidation (following section 1.3.5) reactions have been developed to prepare bimetallic catalysts which have close interaction.

The mechanism of SEA method was first postulated by Brunelle [70] and further refined by Regalbuto [62,71]. Hydroxyl groups on the surface of an oxide can be protonated or deprotonated depending on the pH of the contacting solution. The pH at which the hydroxyl groups are neutral and no precursor-support interactions occur is called the point of zero charge (PZC). As shown in Figure 1.3, above the PZC, the hydroxyl groups deprotonate and become negatively charged, and the surface can electrostatically adsorb cationic metal complexes such as  $[\text{Pt}(\text{NH}_3)_4]^{2+}$  and  $[\text{Ru}(\text{NH}_3)_6]^{3+}$ . Conversely, below the PZC the hydroxyl groups protonate and become positively charged, and anionic metal complexes such as  $[\text{PtCl}_6]^{2-}$  and  $[\text{Ru}(\text{CN})_6]^{4-}$  can be strongly adsorbed. In both cases, the metal complexes are deposited on the support surface with highly-dispersed metal particles with narrow size distributions. The desired weight loading of the catalyst can be achieved by adjusting solution pH and the concentration of

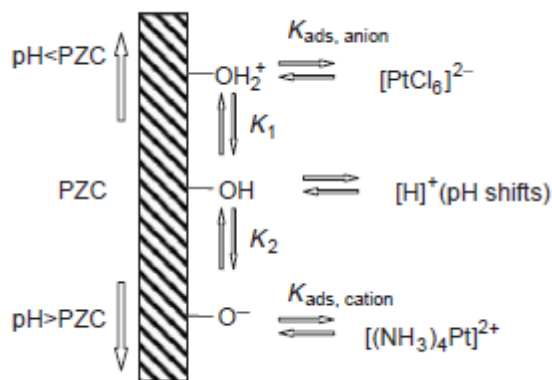


Figure 1.3 Electrostatic adsorption mechanism [62].

metal ions in the solution. Higher weight loadings can be achieved by repeating the SEA sequence, typically after a calcination step to make the initially deposited metal insoluble in the subsequent step.

Bimetallic catalysts can be prepared by simultaneous SEA (co-SEA) or sequential SEA [62,71]. In case of simultaneous SEA, a mixture of cationic precursors of both metals is used if solution pH is above PZC. A mixed monolayer of precursors will be electrostatically adsorbed onto the surface, which results in well-dispersed particles with even distribution and hopefully homogeneous compositions after reduction. If sequential SEA is used, the primary metal is initially deposited by SEA and then oxidized to form a supported metal oxide. If the PZC values of the support and primary metal oxide are different enough, opposite charges can be induced on them so that a secondary metal precursor can be selectively deposited onto the primary metal oxide to form a metal core-shell structure after reduction.

### 1.3.5 Redox

Methods based on reduction-oxidation (redox) reactions have been developed to prepare bimetallic catalysts having close interaction between the two metals. The addition of the second metal takes place exclusively on the monometallic particles of the base catalyst. There are three major types of redox procedures based on various reductants: direct redox reaction, redox reaction of adsorbed reductant, and catalytic reduction [63].

Direct redox reactions methods (also known as galvanic displacement or immersion plating) take place when the primary metal is oxidized by reaction with the oxidized form of a metal salt in solution to effect reduction of the salt [25,28-

30,63,72,73]. Therefore, the redox reaction is driven by the difference in their respective reduction potentials. In practice, this method can be used to deposit a noble metal with a higher standard reduction potential onto a non-noble metal with a lower standard reduction potential. When the difference between reduction potentials of two metals is small, displacement is sluggish and typically occurs only at the more energetic sites (such as corners and edges) of the primary metal. Thus, this direct redox reaction method can potentially be used to prepare bimetallic catalysts with close interaction between the two metals, and also to deposit the second metal selectively on particular sites of the primary metal. This method is usually limited by the accessibility of the primary metal, resulting in passivation of the reaction when a critical portion of the primary metal is covered. Therefore, this method allows for the precise and reproducible control of the surface coverage, which may form up to a one monolayer structure and not three-dimensional depositions. Direct redox reactions (galvanic displacement) will be discussed in more detail in a following Section.

In the adsorbed reductant method, a reductant is selectively pre-adsorbed on the primary metal [22,63,74]. The ions of the second metal are then reduced by this reductant from solution. Dissociatively adsorbed hydrogen is commonly used as the pre-adsorbed reductant for this method; this requires that (1), the primary metal (Pt, Pd, Rh, Ru, etc.) be capable of dissociative adsorption of  $H_2$ , (2), the adsorbed H species is stable in the aqueous solution, and (3), the second metal (Cu, Re, Ir, Rh, Pd, Pt, Au, etc.) is thermodynamically reducible by  $H_2$ . Many combinations of above metals have been prepared and characterized using this method. Even though this method can provide the desired intimate interaction between two metals, it is not applicable for bimetallic

compositions that employ Group IB metals as the primary metal since these metals do not readily dissociatively adsorb hydrogen. It is also rather cumbersome and complex since several successive steps are needed, and the whole process is slow since the solubility of hydrogen in water is quite low. In addition, if the second metal has a higher reduction potential than that of the primary metal, the overall reaction will be complicated since it involves not only a redox reaction by adsorbed reductant but also a direct redox reaction.

The last type of redox reaction method is preparation of bimetallic catalysts by catalytic reduction [25-27,63,72,75]. The catalytic properties of the primary metal are used to activate a reducing agent to effect the reduction of the second metal precursor. Thus, the second metal is placed on the catalytic site of the primary metal where activation of a reducing agent has occurred. This method can be applied to a variety of combination of primary metal and reductants. Some reduction reactions may be structure sensitive due to the nature of the reductant. Therefore, the second metal can be selectively deposited on specific sites of the primary metal. This method provides a way to design bimetallic catalysts which can give optimum activity, selectivity and lifetime for certain reactions. Electroless deposition (ED) is included in this method. It is a catalytic or autocatalytic process for deposition of the second metal precursor onto the primary metal which has activated the reducing agent. Electroless deposition will be discussed in more detail in the following Section.

In addition to the above methods, other techniques such as chemical vapor deposition [22], sol-gel [76], and dendrimer [77] have been also developed to prepare bimetallic catalysts. Each method has advantages and disadvantages, and is used according to the application required by the bimetallic catalysts. Some methods have

little or no control of the metal distribution, thus the close contact between the metals cannot be assured. Methods such as impregnation and precipitation are difficult to achieve uniform bimetallic compositions and often exhibit both monometallic and bimetallic property. Other methods use colloidal or ligated species to help deposit the metals, but the removal of these species may cause agglomeration or segregation which can alter the properties of the catalysts. Redox reaction methods are promising, since they provide the ability to prepare true bimetallic catalyst with controlled composition and sometimes permit the second metal to be deposited on specific sites which can influence the properties of the resulting catalysts. Catalytic deposition, especially electroless deposition, is more attractive for industrial applications, due to its simplicity of preparation and control of the final composition.

## 1.4 Electroless Deposition

### 1.4.1 Background

In 1835, electroless deposition was first mentioned by von Liebig when he used aldehydes to reduce Ag (I) salts to Ag metal [25]. Development in this field was slow until Brenner and Riddell first successfully used electroless deposition to form smooth Ni films in 1946 [25]. They first named the process *electrodeless* plating [78]. Electroless deposition was originally used to describe an autocatalytic process by which a metal was deposited without the use of an external source of electrical current. Much attention has been devoted to find systematic and reproducible electroless deposition solutions which can be used industrially [26]. Since electroless deposition is a simple and inexpensive process, it has been applied in many fields, including electronics, corrosion prevention,

decorative purposes, batteries, and medical devices. Electroless deposition is attractive since most of the metals that can be deposited by electrodeposition can also be deposited electrolessly when proper deposition conditions are used. Currently, electroless deposition has been used for deposition of a wide variety of metals, including Ni, Co, Cu, Cd, Ag, Au, Cr, Sn, Sb, In, Pd, Pt, Ru, Rh, Pb, and Bi [25-27,79]. This method has replaced electrodeposition in many cases due to several practical reasons. It allows plating of very complex shapes and through holes, and produces more dense deposits that show better properties for corrosion prevention and electronics applications than those from electrodeposition [25]. Electroless deposition can selectively deposit metals on certain metal-seeded areas of the substrate, and apply to both conductive and nonconductive surfaces whereas electrodeposition is only practical on conductive materials [25-27,72]. Since ED does not need an external current source, it avoids the problem of current density uniformity that is encountered in electrodeposition. Therefore, it can obtain coatings with more uniform thickness and composition.

Electroless deposition may provide both catalytic and autocatalytic depositions, which are shown in Figure 1.4. Catalytic deposition is a controlled chemical reaction where a second metal ion is selectively reduced on the primary metal that has been activated by a reducing agent. However, if the second metal that has just been deposited can activate the reducing agent, the process becomes autocatalytic since the second metal ion is also deposited on itself [25,28]. It is sometimes difficult to distinguish between catalytic and autocatalytic deposition, since they can take place simultaneously or successively depending on the activation trends of the primary and secondary metals. Nevertheless, electroless deposition always begins with catalytic deposition where the

primary metal acts as catalyst to activate the reducing agent. Since electroless deposition may use an excess of second metal salt and reducing agent relative to monolayer coverage on the primary metal surface, it allows further deposition of multilayers even after the primary metal is completely covered, making it different from galvanic displacement.

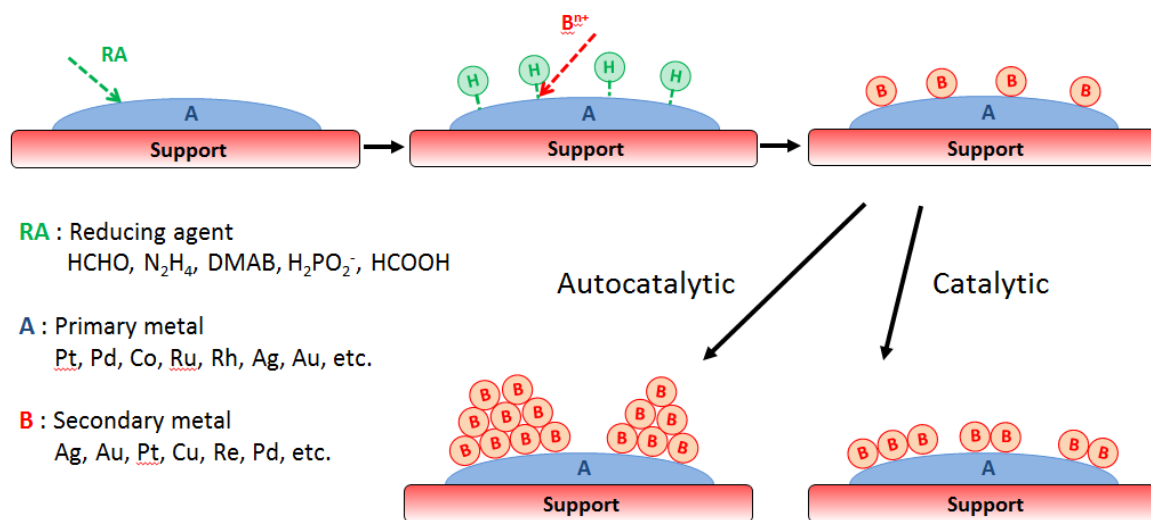


Figure 1.4 Electroless deposition mechanism.

### 1.4.2 Bath Composition

Most electroless deposition baths have similar components. The bath is usually aqueous and consists of a metal ion source, a reducing agent, a complexing agent, and a stabilizer [25,26]. A monometallic supported catalyst is used as substrate for synthesis of bimetallic catalysts. Since these baths are thermodynamically unstable, kinetic stability of the bath must be maintained to obtain successful electroless deposition. Otherwise, the metal ion will be reduced and precipitate from the bath, instead of being deposited on active sites of the primary metal.

### 1.4.2.1 Metal Ion Source

Generally speaking, the metal ion source can be any water soluble salt such as sulfates, chlorides, acetates, and cyanides. Some of the common metal ion sources used for electroless deposition are listed in Table 1.1 [25]. The selection of the metal ion sources depend on stability in the bath, properties of the deposits, and environmental concerns. The effects of impurities and byproducts on the final deposits also play an important role in metal source selection. For instance, secondary metal ions with cyanide ligands act both as complexing agents and high stability ions due to high formation constants of metal cyanides, but their toxicity hinders extensive industrial use. Metal chloride sources are safer but can induce dissolution of certain supports; further, residual chloride ions in the final catalyst may adversely affect catalyst performance.

In electroless deposition, metal precursors should react with reducing species adsorbed on the primary metal, instead of being adsorbed onto the support. To avoid such strong electrostatic adsorption (SEA) of a metal precursor on the support, the selection of

Table 1.1 Common metal ion sources for electroless deposition [25].

Metal	Metal precursors
Ni	NiSO <sub>4</sub> , NiCl <sub>2</sub> , Ni(H <sub>2</sub> PO <sub>2</sub> ) <sub>2</sub> , Ni(CH <sub>3</sub> COO) <sub>2</sub>
Co	CoSO <sub>4</sub> , CoCl <sub>2</sub>
Au	KAu(CN) <sub>2</sub> , KAuCl <sub>4</sub> , Na <sub>3</sub> Au(SO <sub>3</sub> ) <sub>2</sub>
Ag	AgNO <sub>3</sub> , KAg(CN) <sub>2</sub>
Pd	PdCl <sub>2</sub> , Pd(NH <sub>3</sub> ) <sub>4</sub> Cl <sub>2</sub>
Pt	Na <sub>2</sub> Pt(OH) <sub>6</sub> , Pt(NH <sub>3</sub> ) <sub>4</sub> Cl <sub>2</sub> , Na <sub>2</sub> PtCl <sub>6</sub>
Cu	CuSO <sub>4</sub> , KCu(CN) <sub>2</sub>

cationic or anionic metal source needs to be taken into consideration. If we conduct the ED experiment below the point of zero charge (PZC) of the catalyst support where the surface is positive, cationic precursors should be chosen to avoid SEA, and vice versa.

#### 1.4.2.2 Reducing agent

The reducing agent provides electrons to the secondary metal cation that is being reduced. Selection of the reducing agent is also important since it affects the stability of the electroless bath and the rate of the deposition process. Commonly used reducing agents include hydrazine ( $N_2H_4$ ), formaldehyde (HCHO), sodium hypophosphite ( $NaH_2PO_2$ ), sodium borohydride ( $NaBH_4$ ), and dimethylamine borane (DMAB) [25,80]. For electroless deposition to occur, the reducing agent must have a more negative standard reduction potential than the second metal cation that is being reduced. In addition, the order of reducing agent activation on metals should be considered for synthesis of true bimetallic catalysts; the reducing agent should prefer to activate on the surface of the primary metal rather than the secondary metal, in order to produce a bimetallic surface. The catalytic activities of different metals (Au, Pd, Pt, Ag, Ni, Co and Cu) for activating the above reducing agents were measured and compared by Ohno et al. [80]. Figure 1.5 shows comparison of the anodic oxidation potential of these reducing agents for different metals at a reference current density. Catalytic activity increases with decreasing anodic potentials. To prepare a bimetallic catalyst, it is recommended from Figure 1.5 that a reducing agent should be selected when the primary metal has a higher catalytic activity than the secondary metal. Under such circumstance, deposition of the second metal on the first metal (*i.e.*, catalytic deposition) will be favored over autocatalytic deposition. For example, to deposit Ag on Pd, sodium borohydride,

dimethylamine borane and hydrazine would be good choices, as Pd shows higher catalytic activity for these reducing agents. The bath stability of the metal source and reducing agent without the presence of primary metal should be investigated before ED experiment. If the bath is unstable, complexing agents or stabilizing agents should be added or other combinations of metal source and reducing agent should be selected. Another consideration is that reducing agents containing phosphorus and boron may co-deposit with the secondary metal salt or become occluded in the deposition layer to give incorporation of these elements into the metal coating. Other reducing agents such as hydrazine or formaldehyde do not have this kind of problem so they permit an alternative.

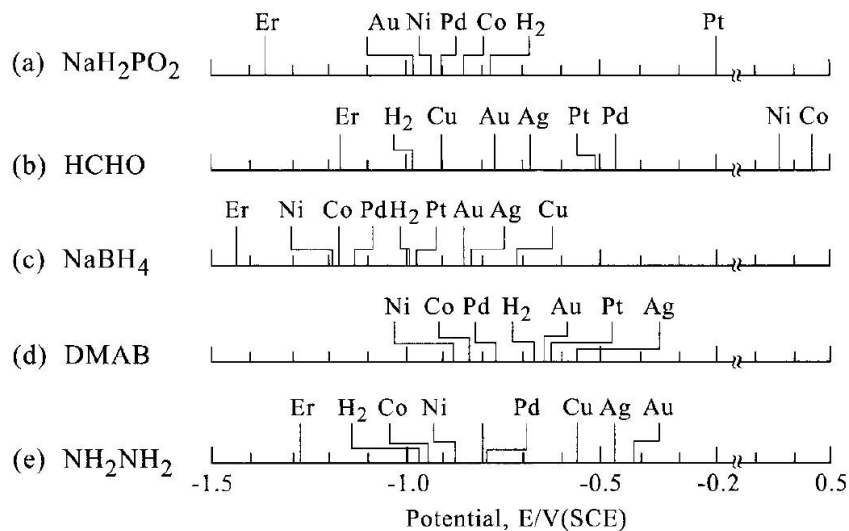


Figure 1.5 Catalytic activities of metals during anodic oxidation of different reducing agents [80].

#### 1.4.2.3 Complexing agent

Complexing agents are employed for several functions to achieve successful electroless deposition. The principal purpose is to increase kinetic stability of the

electroless bath by preventing the precipitation of metal salts as well as the thermal reaction of metals salts with reducing agents [25]. Complexing agents can also be used to change the cationic metal source from cationic to anionic metal or vice versa, to avoid SEA. In some cases as mentioned in Section 1.4.2.1, the metal source itself can also function as a complexing agent, such as for  $\text{Ag}(\text{CN})_2^-$ . The commonly used complexing agents for some metals are listed in Table 1.2 [25]. They work effectively at different pH values, but will not be discussed in detail here. More discussions can be found in reference [81].

Table 1.2 Complexing agents used in the electroless deposition for common metals [25].

Metal	Complexing agents
Ni, Co	propionate, succinate, citrate, EDTA, ethylenediamine
Cu	cyanide, triethyl amine, EDTA, glycolic acid
Au	cyanide, sulfite, citrate, chloride
Ag	cyanide, ammonium
Pd, Pt, Ru	citrate, acetate, ammonium, ethylenediamine

#### 1.4.2.4 Stabilizing agent

Stabilizing agents have similar functions as complexing agents. These chemical compounds are used to prevent the precipitation of the metal ions from the bulk solution and to increase the thermal stability of baths [25]. Reduction of secondary metal salts to form suspended metal nuclei also is catalytic for further metal reduction in the ED bath. Since the concentration of stabilizing agents can determine the rate of deposition, they can be used to optimize the rate of catalytic deposition which may ensure distribution of

the second metal on the primary metal surface. A representative list of commonly used stabilizing agents for some metal salts is listed in Table 1.3.

Table 1.3 Stabilizing agents used for the electroless deposition of common metals [25].

Metal	Stabilizing agents
Ni	metals (S, Se, Te), oxyanions ( $\text{AsO}_2^-$ , $\text{IO}_3^-$ , $\text{MoO}_4^{2-}$ ), metal cations, organic acids
Cu	cyanide, thiourea, mercury compounds, butyrol, propionitrile
Au	cyanide, nitrilotriacetic acid, mercaptosuccinic acid
Ag	cyanide, metal ions ( $\text{Cu}^{2+}$ , $\text{Ni}^{2+}$ , $\text{Co}^{2+}$ , $\text{Zn}^{2+}$ ), $\text{NaSCN}$ , mercaptopropane sulfonate
Pd	mercaptoformazon compounds

#### 1.4.2.5 Bath medium

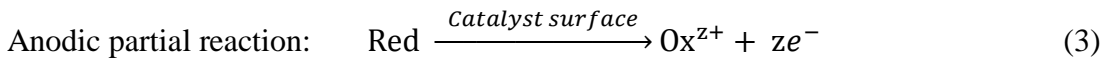
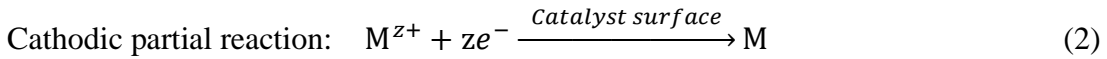
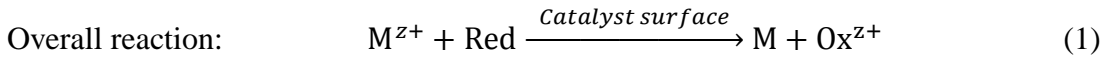
Apart from the above constituents of electroless deposition baths, an aqueous medium is also preferred for most of electroless deposition processes, since it can provide  $\text{OH}^-$  and  $\text{H}^+$  ions to promote the electron transfer. In addition, the pH of the solution may change the oxidation potential of the reducing agent and the ionic charge on the surface of the catalyst support to prevent SEA. Therefore, the composition of an effective electroless deposition bath is based on consideration of all bath factors to achieve a balance between stability and rate of deposition.

### 1.4.3 Mechanism

#### 1.4.3.1 Mixed potential theory

Paunovic [82] and Saito [83] were the first to promote the idea that a simple electrochemical method can be used to model the electroless deposition process. Today, it

is well understood that since cathodic and anodic partial reactions occur simultaneously on the surface of the same substrate, the overall electroless deposition process is electrochemical in nature [26,27,75]. These electroless deposition reactions can be expressed as [26,27,75]:



where  $M^{z+}$  is the metal ion source, Red is the reducing agent, M is the reduced metal and Ox is the oxidized product of reducing agent. The two partial reactions (2) and (3) determine the potential of a surface undergoing electroless deposition, which is called the mixed potential [26,27,75]. This concept can be understood better by the plot shown in Figure 1.6 [26].

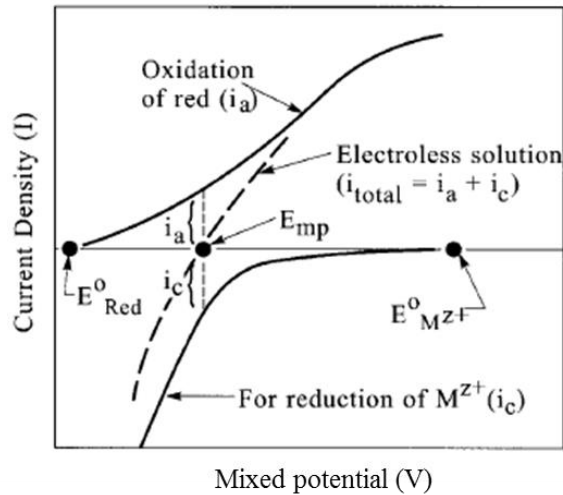


Figure 1.6 Schematic diagram of mixed potential concept [26].

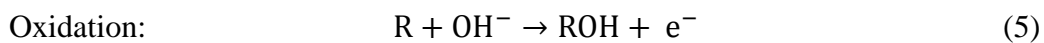
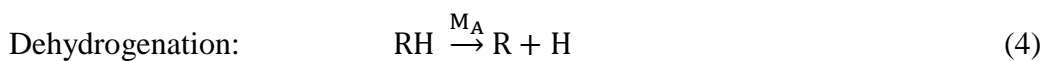
The dashed line represents the electroless deposition process;  $i_a$  and  $i_c$  represent the partial anodic and cathodic currents, respectively. The anodic oxidation and cathodic

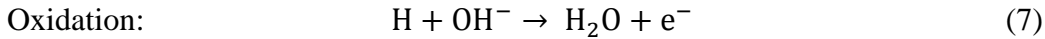
metal deposition take place at the catalytically activated metallic surface. As the partial reactions proceed, they reach their individual equilibrium potentials at  $E_{\text{Red}}^{\circ}$  and  $E_{\text{M}^{z+}}^{\circ}$  on the surface.  $E_{\text{Red}}^{\circ}$  must be more negative than  $E_{\text{M}^{z+}}^{\circ}$  so that the reducing agent Red can function as an electron donor and  $\text{M}^{z+}$  as an electron acceptor. When the difference between these two potentials is too low or negative, the metal reduction process stops. On the other hand, when the difference is too high, decomposition of the bath occurs spontaneously. Somewhere between  $E_{\text{Red}}^{\circ}$  and  $E_{\text{M}^{z+}}^{\circ}$ , when the anodic and cathodic currents are equal, is the potential where electroless deposition takes place, thus this point is called the mixed potential,  $E_{\text{mp}}$ .

#### 1.4.3.2 Unified mechanism

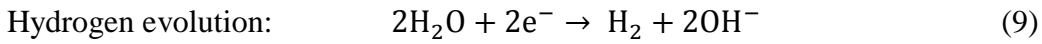
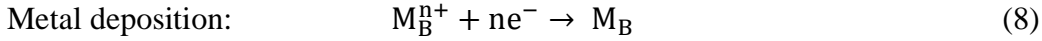
To account for some deficiencies of the mixed potential theory, other mechanisms have been proposed for various electroless deposition processes, but most are specific to particular systems with different reducing agents. However, Van Den Meerakker [84] observed that there are some common characteristics for all electroless systems: (1) evolution of  $\text{H}_2$  gas from the reducing agent, (2) primary metals are effective hydrogenation-dehydrogenation catalysts, (3) poisons for the above hydrogenation-dehydrogenation process act as stabilizing agents, (4) rates of electroless deposition are promoted by an increase of solution pH. He then proposed a unified mechanism that can be employed for all electroless systems:

Anodic:





Cathodic:

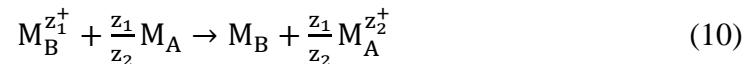


where  $M_A$  and  $M_B$  are the primary and secondary metals; RH represents the reducing agent. RH dissociates to form the radical R and atomic H upon adsorption at the surface of the deposited metal. The electrons supplied by oxidation steps (eqn. (5) and eqn. (7)) go towards metal ion reduction. The above equations are considered to represent the core steps in electroless deposition. However, when it comes the reducing agents such as  $NaH_2PO_2$  and DMAB which contain phosphorus and boron, one or more reactions need to be added to account for co-deposition of P and B along with metals [25,26].

## 1.5 Galvanic displacement

### 1.5.1 Background

In galvanic displacement (also called cementation or immersion plating), cations of more noble metals (secondary metal) with higher reduction potential are spontaneously reduced by the less noble metal (primary metal) with a lower reduction potential [25,28-30,63,72,73], which can be expressed as



where  $M_A$  represents the less noble metal (primary metal) and  $M_B$  is the more noble metal (secondary metal). Upon contact in a solution phase, the base material is oxidized and dissolved into the solution while the metallic ions of the secondary metal in the solution

are reduced on the surface of the base material, which differs from electroless deposition since GD does not require a reducing agent and the surface of the primary metal erodes into solution during GD. At the beginning of the immersion, the rate of the deposition is fastest, since the full primary metal surface is available for reaction. As more of the primary metal is covered by the secondary metal, the rate of deposition decreases. Ideally, the deposition should stop as soon as the entire surface of the primary metal is covered and the coverage should be limited  $\leq 1$  monolayer, depending on the redox stoichiometry.

Over the past decade, galvanic displacement has been used for the development of metal nanostructures with highly active surfaces for electrocatalysts [30], biomedicine [29], and functional coatings [85]. This simple preparation method can be applied to synthesize a wide variety of bimetallic catalysts such as Pd-Ir, Au-Ag, Pd-Ag, Pt-Ag, Pt-Cu, as long as the reduction potentials of the two metals differ sufficiently [29,86-89]. There are several advantages of this method. Firstly, the composition of the final bimetallic catalyst can be controlled by adjusting the initial amount of secondary metal precursor. Secondly, since the secondary metal only deposits on the primary metal, the surface of final product reproduces almost exactly the same shape of base material with only a slight increase in dimensions. Thirdly, some studies [29,90,91] have shown that the oxidation and dissolution of the primary metal begins at certain sites of the base material, giving the ability to target the second metal to some extent. Thus, galvanic displacement is a simple, effective and versatile method to prepare true bimetallic catalysts with close contact of two metals and controlled composition, shape and structure.

### 1.5.2 Bath composition

Compared to electroless deposition, galvanic displacement does not require a reducing agent, which makes the development of galvanic displacement bath much easier since thermal stability of the bath is not an issue. A galvanic displacement bath is simply an aqueous solution consisting of a salt of a metal precursor with optional additive (*i.e.*, complexing agent) at a given temperature and pH. The only requirements to ensure that GD can occur are the metal salt source must have a higher reduction potential than the primary metal and that there is no adsorption of the metal salt on the catalyst support. To avoid SEA of metal precursor onto the support, cationic precursors should be chosen if we conduct the GD experiment under the point of zero charge (PZC) of the catalyst support where the support surface exhibits positive, and vice versa. Displacement temperature can be adjusted according to the desired reaction rate.

## CHAPTER 2:

### EXPERIMENTAL PROCEDURES

## 2.1 List of chemical materials

Pd/SiO<sub>2</sub>: BASF, CD04183, 1.85 wt% Pd on SiO<sub>2</sub> #1, dispersion = 8.6%

SiO<sub>2</sub> #1: BASF, surface area = 100m<sup>2</sup>/g, pore volume = 0.75 cc/g

SiO<sub>2</sub> #2: Evonik Degussa, AEROSIL® OX 50, hydrophilic and fumed, surface area = 50 ± 15 m<sup>2</sup>/g

Potassium silver cyanide (KAg(CN)<sub>2</sub>): Technic, Inc., 99% purity

Potassium dicyanoaurate (KAu(CN)<sub>2</sub>): Sigma-Aldrich, 99% purity

Hydrazine (N<sub>2</sub>H<sub>4</sub>): Sigma-Aldrich, 35 wt% solution

Sodium hydroxide (NaOH): J.T. Baker, pellets

Nitric acid (HNO<sub>3</sub>): BDH, 68.0-70.0%

Hydrochloric acid (HCl): BDH, 36.5-38.0%

Silver nitrate (AgNO<sub>3</sub>): Alfa Aesar, 99.9+%

Palladium nitrate (Pd(NO<sub>3</sub>)<sub>2</sub>): Alfa Aesar, 99.9%

Lanthanum chloride (LaCl<sub>3</sub>): Sigma-Aldrich, 99.999%

Au, Ag, Pd Atomic Absorption standards: EMD, each 1000 mg/L or ppm

## 2.2 Catalyst preparation

### 2.2.1 Ag- and Au-Pd/SiO<sub>2</sub> prepared by electroless deposition

As stated in Section 1.4, an electroless deposition bath is an aqueous solution consisting of a metal source, a reducing agent and optional additives (*i.e.*, stabilizing agent, complexing agent) at a given temperature and pH. The conditions for ED baths in this study were chosen based three requirements. Firstly, there must be no adsorption of the reducible metal salt on the catalyst support, since bimetallic catalyst formation

requires that all reducible metal ions must be deposited on only the primary metal surface. In this case, Ag or Au ions must be deposited only on the Pd surface and not the silica support. Secondly, the thermal stability of the bath with respect to reduction of the reducible metal salt with the reducing agent must exceed the time frame required for electroless deposition, which would avoid the spontaneous precipitation of the metal salt in the solution. Thirdly, the primary metal surface (Pd, in this study) must be capable of activating the reducing agent to provide sites for reduction of the reducible metal ion (Ag or Au, in this study).

Regarding the first requirement, the PZC of the silica support of the base catalyst 1.85 wt% Pd/SiO<sub>2</sub> was approximately pH 4. At pH < 4, the silica support was positively charged and capable of adsorbing the negatively-charged metal anions. Since most aqueous reducing agents are more active at basic conditions (pH ≥ 9), pH 9 was selected for the ED bath in this study. This pH is higher than the PZC of the silica support, so Ag(CN)<sub>2</sub><sup>-</sup> and Au(CN)<sub>2</sub><sup>-</sup> were selected as the metal sources for Ag and Au deposition, respectively, on Pd/SiO<sub>2</sub>. The cyanide salts also provide higher kinetic stability for the ED baths due to their high formation constants, precluding the need for stabilizing agents, and galvanic displacement will be avoided compared to AuCl<sub>4</sub><sup>-</sup> since





the overall potential of the redox system is negative for  $\text{Au}(\text{CN})_2^-$  with  $\text{Pd}^0$ , which means that galvanic displacement is not thermodynamically favored. Galvanic displacement of  $\text{AuCl}_4^-$  with  $\text{Pd}^0$  is slightly positive, suggesting that some GD might occur which could complicate the overall deposition of Au.

The combination of  $\text{Ag}(\text{CN})_2^-$  with  $\text{Pd}^0/\text{SiO}_2$  and  $\text{Au}(\text{CN})_2^-$  with  $\text{Pd}^0/\text{SiO}_2$  were experimentally tested to determine stability of the baths with respect to GD and the absence of SEA on  $\text{SiO}_2$  at pH electroless systems without the addition of reducing agent. The concentrations of  $\text{Ag}(\text{CN})_2^-$  and  $\text{Au}(\text{CN})_2^-$  in the electroless baths were found to be unchanged over time and no  $\text{Pd}^{2+}$  was detected, indicating no dissolution of primary metal Pd or deposition of second metal Ag or Au had occurred. To satisfy bath stabilities, the reducing agent should be selected so that stabilities existed for a satisfactory period of time (at least 2 h) in the absence of  $\text{Pd}^0$  but that reduction readily occurred in the presence of  $\text{Pd}^0$ . In this study, hydrazine ( $\text{N}_2\text{H}_4$ ) was selected as the reducing agent based on anodic oxidation trends for oxidation of hydrazine by different metals [80]. Hydrazine is preferentially oxidized on Pd rather than Ag or Au, making hydrazine an ideal candidate for the catalysts in this study. Hydrazine is activated faster by Pd than Ag or Au so that catalytic deposition of Ag or Au on Pd dominates and the autocatalytic deposition of Ag on Ag or Au or Au is inhibited. This trend was in our interest since we wanted to study and evaluate catalysts with variable and controlled coverages of Ag on Pd and Au on Pd, up to high coverages of each Group 1B metal on Pd. Competitive rates of autocatalytic deposition of Ag and Au limit the ability to achieve high coverages of these components.

To ensure thermal stabilities of the ED baths, the maximum concentrations of  $\text{N}_2\text{H}_4$  with  $\text{Ag}(\text{CN})_2^-$  or  $\text{Au}(\text{CN})_2^-$  were thoroughly explored. Likewise, the effect of deposition temperatures on near-optimum bath compositions was also determined. A master batch of 1.85 wt% Pd/SiO<sub>2</sub> (sieved to 60/80 mesh particles) was used as the base monometallic Pd catalyst. The surface area of the silica was measured by the BET method to be 100 m<sup>2</sup>/g. The dispersion of Pd was determined by hydrogen titration of oxygen pre-covered Pd sites at 40°C using a Micromeritics AutoChem 2920 Automated Analyzer, which is described in detail in Section 2.3.2. The dispersion of 8.6% corresponded to Pd particles of 13.2 nm diameter and  $9.0 \times 10^{18}$  surface Pd sites/g cat. Controlled loadings of Ag and Au on the Pd surface were added using the electroless deposition method. Briefly, potassium silver cyanide ( $\text{KAg}(\text{CN})_2$ ) and potassium dicyanoaurate ( $\text{KAu}(\text{CN})_2$ ) were used as the metal sources, and hydrazine ( $\text{N}_2\text{H}_4$ ) was used as the reducing agent. Initial concentrations of the metal salts were selected based on the desired, theoretical coverage of Ag or Au on Pd, assuming monolayer deposition and 1:1 surface stoichiometry of Ag or Au to Pd. The molar ratio of the reducing agent to metal salt was initially selected at 10:1. To deposit higher amounts of Ag or Au, a 20:1 ratio was used to compensate for time-dependent, thermal decomposition of the reducing agent in the ED bath. Typically, the volume of the electroless bath was 50 – 100 mL for each gram of the monometallic catalyst. The deposition of Ag and Au was conducted at room temperature, and the baths were placed in disposable polyethylene beakers to prevent cross-contamination. The experiments were carried out while stirring on a magnetic stirring plate to minimize external mass transfer limitations. Dropwise addition of a concentrated solution of sodium hydroxide (NaOH) was used to maintain pH of the

bath solution at  $\sim 9.0 \pm 0.5$  during the entire experiment; a pH probe was immersed in the ED bath to monitor the pH throughout the deposition. Baths were prepared by adding all the required components except the monometallic Pd/SiO<sub>2</sub> catalyst. An aliquot ( $\leq 1$  mL) was first taken from the bath to determine the initial Ag or Au concentration. Addition of the monometallic Pd/SiO<sub>2</sub> catalyst initiated the deposition. To monitor the concentration of Ag<sup>+</sup> and Au<sup>+</sup> remaining in the bath, liquid aliquots were periodically taken and filtered using 4.5  $\mu\text{m}$  mesh syringe filters to remove catalyst particles at different time intervals. These liquid samples were diluted and analyzed for Ag and Au concentrations by atomic absorption spectroscopy, which is described in details in Section 2.3.1. After 4 h of deposition time, the slurry was filtered and the catalyst was washed thoroughly with 2 L of de-ionized water to remove unreacted metal and all other soluble ligands and salts. The filtrates were then dried *in vacuo* at room temperature and stored at ambient conditions. Thus, complete series of Ag-Pd/SiO<sub>2</sub> and Au-Pd/SiO<sub>2</sub> bimetallic catalysts were prepared with varying weight loadings of Ag and Au metals on the Pd surface.

### 2.2.2 Pd-Ag/SiO<sub>2</sub> prepared by galvanic displacement

The galvanic displacement bath in this study was an aqueous solution of KAg(CN)<sub>2</sub> at a given temperature and pH. Compared to electroless deposition, galvanic displacement does not require chemical reducing agent, which makes the selection of GD bath conditions easier as we do not need to consider the bath thermal stability. Thus, there are only two requirements. Firstly, GD can occur only when the metal source have a higher reduction potential than the primary metal. Secondly, there must be no adsorption of the metal salt on the catalyst support, since bimetallic catalyst formation requires that

all metal ions must be deposited on only the primary metal surface. For the first requirement, the oxidation potential for  $\text{Ag}^0 = \text{Ag}^+ + \text{e}^-$  was -0.799 V meaning the reduction potential for Pd salts must be greater than +0.799V. From Table 2.1 below, the  $\text{Pd}^{2+}$  salt is basically limited to non-ligated  $\text{Pd}^{2+}$  salts [such as  $\text{Pd}(\text{NO}_3)_2$ ] with a reduction potential of +0.915V. The PZC of the silica support of the base catalyst 2 wt%  $\text{Ag}/\text{SiO}_2$  is pH 4. To avoid SEA of the Pd metal salt onto the support, the positively charged metal cation  $\text{Pd}^{2+}$  must be used below the PZC. This, the bath solution for GD of  $\text{Pd}^{2+}$  was maintained at pH 2.

Table 2.1 Standard reduction potentials for different  $\text{Pd}^{2+}$  salts.

Formula (aqueous)	$E^\circ$ (V)
$\text{Pd}^{2+}$	0.915
$\text{PdCl}_4^{2-}$ (1M HCl)	0.62
$\text{PdBr}_4^{2-}$	0.49
$\text{PdI}_4^{2-}$	0.18
$\text{Pd}(\text{NO}_2)_4^{2+}$	0.34
$\text{Pd}(\text{OH})_2$	0.07
$\text{Pd}(\text{EN})_2^{2+}$	-0.79
$\text{Pd}(\text{NH}_3)_4^{2+}$	0.0
$\text{Pd}(\text{CN})_4^{2-}$	-1.52

The base catalyst 2.0 wt%  $\text{Ag}/\text{SiO}_2$  was prepared by conventional incipient wetness of silver nitrate ( $\text{AgNO}_3$ ) dissolved in de-ionized water and added to AEROSIL® OX 50 hydrophilic, fumed silica with a specific surface area of  $50 \pm 15 \text{ m}^2/\text{g}$ . The fresh catalyst was dried under vacuum in a rotary evaporator at 60 °C before calcination at 300 °C in flowing air for 2 h. Finally, the catalyst was reduced at 300 °C in

flowing 10% H<sub>2</sub>/He for 2 h in a horizontal furnace. The dispersion of Ag was determined by hydrogen titration of oxygen pre-covered Ag sites at 170°C. The detailed chemisorption procedures are described in Section 2.3.2. The dispersion of 4.9% corresponded to Ag particles of 23.8 nm diameter and  $5.52 \times 10^{18}$  surface Ag sites/g cat.

Controlled loadings of Pd were added to the silica-supported Ag surface by galvanic displacement. Briefly, (Pd(NO<sub>3</sub>)<sub>2</sub>) was dissolved in 5% nitric acid (HNO<sub>3</sub>) and used as the metal source of Pd<sup>2+</sup>. Initial concentrations of the metal salts were selected based on the desired, theoretical coverage of Pd on Ag, assuming monolayer deposition and 1:1 surface stoichiometry of Pd on Ag. The volume of the galvanic displacement bath was 100 mL for each gram of the monometallic catalyst. The deposition of Pd was conducted at room temperature in disposable polyethylene beakers to prevent cross-contamination. The experiments were carried out while stirring on a magnetic stirring plate to ensure there were no external mass transfer limitations. A concentrated solution of nitric acid was added dropwise to the bath to maintain pH at  $\sim 2.0 \pm 0.1$  during the entire experiment; a pH probe was immersed in the galvanic displacement bath to monitor the pH throughout the 1 h reaction time. Baths were prepared by adding all the required components except the monometallic Ag/SiO<sub>2</sub> catalyst. An aliquot ( $\leq 1$  mL) was taken from the bath to determine the initial Pd concentration. Addition of 1.0 g Ag/SiO<sub>2</sub> catalyst initiated the deposition. To monitor the concentrations of both Pd<sup>2+</sup> remaining in solution and the Ag<sup>+</sup> displaced in the bath, liquid aliquots were periodically taken at different time intervals and filtered using 0.2  $\mu$ m PTFE membrane syringe filters to remove catalyst particles. These liquid samples were diluted separately and then analyzed for Pd<sup>2+</sup> and Ag<sup>+</sup> concentrations by atomic absorption spectroscopy, which is described in

details in Section 2.3.1. After 1 h of reaction time, the solution was filtered and the filtrate was washed thoroughly with 2 L de-ionized water to remove all soluble salts. The catalyst was then dried *in vacuo* at room temperature and stored at ambient conditions. Thus, a complete series of Pd-Ag/SiO<sub>2</sub> bimetallic catalysts was prepared with varying weight loadings of Pd exchanged on the Ag surface.

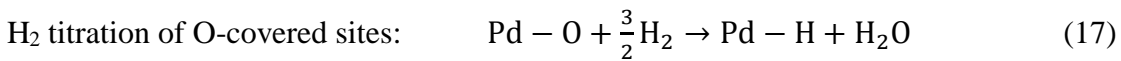
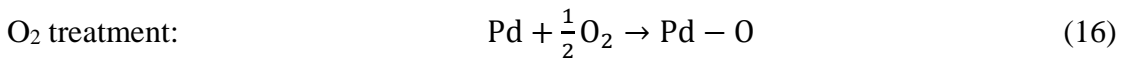
## 2.3 Catalyst characterization

### 2.3.1 Atomic absorption spectroscopy (AA)

Atomic absorption spectroscopy was performed on a PerkinElmer AAnalyst 400 spectrometer to analyze the elemental concentrations of Ag, Au and Pd in ED and GD solutions and solid catalysts. A set of standards with known concentrations were prepared to calibrate the instrument before the actual measurements were conducted. In case of solid catalysts, the weight percentages of metals in the final bimetallic catalysts were determined by digesting 0.04 g of samples in aqua regia (3:1 of HCl to HNO<sub>3</sub> by volume) at 120 °C for 4 h and then diluting with de-ionized water prior to AA analysis. All the liquid samples (both from solid catalysts and aliquots of ED and GD) were further diluted to lower the concentrations of metals within the AA spectroscopy detection limits. For Ag samples (except containing cyanide), 5 vol% HNO<sub>3</sub> was added along with the dilution to keep Ag from oxidation. For Au samples (except containing cyanide), only de-ionized water is needed for the dilution. For Pd samples, 10 vol% HCl and 0.5% LaCl<sub>3</sub> were added to the samples for better sensitivity and accuracy. For the samples containing cyanide, basic solutions were required for the dilution to avoid hazardous HCN formation.

### 2.3.2 Chemisorption

The concentrations of Pd surface sites for the base monometallic Pd/SiO<sub>2</sub> as well as the bimetallic Ag-Pd/SiO<sub>2</sub>, Au-Pd/SiO<sub>2</sub> and Pd-Ag/SiO<sub>2</sub> catalysts were determined by chemisorption using hydrogen pulse titration of oxygen pre-covered Pd sites at 40 °C. Chemisorption was performed using a Micromeritics Autochem II 2920 automated chemisorption analyzer. All samples were reduced *in situ* at 200 °C in 10% H<sub>2</sub>/balance Ar for 2 h and then purged with Ar for 1 h to remove any residual H<sub>2</sub>, before cooling down to 40 °C in Ar. Next, 10% O<sub>2</sub>/balance He was flowed over the catalyst for 30 min to form Pd-O surface sites (see Eq.16), and then purged with Ar for 30 min to remove any residual gas phase oxygen and weakly adsorbed oxygen on the support. Finally, 10% H<sub>2</sub>/balance Ar was dosed until all surface Pd-O species reacted with H<sub>2</sub> to form H<sub>2</sub>O and Pd-H surface species (see Eq.17). For each Pd atom, 1.5 H<sub>2</sub> molecules are accounted. Hence, the amount of consumed H<sub>2</sub> is corresponded to amount of Pd surface sites. Hydrogen consumption was quantitatively measured using a high sensitivity thermal conductivity detector (TCD).

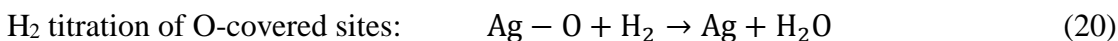
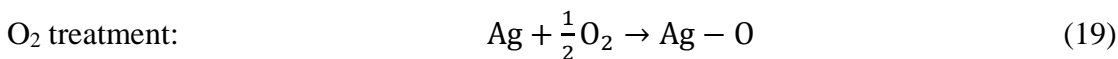


Since Ag or Au is inactive for H<sub>2</sub>-O<sub>2</sub> titration, the coverage  $\theta$  of Ag or Au metals can be calculated from the following Eq.18. The corresponding metallic dispersion and particles size can also be determined.

$$\theta = \frac{\# \text{Pd sites in Pd/SiO}_2 - \# \text{Pd sites in Group IB-Pd/SiO}_2}{\# \text{Pd sites in Pd/SiO}_2} \quad (18)$$

The concentration of Ag surface sites for the base monometallic Ag/SiO<sub>2</sub> catalyst was determined using same chemisorption equipment and same procedures. The only

differences are the temperatures for pretreatment and titration, which were developed by Vannice [92]. The Ag/SiO<sub>2</sub> sample was reduced at 250 °C, and then cooled down to 170 °C for titration. The reactions are shown in Eq.19 and Eq.20. For each Ag atom, a single H<sub>2</sub> molecule is consumed.



### 2.3.3 Powder X-ray diffraction (XRD)

For further reference, powder XRD on 2 wt% Ag/SiO<sub>2</sub> was conducted using a Rigaku Miniflex II benchtop diffractometer with a CuK $\alpha$  radiation source ( $\lambda = 1.5406 \text{ \AA}$ ) operated at 30 kV and 15 mA. Powder sample was loaded on an amorphous glass-backed, low background holder. Scanning was done over the 2 $\theta$  range of 10-80° with sampling width of 0.02° and dwell time of 1 %/min. The diffractometer was fitted with a Rigaku D/tex Ultra silicon strip detector which is capable of detecting nanoparticles in samples with metal loadings as low as 1 wt% and particles as small as 1 nm.

### 2.3.4 Fourier transform infrared spectroscopy (FTIR) of CO adsorption

*In situ* FTIR of CO adsorption on the bimetallic Pd-Ag/SiO<sub>2</sub> prepared by GD was performed by using a Thermo Electron Nicolet Nexus 4700 spectrometer with a liquid nitrogen-cooled MCT-B (mercury-cadmium-telluride B) detector. Approximately 0.030 g catalyst was pressed into a self-supporting pellet with 12 mm diameter and then fixed in a sample holder that was placed in the middle of a cylindrical stainless steel cell. The sample temperature was monitored by a thermocouple placed near the catalyst and

controlled by external heating tape wrapped around the cell. All samples were pretreated *in situ* at 200 °C in flowing 10% H<sub>2</sub>/balance He for 2 h followed by flowing He for 30 min before cooling to room temperature in He. For each sample, a background spectrum of pure metal surface in flowing He was first taken and subtracted from all subsequent spectra. The sample was exposed to 1% CO/balance He for 30 min followed by a flow of pure He for 30 min to remove any gas phase and reversibly-adsorbed CO. The spectra of chemisorbed CO on Pd were continuously collected for 1 h in single beam absorbance mode with a resolution of 4 cm<sup>-1</sup>, and then referenced to the initial He background spectrum. The spectra were baseline corrected and smoothed as needed to remove the noise due to water.

### 2.3.5 X-ray photoelectron spectroscopy (XPS)

XPS measurements of bimetallic Pd-Ag/SiO<sub>2</sub> prepared by GD were conducted using a Kratos Axis Ultra DLD system with a hemispherical energy analyzer and a monochromatic Al K $\alpha$  source operated at 15 keV and 150 W. The X-rays were incident at an angle of 45 ° with respect to the surface normal and the pass energy was fixed at 40 eV for the detailed scans. The powder samples were pressed into a cup of Mo stub and mounted in a catalysis cell that was attached to the XPS main chamber for *in situ* sample pretreatment. After the sample was reduced at 200 °C for 2 h, it was transferred into the UHV chamber for XPS analysis without exposure to air. A charge neutralizer was applied to compensate the residual positive charge present on the non-conductive silica support during photoemission. The Si 2p binding energy was used as a reference and was compared to the literature value of 103.3 eV. The same difference (charging correction)

in eV was applied to all other XPS peaks to give corrected binding energy of Ag 3d and Pd 3d for both monometallic and bimetallic catalysts. For comparison, a reduced and commercially-available 2 wt% Pd/SiO<sub>2</sub> (BASF) was used as reference for the binding energy of Pd<sup>0</sup>.

## 2.4 Catalyst evaluation

The monometallic Pd/SiO<sub>2</sub> and the series of bimetallic Ag-Pd/SiO<sub>2</sub> and Au-Pd/SiO<sub>2</sub> catalysts prepared by ED, as well as the monometallic Ag/SiO<sub>2</sub> and the series of bimetallic Pd-Ag/SiO<sub>2</sub> catalysts prepared by GD were evaluated for selective hydrogenation of acetylene in the presence of excess ethylene. Catalysts were evaluated in a single pass, 0.19 in ID, packed bed, tubular reactor (316 stainless steel). The reactor was encased in a 1.0 in OD, jacketed shell with liquid inlet and exit ports at the bottom and top of the shell, respectively, which was connected to an ethylene glycol/H<sub>2</sub>O recirculation bath to maintain isothermal behavior at 65 °C for this highly exothermic reaction. The reactor was wrapped with heating tape outside the jacket to heat the reactor to 200 °C when the catalyst was pretreated *in situ*. For the monometallic Pd/SiO<sub>2</sub> and the series of bimetallic Ag-Pd/SiO<sub>2</sub> and Au-Pd/SiO<sub>2</sub> catalysts prepared by ED, the reactor was loaded with 0.005 g of catalyst diluted by 0.030 g of the silica support (20/40 mesh) to form the catalyst bed that was supported on glass wool in the middle of the reactor. As for the monometallic Ag/SiO<sub>2</sub> and the series of bimetallic Pd-Ag/SiO<sub>2</sub> catalysts prepared by GD, 0.050 g of catalyst was used. A thermocouple was inserted into the catalyst bed to accurately monitor the reaction temperature and to ensure isothermal behavior. All

catalysts were pretreated *in situ* at 200 °C in flowing 10% H<sub>2</sub>/balance He for 2 h before being cooled to 65 °C for evaluation.

All gas flows were maintained by mass flow controllers. To roughly approximate the tail-end feed of an ethylene cracker, the reaction feed stream for catalyst screening consisted of 1% C<sub>2</sub>H<sub>2</sub>, 20% C<sub>2</sub>H<sub>4</sub>, 5% H<sub>2</sub>, balance He at a total flow rate of 50 SCCM corresponding to a GHSV value of  $6.0 \times 10^5 \text{ h}^{-1}$ . To ensure kinetic measurements were free from external mass transfer limitations, a standard loading (0.005 g) of the most active catalyst, 1.85 wt% Pd/SiO<sub>2</sub>, was evaluated over the flow range 50 – 250 SCCM, corresponding to GHSV values  $6.0 \times 10^5$  to  $3.0 \times 10^6 \text{ h}^{-1}$ . In all cases the turnover frequency (TOF) values for C<sub>2</sub>H<sub>2</sub> conversion varied between 4.2 and 4.6 s<sup>-1</sup> indicating no external mass transfer limitations over this flow range. Acetylene at 1% concentration was added from a pre-mixed cylinder of 10% C<sub>2</sub>H<sub>2</sub>/balance He by making the proper dilution. Both reaction feed and product streams were evaluated using an automated, on-line Hewlett-Packard 5890 Series II gas chromatograph using flame ionization detection. The feed and product analyses were typically made every 1.5 h. In addition to C<sub>2</sub>H<sub>2</sub>, C<sub>2</sub>H<sub>4</sub>, and C<sub>2</sub>H<sub>6</sub>, a number of C<sub>4</sub> hydrocarbons (n-butane, 1-butene, cis-2-butene, trans-2-butene, and 1,3-butadiene) were identified and quantitatively analyzed. These products can be considered as precursors to the “green oil” or C<sub>2</sub> oligomers commonly observed during industrial operation. All C<sub>4</sub> products were combined to give a total product and rates of formation that were normalized to C<sub>2</sub> feeds, *i.e.*, the molar quantities of C<sub>4</sub> products were multiplied by 2. All catalysts exhibited high, initial activities that underwent varying degrees of deactivation for the approximately first 20 h on line. Therefore, all the summary reaction data reported here were based on stable catalyst

performance after 20 h on line to eliminate transient behavior. Similar deactivation trends have been observed by others and have been attributed to carbon-based fouling due to C<sub>2</sub>H<sub>2</sub> oligomers on fresh catalyst surfaces.

Conversion of C<sub>2</sub>H<sub>2</sub> and selectivity of C<sub>2</sub>H<sub>2</sub> to C<sub>2</sub>H<sub>4</sub>, C<sub>2</sub>H<sub>6</sub> and C<sub>4</sub>s were also defined from the following relationships:

$$\text{Conversion of C}_2\text{H}_2 = \frac{\text{C}_2\text{H}_2 \text{ reacted}}{\text{C}_2\text{H}_2 \text{ (in)}} \quad (21)$$

$$\text{Selectivity of C}_2\text{H}_2 \text{ to C}_2\text{H}_4 = \frac{\text{C}_2\text{H}_2 \text{ reacted}}{\text{C}_2\text{H}_2 \text{ reacted} + \text{C}_2\text{H}_6 \text{ formed} + \text{C}_4\text{s formed} \times 2} \quad (22)$$

$$\text{Selectivity of C}_2\text{H}_2 \text{ to C}_2\text{H}_6 = \frac{\text{C}_2\text{H}_6 \text{ formed}}{\text{C}_2\text{H}_2 \text{ reacted} + \text{C}_2\text{H}_6 \text{ formed} + \text{C}_4\text{s formed} \times 2} \quad (23)$$

$$\text{Selectivity of C}_2\text{H}_2 \text{ to C}_4\text{s} = \frac{\text{C}_4\text{s formed} \times 2}{\text{C}_2\text{H}_2 \text{ reacted} + \text{C}_2\text{H}_6 \text{ formed} + \text{C}_4\text{s formed} \times 2} \quad (24)$$

$$\text{C}_2\text{H}_2 \text{ reacted} = \text{C}_2\text{H}_2 \text{ (in)} - \text{C}_2\text{H}_2 \text{ (out)} \quad (25)$$

$$\text{C}_2\text{H}_6 \text{ formed} = \text{C}_2\text{H}_6 \text{ (out)} - \text{C}_2\text{H}_6 \text{ (in)} \quad (26)$$

$$\begin{aligned} \text{C}_4\text{s formed} = & \text{n-C}_4\text{H}_{10} \text{ (out)} + \text{t-2-C}_4\text{H}_8 \text{ (out)} + \text{1-C}_4\text{H}_8 \text{ (out)} + \text{c-2-C}_4\text{H}_8 \text{ (out)} + \\ & \text{1,3-C}_4\text{H}_6 \text{ (out)} \end{aligned} \quad (27)$$

where (in) and (out) represent the feed stream and the product stream, respectively. This method of calculation cannot accurately be used for C<sub>2</sub>H<sub>4</sub> hydrogenation, since C<sub>2</sub>H<sub>4</sub> is a reaction product from selective C<sub>2</sub>H<sub>2</sub> hydrogenation, and is also present in great excess as a feed component, making gas chromatographic analysis inaccurate.

For the monometallic Pd/SiO<sub>2</sub> and the series of bimetallic Ag-Pd/SiO<sub>2</sub> and Au-Pd/SiO<sub>2</sub> catalysts prepared by ED, the kinetic measurements for acetylene hydrogenation

were studied using the same reactor system. In order to maintain differential conversion conditions, flow rates were varied between 50 and 200 SCCM and the reaction temperature was lowered from 65 to 50 °C. For determination of C<sub>2</sub>H<sub>2</sub> reaction orders, partial pressures were varied between 0.005 – 0.015 atm while holding P<sub>H<sub>2</sub></sub> constant at 0.05 atm, and for calculation of H<sub>2</sub> dependencies, partial pressures ranged between 0.02 – 0.10 atm and P<sub>C<sub>2</sub>H<sub>2</sub></sub> was kept constant at 0.01 atm. The activation energies at differential conversion conditions were determined between 40 to 80 °C using the standard feed composition of 1% C<sub>2</sub>H<sub>2</sub>, 20% C<sub>2</sub>H<sub>4</sub>, 5% H<sub>2</sub>, balance He.

## CHAPTER 3:

### SELECTIVE HYDROGENATION OF ACETYLENE IN EXCESS ETHYLENE USING AG- AND AU-PD/SiO<sub>2</sub> BIMETALLIC CATALYSTS PREPARED BY ELECTROLESS DEPOSITION

---

Reprinted with permission from [Y. Zhang, W. Diao, C. T. Williams, J. R. Monnier,  
Appl. Catal. A 469 (2014) 419-426].

DOI: 10.1016/j.apcata.2013.10.024

Copyright [2014] Elsevier

### 3.1 Abstract

Selective hydrogenation of acetylene in excess ethylene has been investigated for a series of Ag- and Au-Pd/SiO<sub>2</sub> bimetallic catalysts having incremental surface coverages of Ag and Au on the Pd surface. The catalysts were prepared by electroless deposition and characterized by atomic absorption spectroscopy and selective chemisorption. Both Ag- and Au-Pd/SiO<sub>2</sub> catalysts showed increased selectivity of acetylene conversion to form ethylene, rather than ethane, at high coverages. The catalyst performance results suggest that at high coverages of Ag or Au on Pd, that result in small ensembles of Pd sites, acetylene is adsorbed as a  $\pi$ -bonded species that favors hydrogenation to ethylene. At low coverages, where ensemble sizes of contiguous Pd surface sites are much larger, acetylene is strongly adsorbed as a multi- $\sigma$ -bonded species which preferentially forms ethane, lowering the selectivity to ethylene. Both kinetic analyses and the calculated turnover frequencies of acetylene conversion and ethane formation were consistent with the above explanation. The similar performance trends for Ag- and Au-Pd/SiO<sub>2</sub> suggest that the bimetallic effect for these catalysts is geometric and not electronic in nature.

### 3.2 Introduction

Ethylene is used as a starting point for many chemical intermediates in the petrochemical industry. The yearly demand for ethylene is over 150 million tons with an annual growth rate of 3.5% [5]. It is predominantly produced through steam cracking of higher hydrocarbons (ethane, propane, butane, naphtha, and gas oil). During the cracking process, a small amount of acetylene is produced as a side product. However, acetylene must be removed since it acts as a poison for ethylene polymerization catalysts at even

ppm concentrations ( $> 5$  ppm) [93]. Thus, the selective hydrogenation of acetylene to ethylene is an important process for the purification of ethylene. Conventional, low weight loading Pd catalysts are used for this selective reaction in high concentration ethylene streams. Selectivity of acetylene to ethylene is a key objective, since over hydrogenation of acetylene to ethane results in a decrease in yield and must be recycled back to the ethane cracking unit.

To understand the factors that influence the selectivity in acetylene hydrogenation, it is important to consider the adsorption modes of acetylene on the catalyst surface. Figure 3.1 shows identified adsorption modes of acetylene on a Pd surface, some in the presence of pre-adsorbed H [47,94-96]. Both associative and dissociative acetylene adsorption can occur. Margitfalvi et al. [97] showed that the adsorption mode of multi- $\sigma$  bonded ethylidyne can lead to the formation of ethane as it undergoes sequential hydrogenation steps: ethylidyne  $\rightarrow$  ethylidene  $\rightarrow$  ethyl  $\rightarrow$  ethane [96,97]. The formation of ethylidyne requires Pd ensembles that have three adjacent adsorption sites on the catalyst surface. Therefore, it is reasonable to assume the selectivity of acetylene hydrogenation can be controlled by changing the ensemble sizes of catalytic surface atoms to influence the forms of the adsorbed species on the catalyst surface. In more recent work, Neurock [98] has used a combination of Monte Carlo and DFT computations to study hydrogenation of acetylene and ethylene mixtures over Pd(111) and a Pd<sub>50%</sub>Ag<sub>50%</sub> structure on the Pd(111) surface and concluded that while strongly-adsorbed, three-fold ethylidyne species are adsorbed on Pd ensembles on the (111) surface, they are largely unreactive and lead to catalyst fouling. His calculations suggest that a three-fold, adsorbed vinyl species ( $C=CH_2$ ) is adsorbed on the Pd surface

which is reactive for the formation of both ethylene and some of the ethane. Addition of Ag to the Pd surface lowers the overall rate of hydrogenation but shifts product selectivity to ethylene. What is common between three-fold, adsorbed ethylidyne and adsorbed vinyl species is that large Pd ensembles favor strongly adsorbed, multi- $\sigma$ -intermediates that favor the formation of ethane.

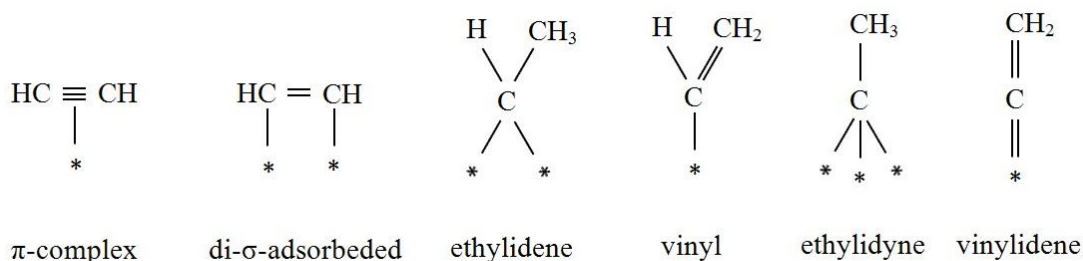


Figure 3.1 Adsorption modes of acetylene on Pd surface [47,94-96].

Thus, over the years, bimetallic Pd catalysts have been developed for the selective hydrogenation of acetylene. Various additives, such as Ag, Ni, Cu, Au, Pb, Tl, Cr and K, have been reported to improve the performance of Pd catalysts, especially in achieving high selectivity for ethylene production [16,19,99,100]. However, the bimetallic effects of the above additives are not yet well understood, possibly because the conventional methods of bimetallic catalyst preparation (co-impregnation and successive impregnation) result in both monometallic and bimetallic particles with varying compositions which make it difficult to determine the position of the two metallic components. The bimetallic interaction occurs only when the two metallic components form bimetallic surface compositions instead of separate particles. An alternative method to prepare bimetallic catalysts with controlled and proximal contact between the two metals is electroless deposition (ED), which can be applied to a wide range of metals. ED is an industrially feasible method which has been widely studied in our laboratory to

synthesize many different bimetallic catalyst compositions [31,32,34,35,39,101-103]. Since the ED process is kinetically controlled, the final composition of a particular bimetallic catalyst can be controlled to give rather precise combinations of the two metallic components.

In this paper, catalyst evaluation and kinetic data are presented for the selective hydrogenation of acetylene in excess ethylene over Ag-Pd/SiO<sub>2</sub> and Au-Pd/SiO<sub>2</sub> catalysts prepared by the ED method. The goals of this paper are not only to discuss the improvements in catalysts selectivity of acetylene to ethylene during acetylene hydrogenation, but also to illustrate the roles of Ag and Au additives on the adsorption modes of acetylene on Pd.

### 3.3. Results and discussion

A series of Ag-Pd/SiO<sub>2</sub> and Au-Pd/SiO<sub>2</sub> bimetallic catalysts were prepared with increasing coverage of Ag and Au on Pd. Table 3.1 shows a summary of the Ag-Pd/SiO<sub>2</sub> and Au-Pd/SiO<sub>2</sub> catalysts that were evaluated for the hydrogenation of acetylene. Even though catalysts with coverages of Ag and Au lower than those shown in Table 3.1 were prepared, they were not evaluated since there were no apparent reaction effects at the lower Group IB coverages. To achieve the highest coverages of Ag and Au on Pd, autocatalytic deposition of Ag on Ag and Au on Au also occurred, which is observed clearly in Figure 3.2. Transition from catalytic deposition to autocatalytic deposition occurs at approximately 0.4 monolayer of Ag or Au metal deposited on Pd. Below this level of deposition, catalytic deposition predominates. Above this point, both catalytic and autocatalytic depositions occur, so the actual coverage deviates substantially from the

theoretical coverage, where theoretical coverage in monolayers (ML) is defined as monodisperse coverage of Ag or Au on Pd surface sites, assuming 1:1 adsorption stoichiometry. In order to obtain the highest fractional coverages of Ag and Au on Pd, it was necessary to deposit considerably more than one theoretical monolayer amount of Ag and Au. Thus, complete coverage can still be attained after substantial autocatalytic deposition. In all cases, autocatalytic deposition increased as the concentration of the second metal increased on the surface of Pd, as expected for kinetically-controlled deposition processes. Since both Ag and Au were inactive for hydrogenation (2 wt% Ag/SiO<sub>2</sub> and 2 wt% Au/SiO<sub>2</sub> showed no activity for either C<sub>2</sub>H<sub>2</sub> or C<sub>2</sub>H<sub>4</sub> hydrogenation), the formation of multilayer aggregates on the Pd surface should have no significant effects on catalyst performance.

Table 3.1 Ag-Pd/SiO<sub>2</sub> and Au-Pd/SiO<sub>2</sub> bimetallic catalysts that were evaluated for acetylene hydrogenation. Base catalyst is 1.85 wt% Pd/SiO<sub>2</sub>. Theoretical coverage in monolayers (ML) represents monodisperse coverage of Ag or Au on Pd surface, assuming 1:1 adsorption stoichiometry.

Ag wt%	Ag mol%	Theoretical coverage (ML)	Actual coverage ( $\theta_{Ag}$ )	Au wt%	Au mol%	Theoretical coverage (ML)	Actual coverage ( $\theta_{Au}$ )
0.19	0.0018	1.16	0.44	0.28	0.0014	0.93	0.44
0.25	0.0023	1.52	0.53	0.58	0.0029	1.93	0.54
1.07	0.0099	6.52	0.73	2.19	0.0111	7.31	0.69
1.20	0.0111	7.31	0.83	3.50	0.0178	11.67	0.84
1.55	0.0144	9.44	0.85	4.40	0.0223	14.68	0.91
2.05	0.0190	12.49	0.91	5.01	0.0254	16.71	0.96
2.10	0.0195	12.79	0.99				

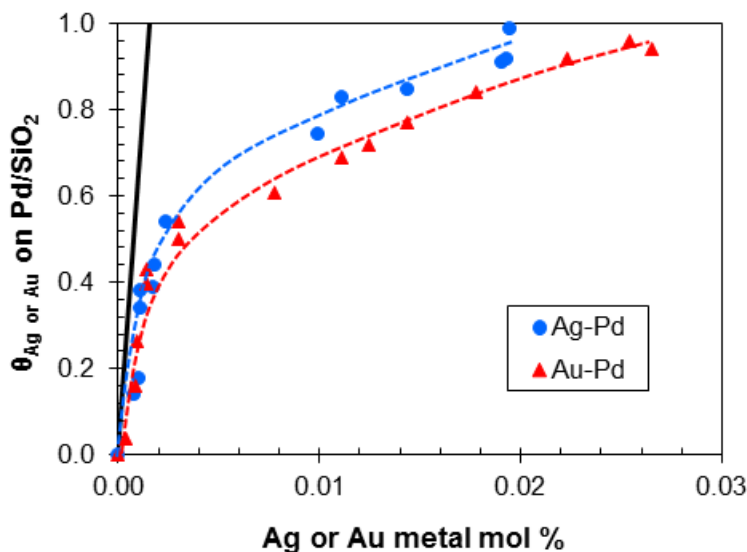


Figure 3.2 Actual coverage of Ag or Au on Pd/SiO<sub>2</sub> as a function of moles of Ag or Au deposited. Black line is the theoretical coverage of Ag or Au metal on Pd surface at a 1:1 deposition stoichiometry. Dashed lines show coverage based on chemisorption of Pd sites.

The Ag-Pd/SiO<sub>2</sub> and Au-Pd/SiO<sub>2</sub> catalysts that are listed in Table 3.1 were evaluated for selective hydrogenation of acetylene in the presence of ethylene; the results are summarized in Figures 3.3 and 3.4, respectively. Figure 3.3A shows conversion of acetylene and selectivity of hydrogenation of acetylene to form ethylene as a function of Ag coverage on Pd/SiO<sub>2</sub>. The base Pd/SiO<sub>2</sub> catalyst exhibited C<sub>2</sub>H<sub>2</sub> conversion of ~60%, which remained essentially constant over the range of  $\theta_{\text{Ag}}$  from 0 – 0.7. Similarly, over this same range, the selectivity to C<sub>2</sub>H<sub>4</sub> remained at approximately 50%. The conversion decreased sharply at  $\theta_{\text{Ag}} > 0.7$ , while the selectivity for C<sub>2</sub>H<sub>2</sub> conversion increased notably, rising to 90% at  $\theta_{\text{Ag}} > 0.9$ ; at these high Ag coverages, the remaining Pd ensembles are necessarily very small, changing the modes of acetylene adsorption. The results for the Au-Pd/SiO<sub>2</sub> series of catalysts in Figure 3.4 show similar behavior. Conversion and selectivity remain essentially constant up to Au coverages of 0.7. At higher Au coverages, the C<sub>2</sub>H<sub>2</sub> conversion decreases and the selectivity towards C<sub>2</sub>H<sub>2</sub>

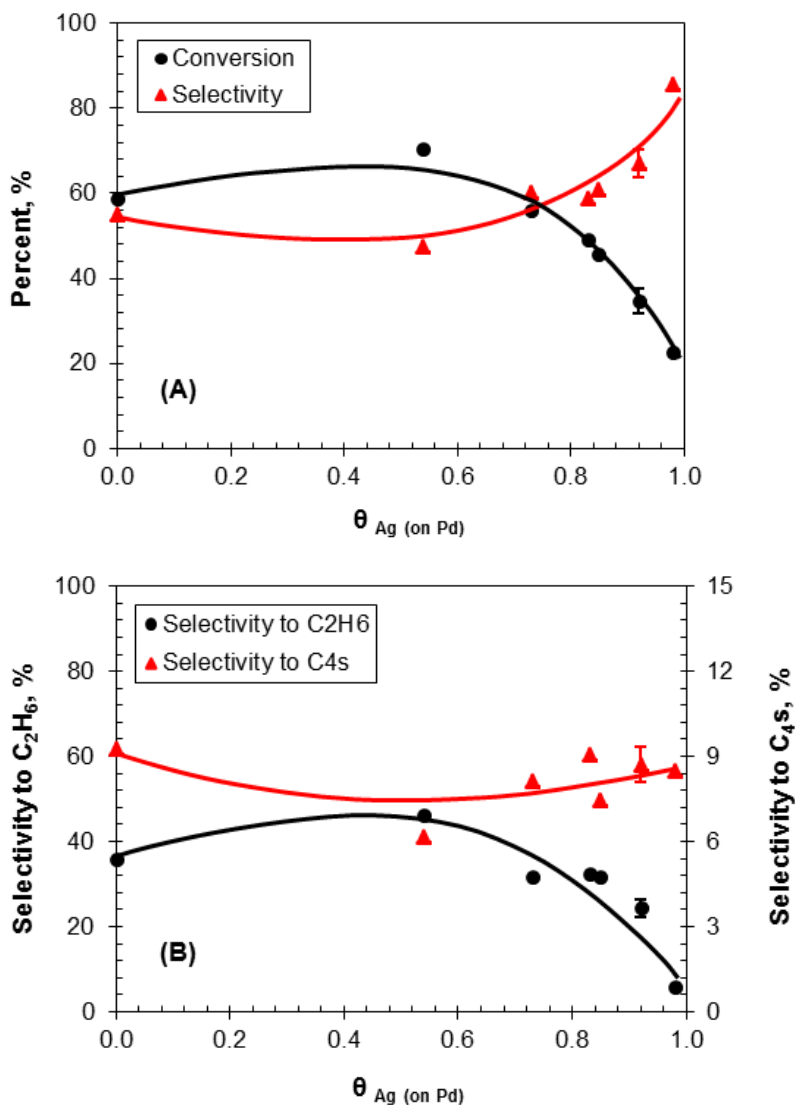


Figure 3.3 (A) Conversion of acetylene and selectivity of acetylene to ethylene and (B) selectivity of acetylene to ethane and C<sub>4</sub>s as a function of Ag coverage on Pd/SiO<sub>2</sub>. Reaction conditions: 65 °C and feed composition of 1% C<sub>2</sub>H<sub>2</sub>, 5% H<sub>2</sub>, 20% C<sub>2</sub>H<sub>4</sub>, and balance He at GHSV = 6.0 × 10<sup>5</sup>. Representative error bars for all data are shown for samples having  $\theta_{\text{Ag}} = 0.92$ .

conversion increases similarly to the Ag-Pd/SiO<sub>2</sub> series. Somewhat surprisingly, for both the Ag-Pd and Au-Pd series of catalysts the selectivities to C<sub>4</sub> products are relatively constant at 8 – 10% based on C<sub>2</sub>H<sub>2</sub> conversion. The C<sub>4</sub> products are derived from C<sub>2</sub>H<sub>2</sub>, and not C<sub>2</sub>H<sub>4</sub>, since no C<sub>4</sub> products were observed when C<sub>2</sub>H<sub>2</sub> was not present in the feed. The sites that give rise to C<sub>4</sub> formation do not appear to be affected by the presence of

either Ag or Au on the Pd surface, suggesting that ensemble effects are not responsible for oligomerization of  $C_2H_2$ . Others [47] have speculated that influences of the support may be a factor in the formation of  $C_4$  products, such as those that exist at the Pd-support interface. These sites would not be affected by the presence of either Au or Ag on the Pd surface.

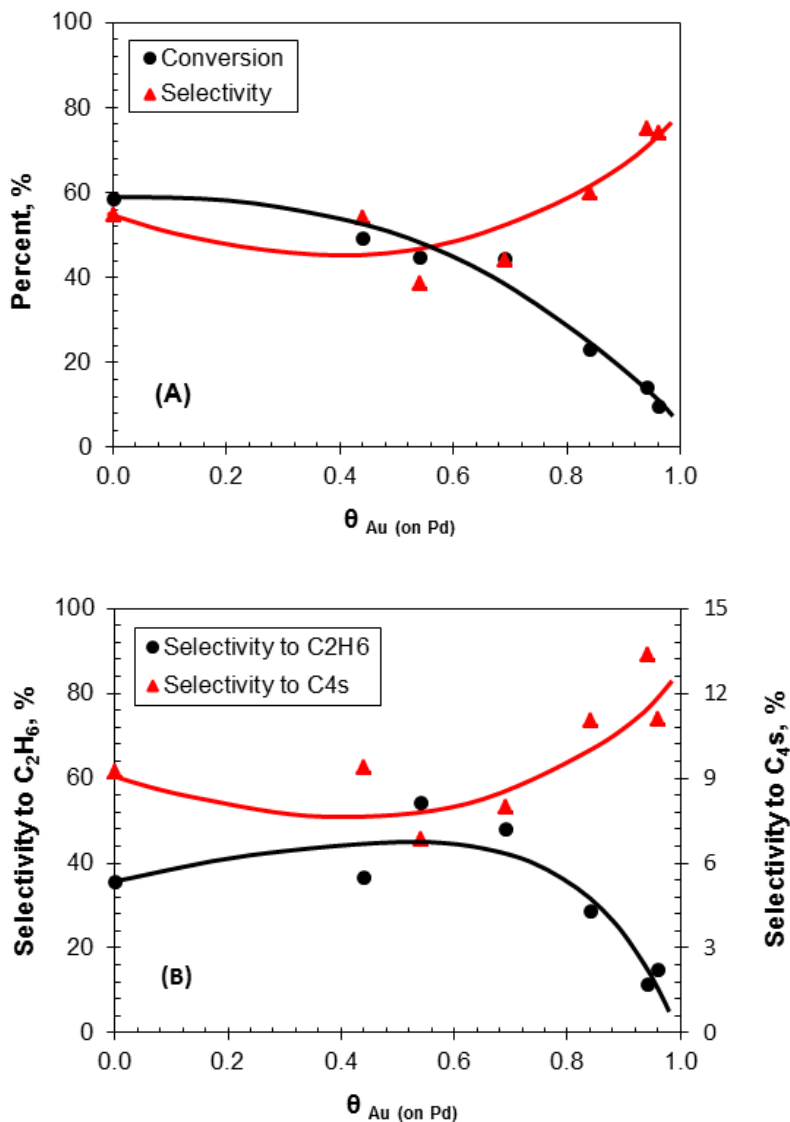


Figure 3.4 (A) Conversion of acetylene and selectivity of acetylene to ethylene and (B) selectivity of acetylene to ethane and C4s as a function of Au coverage on Pd/SiO<sub>2</sub>.

Somorjai [104] has reported that ethylidyne (Figure 3.1) was formed rapidly upon exposure of  $C_2H_4$  to a Pt(111) surface at  $\sim 300$  K; similarly, adsorption of  $C_2H_2$  in the presence of pre-adsorbed H also formed ethylidyne at 350 K. This mode of strong adsorption required a minimum of three contiguous Pt atoms, preferably on (111) surfaces according to Somorjai. Hydrogenation of such intermediates resulted primarily in the formation of ethane. Since Pd is similar to Pt in catalytic reactivity trends, adsorption of  $C_2H_2$  and  $C_2H_4$  on the Pd(111) surface should exhibit the same pattern as the adsorption of  $C_2H_2$  and  $C_2H_4$  on the Pt(111) surface. In fact, Medlin [105] has calculated that  $C_2H_2$  is preferentially adsorbed over the three-fold hollow sites on the (111) surfaces of Pt, Pd, and Rh, confirming similar adsorption modes for these metals. However, Medlin concluded that the adsorbed acetylene species reactive toward selective hydrogenation was not the highly coordinated species which was bound very strongly to the metal surface. Instead, the high-coordination sites likely become irreversibly blocked by strongly adsorbed acetylene leaving exposed only the low coordination sites for reversible  $C_2H_2$  adsorption and subsequent hydrogenation. The computational results of Neurock [98] likewise support the results of Medlin [105] and Somorjai [104] that adsorbed ethylidyne is catalytically inactive and/or non-selective to ethylene. Finally, Norskov [106,107] has also used computational methods and found that the heats of adsorption of acetylene and ethylene were the main factors that determined activity and selectivity for hydrogenation on Pd surfaces. Because acetylene and ethylene adsorption energies scaled with the carbon-surface bond energies, ethylene which adsorbed as a di- $\sigma$ -species was adsorbed at approximately  $\frac{1}{2}$  the strength of  $C_2H_2$  (tetra- $\sigma$ -species). To be both active for  $C_2H_2$  hydrogenation and selective for  $C_2H_4$  formation, a Pd catalyst must

have sites that bind acetylene strongly enough to undergo hydrogenation, but weakly enough to permit desorption as  $C_2H_4$ . This condition is best achieved, not on planar (111) surfaces, but on sites where multi- $\sigma$ -bonded species are not formed. Pd surfaces with subsurface carbon or partially covered with other metals such as Ag provided the proper balance of activity and selectivity.

Finally, Freund [108] has also studied the adsorption of ethylene and co-adsorption of ethylene and  $H_2$  on alumina-supported Pd catalysts and concluded that the strength of  $C_2H_4$  adsorption increased gradually with increasing particle size, which led to a redistribution of  $\pi$ -bonded and di- $\sigma$  bonded ethylene, the latter preferentially adsorbed on the large particles. Similarly, Li and Shen [109] investigated ethylene adsorption on Pd/SiO<sub>2</sub>, Pd-Ag(1:1)/SiO<sub>2</sub> and Pd-Ag(1:4)/SiO<sub>2</sub> catalysts at room temperature and found that tri- $\sigma$ -bonded ethylidyne, di- $\sigma$  bonded surface species, and a  $\pi$ -bonded species were formed on the Pd/SiO<sub>2</sub> catalyst and among the three adsorption modes ethylidyne was the predominant species. The  $\pi$ -bonded and di- $\sigma$  bonded species was formed on Pd-Ag(1:1)/SiO<sub>2</sub> while only  $\pi$ -bonded was found on Pd-Ag(1:4)/SiO<sub>2</sub>. Their work showed that with addition of Ag the principal mode of ethylene adsorption was altered from ethylidyne to a  $\pi$ -bonded species.

Because the coverage of Ag and Au on the Pd surface can be systematically changed by electroless deposition, it is possible to observe the transition for multi- $\sigma$  to  $\pi$ -adsorbed species. At low coverages of Ag on Pd, there is an abundance of contiguous Pd surface sites where the strongly adsorbed acetylene and ethylene are adsorbed as multi- $\sigma$ -adsorbed species. The formation of ethylidyne is favored when there are three adjacent adsorption sites on the catalyst surface, or if 1,1,2,2-tetra- $\sigma$ -adsorbed acetylene is the

preferred mode of adsorption, four adjacent Pd surface sites would be required. These species favor hydrogenation of acetylene to form ethane, rather than ethylene. In addition, the excess ethylene in the feed stream (at typical ethane cracking conditions) can also adsorb as ethylidene, or 1,2-di- $\sigma$ -ethylene and be hydrogenated to ethane. However, at high coverages of Ag most of the Pd surface is covered by Ag, leaving only small Pd ensembles, or even single atom sites of Pd on the surface. In this case, acetylene is more weakly adsorbed as a  $\pi$ -bonded species requiring potentially only a single Pd surface site, which favors formation of ethylene.

In earlier work from our group [103] FTIR of adsorbed CO on Pd surfaces as a function of Ag coverage was used to identify the positions of Ag deposition; Ag deposition was favored on the Pd (111) surface up to  $\sim \theta_{\text{Ag}} = 0.4$ ; FTIR peaks for three-fold adsorption of CO that is favored on (111) surfaces was strongly suppressed over this range of Ag coverage. Deposition of Ag from  $\sim \theta_{\text{Ag}} = 0.4$ – $0.75$  then occurred primarily on (1 0 0) sites as evidenced by decreasing peak intensities for two-fold adsorption of CO as Ag coverage increased. Only when Ag coverages were above  $\sim \theta_{\text{Ag}} = 0.8$  was Ag deposited on the corner and edge sites of Pd, where peak intensities of linearly-bound CO decreased with higher Ag coverages. Interestingly, for Au deposition on the same base Pd/SiO<sub>2</sub> catalyst, FTIR of CO indicated that Au was deposited in a rather non-discriminate manner on all surface facets and sites of the Pd surface [39]. However, since the Pd particles in this study were quite large (average particle diameter of 13.2 nm), the Pd surface was composed primarily of (1 1 1) facets with lesser amounts of (1 0 0) and even smaller amounts of coordinatively-unsaturated corner and edge sites [110]. Thus, even if Au deposition was random while Ag was directed primarily on (1 1 1) surfaces,

the positions of IB deposition would necessarily be the same to give similar behavior for C<sub>2</sub>H<sub>2</sub> hydrogenation. Thus, both Ag-Pd and Au-Pd catalysts should have similar IB coverage effects for selective C<sub>2</sub>H<sub>2</sub> hydrogenation. The existence of only linear CO adsorption at high Ag and Au coverages suggests that only isolated Pd sites or very small Pd ensembles were responsible for acetylene hydrogenation. Li and Shen [109] observed similar CO adsorption results on Pd/SiO<sub>2</sub>, Pd-Ag(1:1)/SiO<sub>2</sub> and Pd-Ag(1:4)/SiO<sub>2</sub>. Both bridged and linear adsorbed CO were seen on the Pd/SiO<sub>2</sub> catalyst, but on the surface of Pd-Ag/SiO<sub>2</sub> catalysts linearly adsorbed CO was the main species.

Because the concentration of Pd surface sites decreases with Ag and Au coverage, it is necessary to determine specific activities of these catalysts in terms of turn over frequency (TOF), or the activity per exposed Pd site. Figure 3.5 shows the TOF values for C<sub>2</sub>H<sub>2</sub> conversion and C<sub>2</sub>H<sub>6</sub> formation for the Ag-Pd and Au-Pd series of catalyst. The TOF for C<sub>2</sub>H<sub>2</sub> conversion and C<sub>2</sub>H<sub>6</sub> formation were calculated as follows:

$$\text{TOF of C}_2\text{H}_2 \text{ conversion} = \frac{\text{number of C}_2\text{H}_2 \text{ molecules reacted}}{\text{number of Pd surface sites} \times \text{time (s)}} \quad (28)$$

$$\text{TOF of C}_2\text{H}_6 \text{ formation} = \frac{\text{number of C}_2\text{H}_6 \text{ molecules formed}}{\text{number of Pd surface sites} \times \text{time (s)}} \quad (29)$$

where the number of Pd surface sites was determined from chemisorption results for each sample. The TOF values for C<sub>2</sub>H<sub>6</sub> formation were relatively constant between 0 and 0.9 Ag and Au coverages. Conversely, the TOF values for C<sub>2</sub>H<sub>2</sub> conversion increased markedly at high Group IB coverages, consistent with the assumptions proposed earlier for conversion and selectivity requirements. At low coverages, much of the acetylene is strongly adsorbed as multi-σ species, which requires more Pd surface sites than for π-bonded species at high coverage. Thus, one explanation for the lower TOF of C<sub>2</sub>H<sub>2</sub>

conversion at low Ag coverage is there are fewer adsorbed  $C_2H_2$  molecules per Pd surface site. Hydrogenation of these strongly bound ethynidyne species leads to the preferable formation of  $C_2H_6$  while hydrogenation of  $\pi$ -complex species favors the formation of ethylene.

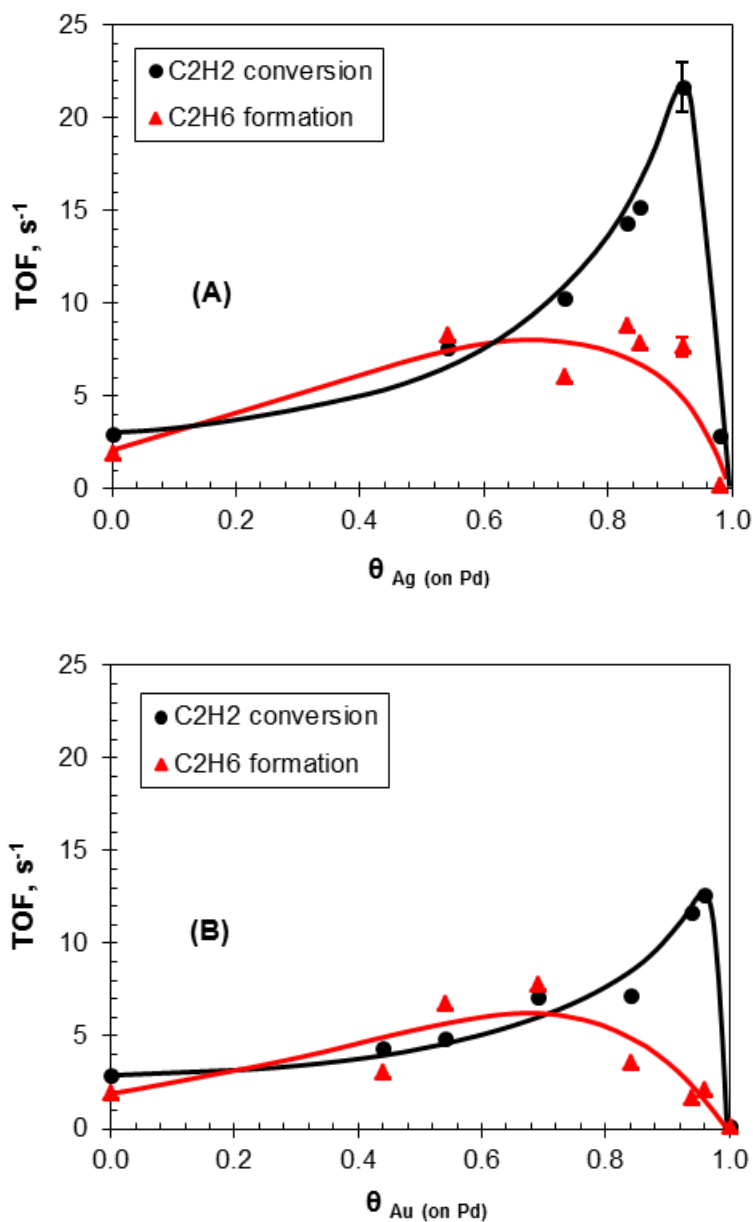


Figure 3.5 Effect of (A) Ag and (B) Au coverage on Pd for TOF of acetylene hydrogenation.

Further, Somorjai [111] has shown that during ethylene hydrogenation the relative hydrogenation rates of the species adsorbed on the Pt(111) surface are as follows:  $\pi$ -bonded ethylene  $\gg$  di- $\sigma$  bonded ethylene  $\gg$  ethynidyne and vinylidene. It would be expected that hydrogenation of ethynidyne also occurs more slowly than  $\pi$ -bonded acetylene on Pd(111) surfaces during acetylene hydrogenation. The shift to  $\pi$ -adsorbed  $C_2H_2$  also increases the rate of  $C_2H_4$  formation per Pd site and simultaneously decreases the rate of  $C_2H_6$  formation, giving the behavior seen in Figure 3.5.

The TOF values for acetylene conversion and  $C_2H_6$  formation for Au-Pd/SiO<sub>2</sub> are also quite similar to the corresponding values for Ag-Pd/SiO<sub>2</sub>. Although there are measurable differences in the TOF values, 22 and 12 s<sup>-1</sup> for Ag-Pd and Au-Pd, respectively, the difference is not significant enough to argue for different types of bimetallic effects. Rather, the similar performances for Ag-Pd and Au-Pd catalysts suggest the bimetallic effect for these two series catalysts is geometric and not electronic in nature, since the electronic properties of Ag and Au should be different enough to cause measurable differences in catalyst performance.

The kinetics of acetylene hydrogenation in excess ethylene over the monometallic Pd/SiO<sub>2</sub> and bimetallic Ag-Pd/SiO<sub>2</sub> catalysts were then investigated to verify the above hypotheses. The optimal Ag-Pd/SiO<sub>2</sub> catalyst with 0.92 coverage of Ag on Pd was used here for kinetic study. Figure 3.3A shows that the  $C_2H_2$  conversion was ~60% for 5 mg Pd/SiO<sub>2</sub> and ~35% for 5 mg Ag-Pd/SiO<sub>2</sub> with 0.92 Ag coverage at 65 °C and a total flow rate of 50 SCCM. In order to obtain differential conversion of  $C_2H_2$ , reaction temperature was lowered to 50 °C and flow rates were changed as needed between 50 and 200 SCCM.

The  $C_2H_2$  pressure dependencies for Pd/SiO<sub>2</sub> and Ag-Pd/SiO<sub>2</sub> are shown in Figure 3.6 at a reaction temperature of 50 °C and constant H<sub>2</sub> pressure of 0.05 atm (5%) over a  $C_2H_2$  pressure range from 0.005 (0.5%) to 0.015 atm (1.5%). The plots give good straight line fits with reaction orders of  $-0.67 \pm 0.06$  for Pd/SiO<sub>2</sub> and  $-0.20 \pm 0.04$  for Ag-Pd/SiO<sub>2</sub>. The  $-0.67$  reaction order for Pd/SiO<sub>2</sub> is in good agreement with the values of  $-0.55$  to  $-0.67$  observed by Bond [112] and  $-0.66$  by Tysoe [113]. Further, in the more recent work of Neurock [98] calculations gave  $C_2H_2$  reaction orders of  $-0.4$  and  $-0.21$  for Pd(111) and Ag-Pd(111), respectively, showing less kinetic inhibition by  $C_2H_2$  on the Ag-modified Pd(111) surface. The negative  $C_2H_2$  pressure dependencies for both Pd/SiO<sub>2</sub> and Ag-Pd/SiO<sub>2</sub> catalysts confirm that the  $C_2H_2$  is strongly adsorbed on the Pd surface. The more negative reaction order for Pd/SiO<sub>2</sub> than Ag-Pd/SiO<sub>2</sub> implies that  $C_2H_2$  is more strongly

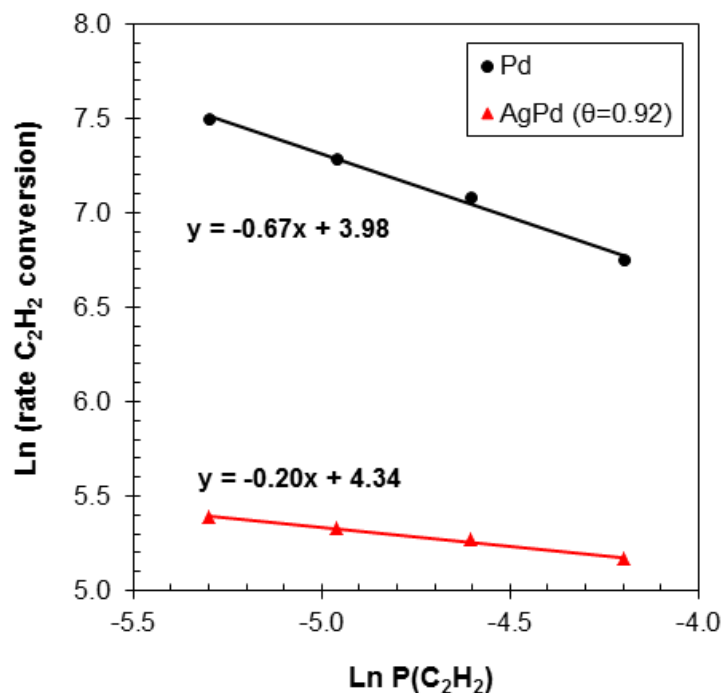


Figure 3.6 The  $C_2H_2$  pressure dependencies for Pd/SiO<sub>2</sub> and Ag-Pd/SiO<sub>2</sub> ( $\theta_{Ag} = 0.92$ ) at 50 °C and H<sub>2</sub> pressure of 0.05 atm.

adsorbed on the former catalyst, consistent with the earlier hypothesis that  $C_2H_2$  is more strongly adsorbed as ethynidyne at low coverage and weakly adsorbed as a  $\pi$ -bonded species at higher coverages of Ag.

The  $H_2$  pressure dependences for these two catalysts were measured at 50 °C and constant  $C_2H_2$  pressure of 0.01 atm (1%) over a  $H_2$  pressure range from 0.02 (2.0%) to 0.10 (10%) atm. The plots shown in Figure 3.7 also give good fits for reaction orders of  $1.17 \pm 0.11$  for Pd/SiO<sub>2</sub> and  $1.18 \pm 0.10$  for Ag-Pd/SiO<sub>2</sub>, which are also in agreement with the values 1.0 – 1.4 measured by Bond [112] and 1.04 by Tysoe [113]. Neurock's [98] results also showed first order dependencies in  $H_2$  pressure for both Pd(111) and Ag-Pd(111) surfaces. The clear first order  $H_2$  pressure dependences suggest that hydrogen is weakly adsorbed on the Pd surface of both catalysts relative to the hydrocarbon species.

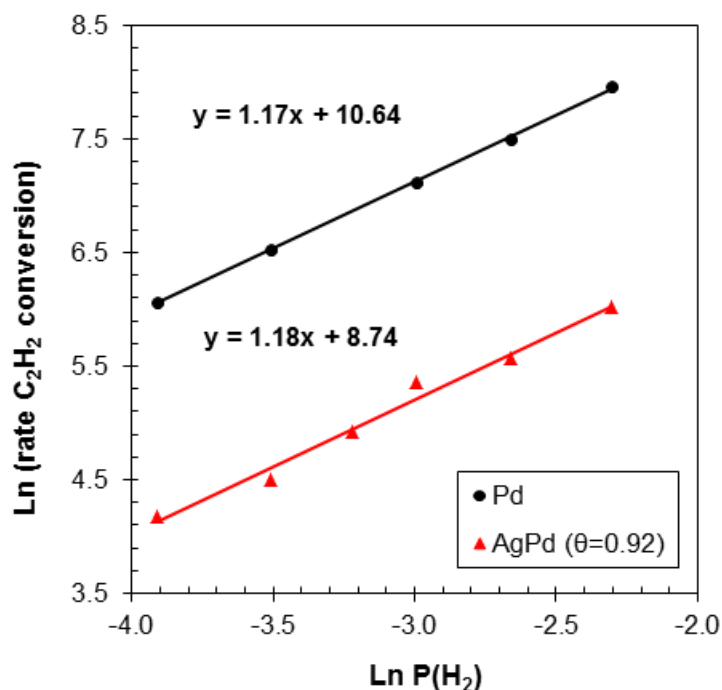


Figure 3.7 The  $H_2$  pressure dependences for Pd/SiO<sub>2</sub> and Ag-Pd/SiO<sub>2</sub> ( $\theta_{Ag} = 0.92$ ) at 50 °C and  $C_2H_2$  pressure of 0.01 atm.

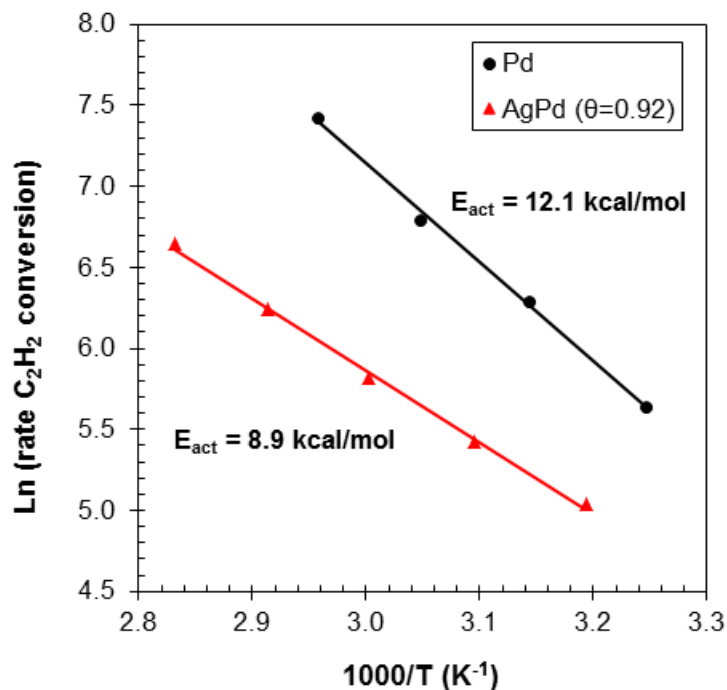


Figure 3.8 Arrhenius plots for the temperature dependencies of C<sub>2</sub>H<sub>2</sub> conversion for (A) Pd/SiO<sub>2</sub> and (B) Ag-Pd/SiO<sub>2</sub> ( $\theta_{\text{Ag}} = 0.92$ ) at C<sub>2</sub>H<sub>2</sub> pressure of 0.01 atm and H<sub>2</sub> pressure of 0.05 atm.

The temperature dependencies for acetylene conversion using these two catalysts were measured by changing the temperature from 40 °C to 80 °C at C<sub>2</sub>H<sub>2</sub> and H<sub>2</sub> partial pressures of 0.01 and 0.05 atm, respectively. The apparent activation energy for Pd/SiO<sub>2</sub> shown in Figure 3.8 is  $12.1 \pm 0.8$  kcal/mol in good agreement with 11.0 kcal/mol by Bond [112] and 10.6 kcal/mol by Inoue et al. [114]. The activation energy for Ag-Pd/SiO<sub>2</sub> is substantially lower at  $8.9 \pm 0.6$  kcal/mol, which is consistent with less strongly adsorbed C<sub>2</sub>H<sub>2</sub> for Ag-Pd/SiO<sub>2</sub> at the generally accepted rate determining step of the surface reaction between adsorbed C<sub>2</sub>H<sub>2</sub> and H [98]. Again both activation energy values agree quite well with the trend seen by Neurock [98], specifically, 7.7 – 10.5 kcal/mol for Pd(111) and 6.2 – 7.4 kcal/mol for Ag-Pd(111). The combination of lower activation energy and less negative reaction order in C<sub>2</sub>H<sub>2</sub> pressure explains why the TOF values for

optimum compositions of Ag-Pd are much higher than for Pd catalysts. The reaction rates for C<sub>2</sub>H<sub>2</sub> conversion over Pd/SiO<sub>2</sub> and Ag-Pd/SiO<sub>2</sub> can be stated as follows, where R has the standard value of 1.986 cal/ °K-mol:

For Pd/SiO<sub>2</sub>,

$$\text{rate} = k_1 e^{-\frac{12100 \pm 800}{RT}} [p(\text{C}_2\text{H}_2)]^{-0.67 \pm 0.06} [p(\text{H}_2)]^{1.17 \pm 0.11}$$

For Ag-Pd/SiO<sub>2</sub> ( $\theta_{\text{Ag on Pd}} = 0.92$ ),

$$\text{rate} = k_2 e^{-\frac{8900 \pm 600}{RT}} [p(\text{C}_2\text{H}_2)]^{-0.20 \pm 0.04} [p(\text{H}_2)]^{1.18 \pm 0.10}$$

### 3.4 Conclusions

Electroless deposition has been shown to be a very good method for preparation of Ag-Pd/SiO<sub>2</sub> and Au-Pd/SiO<sub>2</sub> bimetallic catalysts with selective and controlled coverages of Ag and Au on Pd. The resulting families of catalysts make it more straightforward to draw correlations between catalyst performance and bimetallic surface compositions. Selectivity of acetylene to ethylene and TOF for acetylene conversion are enhanced at high coverages of Ag or Au on Pd, implying that the transition of adsorption mode of acetylene on Pd surface from strongly adsorbed ethylidyne on large Pd ensembles to weakly adsorbed  $\pi$ -bonded species on small Pd ensembles, is responsible for selective conversion of acetylene to ethylene. This explanation of adsorption mode is further confirmed by the kinetics of acetylene hydrogenation. The presence of optimal coverages of either Ag or Au on Pd lower the reaction order in C<sub>2</sub>H<sub>2</sub> from -0.67 to -0.20 for Pd and Ag-Pd, respectively. Both catalysts exhibit first order kinetics for H<sub>2</sub> pressures, indicating the surface is near fully covered by adsorbed C<sub>2</sub>H<sub>2</sub>. Likewise, the apparent activation energies for C<sub>2</sub>H<sub>2</sub> conversion decrease from 12.1 kcal/mol to 8.9

kcal/mol at high coverages of Ag on Pd. The combination of lower activation energy and less negative reaction order in  $C_2H_2$  pressure explains why the TOF values for optimum compositions of Ag-Pd are much higher than for Pd catalysts. The similar performance trends for Ag- and Au-Pd/SiO<sub>2</sub> indicate that the bimetallic effect for these catalysts is likely geometric and not electronic in nature.

## CHAPTER 4:

### PD-AG/SiO<sub>2</sub> BIMETALLIC CATALYSTS PREPARED BY GALVANIC DISPLACEMENT FOR SELECTIVE HYDROGENATION OF ACETYLENE IN EXCESS ETHYLENE

---

Reproduced from reference [Y. Zhang, W. Diao, J. R. Monnier, C. T. Williams, *Catal. Sci. Technol.* 5 (2015) 4123-4132] with permission from Royal Society of Chemistry.

[DOI: 10.1039/C5CY00353A](https://doi.org/10.1039/C5CY00353A)

#### 4.1 Abstract

A series of bimetallic Pd-Ag/SiO<sub>2</sub> catalysts were prepared by galvanic displacement with increasing loadings of Pd on Ag. The catalysts were characterized by atomic absorption spectroscopy, Fourier-transform infrared spectroscopy of CO adsorption and X-ray photoelectron spectroscopy. An actual Pd deposition beyond the theoretical limit for galvanic displacement suggested that the large difference in surface free energy for Pd and Ag resulted in Pd diffusion into the bulk of Ag particles, or Ag diffusion to the surface to provide fresh Ag atoms for further galvanic displacement. Characterization results indicated that on this series of catalysts the Pd atoms are distributed in very small ensembles or possibly even atomically on the Ag surface, and there was a transfer of electrons from Pd to Ag at all Pd loadings. For comparison, the catalysts were also evaluated for the selective hydrogenation of acetylene in excess ethylene at the conditions used in our previous study of the reverse Ag-Pd/SiO<sub>2</sub> catalysts. The selectivities for C<sub>2</sub>H<sub>4</sub> formation remained high and constant due to the geometric effects that Pd atom existed as small ensembles. However, the electronic effects resulted in lower selectivities for C<sub>2</sub>H<sub>4</sub> formation than those from the catalysts with high coverage of Ag on Pd.

#### 4.2 Introduction

It has long been recognized that Pd provides superior performance on both activity and selectivity for the hydrogenation of acetylene to ethylene [8,44]. However, at high acetylene conversion the formation of ethane, C<sub>4</sub> and C<sub>6</sub> hydrocarbons is accelerated, which leads to the formation of carbonaceous residues that decrease the

catalyst lifetime. To increase the selectivity to ethylene, Pd-based catalysts are usually modified with promoters, such as Ag, Ni, Cu, and K etc [16,19,99,100]. However, the bimetallic effects of the above additives are still not well understood, probably due to the conventional catalyst preparation methods that result in both monometallic and bimetallic particles with varying compositions. In our previous work [42], we used electroless deposition (ED) [31,32,34,102,103] to prepare a series of Ag- and Au-Pd/SiO<sub>2</sub> bimetallic catalysts with selective and controlled coverages of Ag and Au on Pd. The similar performance trends of enhanced selectivity of acetylene to ethylene at high coverages for Ag- and Au-Pd/SiO<sub>2</sub> suggested that the bimetallic effect for these catalysts was geometric and not electronic in nature. That is, at high coverages with smaller ensembles of Pd sites, acetylene is weakly adsorbed as a  $\pi$ -bonded species, which favors the hydrogenation to ethylene. On the other hand, acetylene is bonded in a multi- $\sigma$  mode on larger ensembles of Pd and desorbs only as fully hydrogenated C<sub>2</sub>H<sub>6</sub>. Therefore, inspired by these previous results, the primary goal of this work was to prepare a series of reverse bimetallic catalysts (*i.e.* where Pd is deposited onto the Ag surface) in order to further explore the nature of bimetallic effects for the selective hydrogenation of acetylene.

For the synthesis of Pd-Ag bimetallic catalysts, galvanic displacement (GD) of Ag<sup>0</sup> by Pd<sup>2+</sup> salts has been chosen. GD occurs when a base material is displaced by a metallic ion in solution that has a higher reduction potential than the displaced metal ion [28-30]. The base material is dissolved into the solution while the metallic ions in the solution are reduced on the surface of the base material. This method is different from ED, in that GD does not require chemical reducing agents since the base metal itself already serves as the reducing agent. However, this redox reaction is usually limited by

the accessibility of the base metal, resulting in passivation of the reaction when the entire surface of the base metal is covered [28].

Over the past decade, GD has been widely used for the development of metal nanostructures with highly active surfaces for a variety of applications such as electrocatalysts [30,115-121], biomedicine [29], functional coatings [85,122], and deposition of metals on semiconductors [28,123]. Xia *et al.*[29,86-88] have thoroughly studied the mechanism of GD for tuning the properties of metal nanostructures through adjustment of composition, size, shape and morphology. Complex hollow nanostructures of Pd-Ir, Au-Ag, Pd-Ag, and Pt-Ag have been generated with potential for many applications. Yan *et al.* [30,119-121] also developed electrocatalysts with Pd-Au, Pt-Cu, Pt-Pd nanotubes or nanowires prepared by GD for the oxygen reduction and methanol oxidation reactions. Lee *et al.* [116-118] have investigated the performance of different forms of hollow and porous Pd-Ag or Pt-Ag nanomaterials prepared by GD as electrocatalysts for the oxygen reduction reaction. Maboudian and Carraro [28,85,122,123] have used GD to coat Au, Pt, Ag and Cu onto Si in thin film or nanoparticle forms for surface-enhanced Raman spectroscopy, and for improved interfacial behavior of semiconductors.

Although GD has been widely used in synthesizing electrocatalysts, it has had little application for the development of catalysts used in hydrogenation reactions. Sykes *et al.* [124] investigated the partial hydrogenation of phenylacetylene using PdCu alloy nanoparticles prepared by GD, which showed improvement in activity and selectivity compared to the corresponding monometallic catalysts. Li *et al.* [125] demonstrated that Pd/Co-B catalysts prepared by GD were extremely active and more selective than

monometallic Pd and a Co-B amorphous alloy for liquid-phase hydrogenation of 2-ethyl-2-hexenaldehyde to 2-ethyl-1-hexanol. Zhou *et al.* [126] used modified GD to prepare hollow Pt-Ni alloy nanospheres for liquid phase hydrogenation of p-chloronitrobenzene to p-chloroaniline. Such materials showed much higher activity, enhanced selectivity, and better durability than solid Pt nanoparticles.

In the present case, to be comparable with our previous work [42], SiO<sub>2</sub>-supported Ag has been chosen as the base material for the preparation of various levels of Pd deposited by GD. From examination of standard reduction potentials, it is thermodynamically favorable for Pd<sup>2+</sup> reduction to occur and to deposit on the Ag surface while Ag<sup>0</sup> is oxidized to Ag<sup>+</sup> (Pd<sup>2+</sup> + 2e<sup>-</sup> = Pd<sup>0</sup>, E<sup>o</sup> = 0.915V; Ag<sup>+</sup> + e<sup>-</sup> = Ag<sup>0</sup>, E<sup>o</sup> = 0.799V). These bimetallic compositions have been characterized by Fourier-transform infrared (FTIR) spectroscopy of CO adsorption and X-ray photoelectron spectroscopy (XPS); catalysts have also been evaluated for the selective hydrogenation of acetylene in excess ethylene at the conditions used in our previous publication<sup>7</sup>. The results indicate that GD of Pd readily occurs but that catalyst surfaces are enriched in Ag due to diffusion of the Pd and/or the Ag components. Selectivity of acetylene hydrogenation is increased when small ensembles of Pd are located on the Ag surface.

#### 4.3 Results and discussion

Silver dispersion and surface sites were measured for the base 2 wt% Ag/SiO<sub>2</sub> material prepared by incipient wetness. From chemisorption using H<sub>2</sub> titration of O-precovered Ag sites at 170 °C (H<sub>2</sub> titration uptake curves shown in Figure 4.1 in Supplementary Information), the average Ag dispersion was 4.9%, which corresponds to

an average Ag particle size of 23.8 nm and  $5.52 \times 10^{18}$  Ag surface sites per gram of catalyst, assuming spherical particle shape. This concentration of Ag surface sites was then used to calculate the theoretical coverage of Pd on Ag during GD. For further characterization, powder X-ray diffraction (XRD) on 2 wt% Ag/SiO<sub>2</sub> was performed and the profile was shown in Figure 4.2 in Supplementary Information. The Ag particle size obtained from refinement of the XRD pattern was 19.6 nm, which is in good agreement with the chemisorption result.

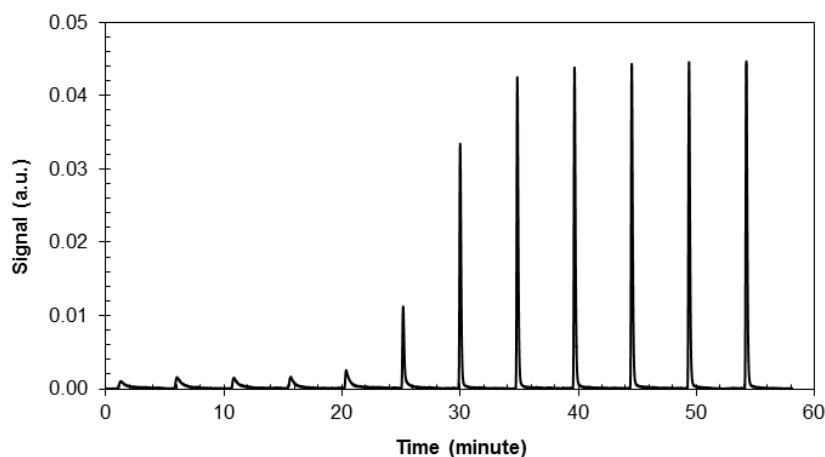


Figure 4.1 Uptake curves for H<sub>2</sub> titration of O-precovered Ag sites at 170 °C for 2 wt% Ag/SiO<sub>2</sub>.

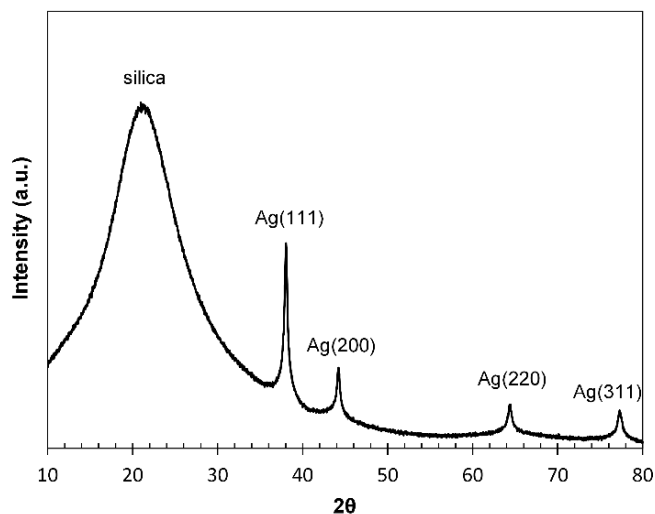


Figure 4.2 XRD pattern of 2 wt% Ag/SiO<sub>2</sub>.

The formation of true bimetallic Pd-Ag/SiO<sub>2</sub> catalysts prepared by GD requires that the Pd<sup>2+</sup> cations should only react with Ag sites and not be adsorbed on the silica support. To prevent the unwanted strong electrostatic adsorption of Pd<sup>2+</sup> cations onto silica, the pH of the galvanic displacement bath should be maintained below the point of zero charge (PZC) of the support where the SiO<sub>2</sub> surface is positively charged and cannot adsorb cations [62,70]. The PZC of the silica support used in this study was ~ pH 3.5, so the pH of the bath was maintained at 2.0 ± 0.1. The blank experiment with a bath of Pd<sup>2+</sup> and silica support at pH 2 was conducted, and there was no observed physisorption of Pd<sup>2+</sup> on the silica support under this condition. On the other hand, at this condition it is thermodynamically favorable for Pd<sup>2+</sup> reduction to occur by oxidation of Ag<sup>0</sup> to Ag<sup>+</sup>. However, when the reaction was conducted in the pH 2 solution containing HNO<sub>3</sub>, it was found that Ag<sup>0</sup> metal might be not only displaced by Pd<sup>2+</sup> but also be oxidized by HNO<sub>3</sub>. Thus, the dissolution of Ag metal from 2 wt% Ag/SiO<sub>2</sub> in pH 2 HNO<sub>3</sub> solution was investigated prior to the GD experiments. From Figure 4.3, it can be seen that the amount of Ag dissolution increased asymptotically with time to approximately 20 μmoles/g cat, or approximately 10% of the total Ag content dissolved within 1 h. The limiting value of 20 μmoles/g cat also suggests that only some of the Ag is susceptible to dissolution, such as those Ag atoms existing at corners and edges of 23.8 nm Ag particles. Therefore, to determine the concentration of displaced Ag<sup>+</sup> from 2 wt% Ag/SiO<sub>2</sub> due to GD, the amount of Ag<sup>+</sup> from HNO<sub>3</sub>-facilitated Ag dissolution was subtracted from the total solution concentration of Ag<sup>+</sup>. The remaining amount of Ag<sup>+</sup> was labeled as “corrected Ag<sup>+</sup>” in figures and tables.

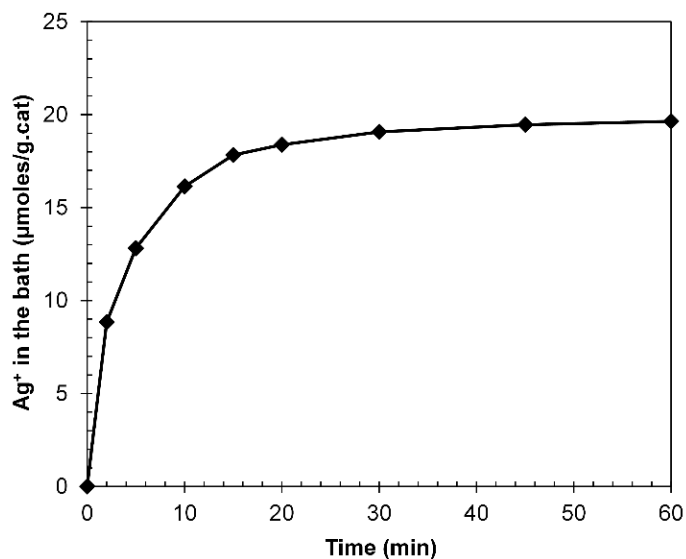


Figure 4.3 Ag dissolution from 2 wt% Ag/SiO<sub>2</sub> in pH 2 HNO<sub>3</sub> solution at room temperature.

A series of bimetallic Pd-Ag/SiO<sub>2</sub> catalysts were prepared with increasing loadings of Pd on Ag. The time-dependent metal displacement profiles are illustrated in Figure 4.4. Both the concentrations of deposited Pd<sup>2+</sup> and corrected displaced Ag<sup>+</sup> were monitored during the experiments. For rigorous GD, the ratio of deposited Pd<sup>2+</sup>/displaced Ag<sup>+</sup> is 1:2 for the reaction  $\text{Pd}^{2+} + 2\text{Ag}^0 \rightarrow \text{Pd}^0 + 2\text{Ag}^+$ . The Pd coverage should then be limited to 0.5 monolayers on Ag, since two Ag surface atoms are required for each Pd<sup>2+</sup> deposited. However, the 0.03, 0.09, 0.28, and 0.32 wt% Pd-Ag samples shown in Figure 4.4A correspond to 0.3, 0.9, 2.9, and 3.3 theoretical monolayers coverage on Ag, when Ag dissolution is not taken into account. The analyzed compositions of the catalysts are summarized in Table 4.1 and indicate that for the higher Pd loadings substantial loss of Ag has occurred, primarily by galvanic displacement (dissolution of Ag<sup>+</sup> in the acidic solution is less important for the higher Pd loadings). For the samples designated as 0.39 and 0.44 wt% Pd, the molar ratios of [Ag]/[Pd] are only about 2.5, corresponding to a

bulk empirical formula of  $\text{Ag}_{0.7}\text{Pd}_{0.3}$ . Thus, extensive mixing of Ag and Pd in the bimetallic particles has occurred.

The increased Pd deposition beyond the theoretical limit for GD indicates one of two possibilities. First, there were perhaps defects on the Ag surface that permitted access of  $\text{Pd}^{2+}$  to more Ag metal sites in the sub-surface region. Alternatively, there was

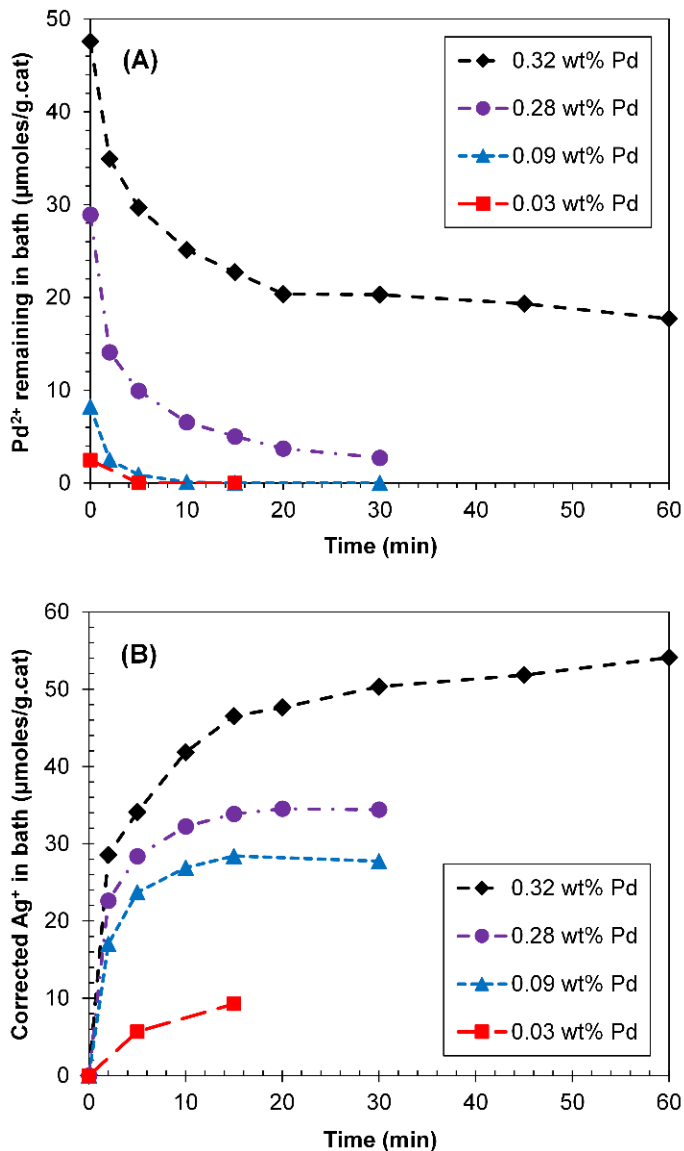


Figure 4.4 Time-dependent galvanic displacement profiles of (A) deposited  $\text{Pd}^{2+}$  from bath solution and (B) galvanically displaced  $\text{Ag}^+$  from 2 wt%  $\text{Ag}/\text{SiO}_2$  at room temperature with different initial  $\text{Pd}^{2+}$  concentrations.

Table 4.1 Composition of Pd-Ag catalysts after galvanic displacement experiments. Actual catalyst compositions based on analyzed Ag and Pd loadings, not predictive stoichiometries.

Catalyst Designation	Initial Ag loading (%)	Final Ag loading after dissolution and GD (%)	Ag loss based on AA analysis (%)	Actual metal composition of catalyst	Molar ratio of Ag to Pd
2 wt% Ag/SiO <sub>2</sub>	2.0	—	—	2 wt% Ag	—
0.03 wt% Pd	2.0	1.71	14.5	0.03 wt% Pd - 1.71 wt% Ag	56.2
0.09 wt% Pd	2.0	1.50	25.0	0.09 wt% Pd - 1.50 wt% Ag	16.4
0.28 wt% Pd	2.0	1.42	29.0	0.28 wt% Pd - 1.43 wt% Ag	5.0
0.32 wt% Pd	2.0	1.21	39.5	0.32 wt% Pd - 1.21 wt% Ag	3.7
0.39 wt% Pd	2.0	1.01	49.5	0.39 wt% Pd - 1.01 wt% Ag	2.6
0.44 wt% Pd	2.0	1.02	49.0	0.44 wt% Pd - 1.02 wt% Ag	2.3

diffusion of Pd into the bulk of Ag particles, or more likely, migration of Ag to the surface. Indeed, the surface free energy of Ag metal is lower than that of Pd metal based on calculated and experimental results from others [127-130]. Mezey [129] reported surface free energies (SFE) of 2043 and 1302 ergs/cm<sup>2</sup> for Pd and Ag metallic surfaces at 298 K, respectively, indicating that it is thermodynamically preferred for Ag to diffuse to the surface of a Ag-Pd bimetallic particle. Tang [130] has also calculated the SFE values of specific Ag facets and estimated the free energies of the two most common facets of Ag particles, the (111) and (100) surfaces, are 881 and 948 ergs/cm<sup>2</sup>, further showing the thermodynamic favorability for Ag diffusion to the surface of Pd-Ag bimetallic particles. In support of the first possibility, Xia *et al.* [131] reported that when Na<sub>2</sub>PdCl<sub>4</sub> was added to a suspension of Ag nanocubes, etch pits developed on the surfaces of the nanocubes,

primarily at the corners. Oxidation within the etch pits removed Ag (as  $\text{Ag}^+$ ) from the interior rather than the surface of the nanocubes to simultaneously reduce Pd on the exterior of the Ag nanocubes. Although the supported Ag particles in this study likely exist as spherical particles, there are still corners and edges that might provide etch pits for access to the interior of the Ag particles. However, the more likely explanation is that the large difference in SFE values for Ag and Pd result in Ag diffusion to the surface to provide fresh Ag atoms for galvanic displacement with  $\text{Pd}^{2+}$ .

It can be seen in Figure 4.4A that the displacement reaction is initially first order in  $\text{Pd}^{2+}$ , but as the Ag surface becomes depleted the rate of displacement decreases. Explicit plots of first order reaction for  $\text{Pd}^{2+}$  disappearance vs. time for 0.09 – 0.32 wt% Pd-Ag samples are shown in Figure 4.5 in Supplementary Information. A straight line correlation for  $\ln [\text{Pd}^{2+}]$  disappearance vs. time confirms that the displacement reaction is initially first order in  $\text{Pd}^{2+}$ . Figure 4.4B shows, as mentioned earlier, the concentration of corrected  $\text{Ag}^+$ , which is the actual amount of the galvanically-displaced  $\text{Ag}^+$ . The decrease in  $\text{Pd}^{2+}$  and increase in corrected  $\text{Ag}^+$  in the solution confirm that GD does occur. For the 0.32 wt% Pd-Ag sample the reaction was conducted with a much higher initial concentration of  $\text{Pd}^{2+}$  in an attempt to achieve more deposition. However,  $\text{Pd}^{2+}$  deposition ceased after around 30 min, leaving more than 20  $\mu\text{moles Pd}^{2+}/\text{g cat}$  in solution to give a similar amount of deposition as the 0.28 wt% Pd-Ag sample, indicating that galvanic displacement has reached an upper limit and is not kinetically dependent on the concentration of  $\text{Pd}^{2+}$  remaining in solution. To determine whether higher temperatures increased displacement, bath temperatures of 50 and 75  $^{\circ}\text{C}$  were examined and the corresponding kinetic curves of deposited  $\text{Pd}^{2+}$  and displaced  $\text{Ag}^+$  are shown in

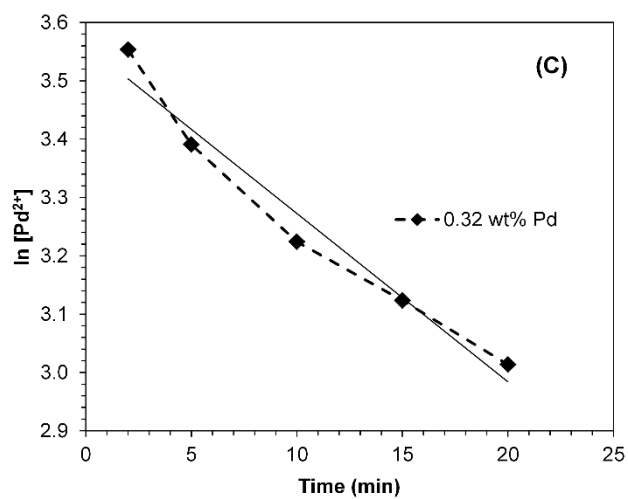
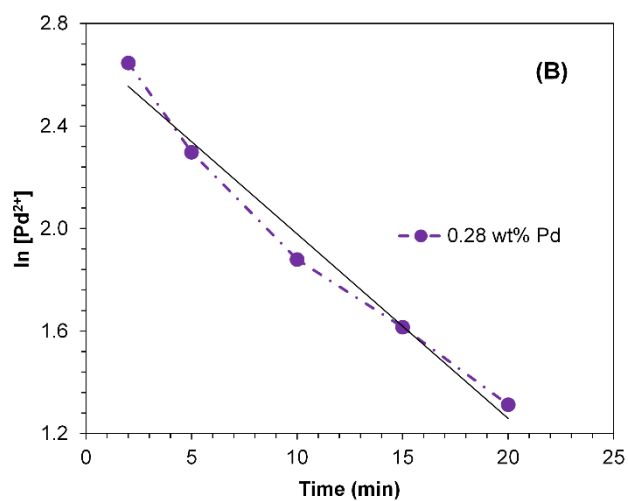
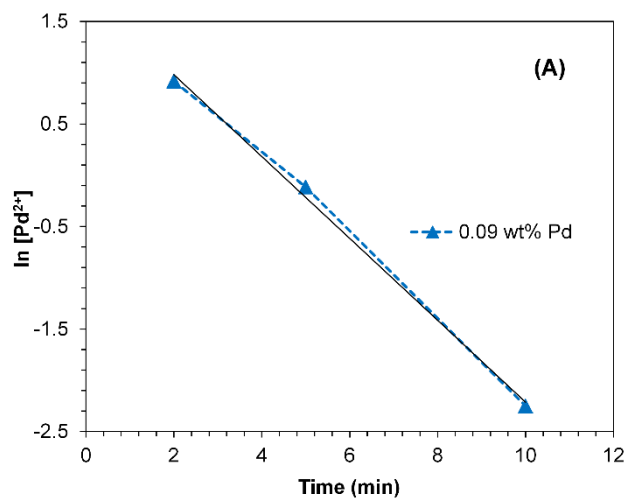


Figure 4.5 First order plots for Pd<sup>2+</sup> disappearance vs. time for (A) 0.09, (B) 0.28, (C) 0.32 wt% Pd on Ag/SiO<sub>2</sub>. A straight line correlation confirms first order dependency.

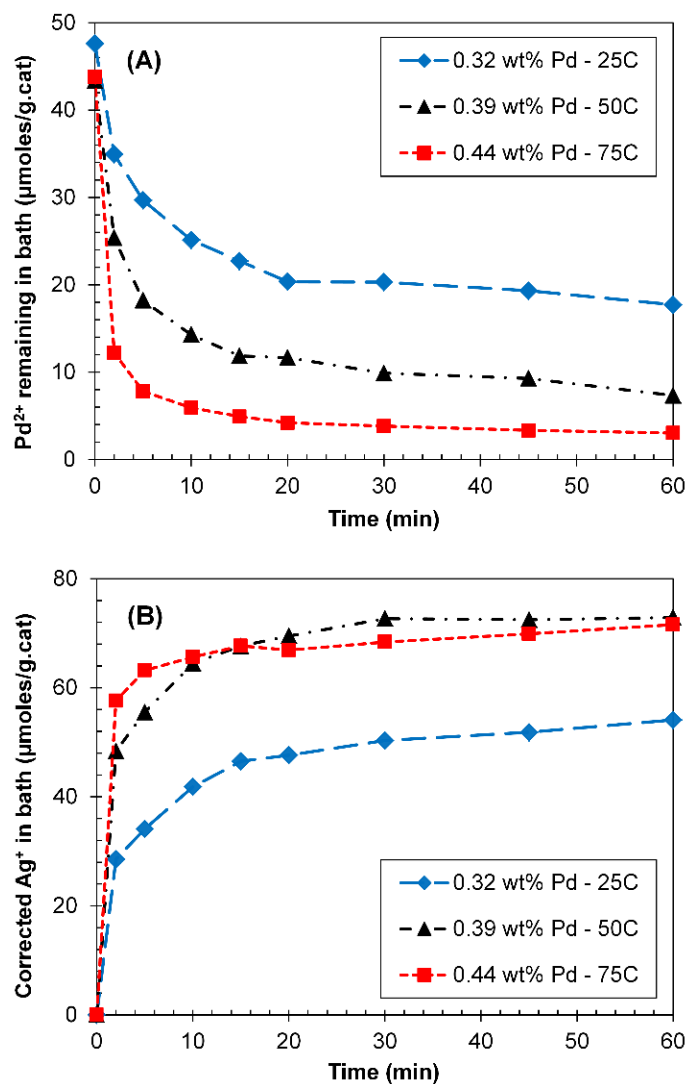


Figure 4.6 Time-dependent galvanic displacement profiles of (A) deposited Pd<sup>2+</sup> from bath solution and (B) galvanically displaced Ag<sup>+</sup> from 2 wt% Ag/SiO<sub>2</sub> at 25, 50 and 75 °C with same initial Pd<sup>2+</sup> concentration.

Figure 4.6A and Figure 4.6B, respectively. The results shows that galvanic displacement increased at higher temperatures, suggesting that activated diffusion of Ag to the surface occurred during GD, again due to differences in the surface free energies of Ag and Pd.

To determine the concentrations of surface Pd on Ag, the standard H<sub>2</sub>-O<sub>2</sub> titration at 40 °C used for Pd metal [31,42] was conducted for all samples. For the highest Pd weight loading sample (0.44 wt% Pd-Ag),  $2.49 \times 10^{19}$  Pd atoms/g cat were deposited on

the Ag surface. However, there was no significant H<sub>2</sub> uptake for this sample as well as for all other samples, suggesting that the surface was highly enriched with Ag. This is inconsistent with the observation that during the preparation of samples with high Pd weight loadings, the GD reaction stopped suggesting there were no exposed Ag atoms. Such contradictory results might be caused by the pretreatment step during the chemisorption. The 2 h reduction at 200 °C for Pd-Ag samples may cause Ag atoms with lower surface energy to move from the bulk to the surface or possibly drive Pd atoms with higher surface energy into the subsurface of Ag. The effects are the same; Ag becomes enriched at the surface of the bimetallic particle. The Pd-Ag system is a well-known binary alloy [132] and such migration of Pd into the bulk and/or Ag moving to the surface may result in the formation of a Pd-Ag alloy near the catalyst surface.

To explore further the distribution of Pd atoms on the Ag surface, FTIR spectroscopy of CO adsorption at room temperature was conducted on the *in situ* reduced, monometallic Ag/SiO<sub>2</sub> and bimetallic Pd-Ag/SiO<sub>2</sub> catalysts. Representative spectra for the different Pd loadings are shown in Figure 4.7. There were no CO vibrations observed for Ag/SiO<sub>2</sub> sample, which is in agreement with the observations of Rodriguez *et al.* [133] that Ag<sup>0</sup> is inactive for CO adsorption. The FTIR spectra of the CO adsorption on the commercial 1.85 wt% Pd/SiO<sub>2</sub> catalyst was previously published by our group [103]. For Pd-Ag/SiO<sub>2</sub> samples, a single CO stretching band was observed in the 2000-2100 cm<sup>-1</sup> region with the peak centered at approximately 2046 cm<sup>-1</sup>, which was attributed to linearly adsorbed CO on fully reduced Pd sites [103,134,135]. However, bridge-bond CO between 1800-2000 cm<sup>-1</sup> was not observed. This result indicates that some surface Pd is present and that the Pd atoms are distributed in very small ensembles,

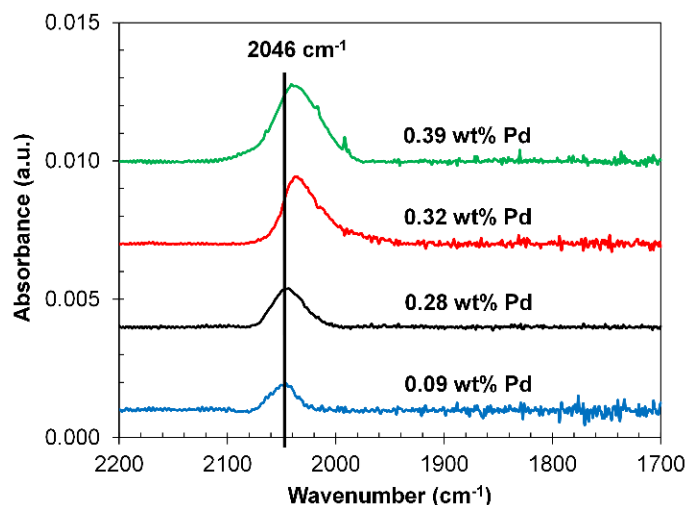


Figure 4.7 FTIR spectra for CO adsorption on various Pd-Ag/SiO<sub>2</sub> bimetallic catalysts.

possibly even atomically, on the Ag surface. The scarcity of Pd sites may also indicate that the 200 °C reduction treatment contributes to a Ag-rich surface, either by diffusion of Pd to into the bulk or migration of the Ag to the surface, to leave only a scattered distribution of Pd atoms on the surface. However, the much lower value of SFE for Ag suggests that subsurface Ag atoms migrate to the surface, covering the Pd atoms to give a Ag-enriched bimetallic surface. The peak intensity increases gradually with increasing Pd weight loadings, indicating that the bulk particles become more saturated with Pd atoms at higher weight loadings and that more Pd atoms remain exposed on the surface. It is also possible that exposure to CO for the FTIR experiments may cause Pd atoms to migrate to the surface of the catalyst due to the high heat of adsorption for CO on Pd [136]; however, the Pd-catalyzed activity of these compositions for C<sub>2</sub>H<sub>2</sub> hydrogenation (later point in this manuscript) suggest the surface Pd sites were initially present, but too low for accurate chemisorption.

In addition to changes in peak intensity, shifts in vibrational band positions were observed with addition of Pd to Ag. Typically, CO coverages increase with more Pd on

the surface, which results in greater CO dipole-dipole interactions and an accompanying shift to higher frequencies [134]. Conversely, in the present case (Figure 4.7) peaks for CO adsorption shift to lower frequencies as the Pd weight loadings increased. This is consistent with what was observed in a previous study from our group [134] for Ag-Pd/SiO<sub>2</sub> prepared by ED of Ag on Pd. In that case, the CO adsorption peaks shifted to higher frequencies as the deposited Ag diluted the Pd surface into smaller ensembles. It was proposed that the frequency shift was related to an electronic effect between Pd and Ag. XPS analyses showed the Ag 3d<sub>5/2</sub> binding energy (BE) was shifted to lower values when deposited on Pd; as the surface coverage of Ag on Pd increased, the BE shift decreased from 0.7 to 0.1. The BE shifts decreased with coverage because the higher surface coverages of Ag resulted in autocatalytic deposition to form three dimensional aggregates of Ag that were more similar to bulk Ag metal particles. The BE shift was maximized at the lowest level of deposition since the Ag was essentially distributed in a monodisperse manner on the Pd surface to give the maximum e<sup>-</sup> transfer from Pd to Ag. The direction of the CO stretching frequency shift suggested that the decrease of the electron density of surface Pd atoms lowered the back donation from non-bonding electrons of Pd to the π\* orbitals of CO. This electronic interaction appeared to outweigh any shift to lower frequencies due to lower dipole-dipole interactions.

In the present study, e<sup>-</sup> transfer from Pd to Ag should be maximized for the lowest levels of galvanically-exchanged Pd since the number of Pd-Ag interactions (e<sup>-</sup> transfer from Pd to Ag) is highest at these conditions. For the 0.09 wt% Pd sample, the empirical formula of the bimetallic particles corresponds to Ag<sub>0.94</sub>Pd<sub>0.06</sub> to give a very dilute Pd composition, which should exhibit the greatest extent of Pd-Ag interaction. This results in

less electron donation from non-bonding electrons of Pd to the  $\pi^*$  orbitals of CO to give a higher C-O bond order and an upshifted C-O stretching frequency.

To examine the surface/near-surface of the Pd-Ag samples, XPS measurements were performed with detailed scans of the Pd 3d and Ag 3d orbitals, and the binding energies were compared with the values obtained from the monometallic (reference) catalysts. The Si 2p peak of the support was used as an internal standard to confirm the peak positions, and all peak intensities for Pd 3d and Ag 3d were normalized to Si 2p peak intensity for comparison. Results shown in Figure 4.8A confirm there was Pd at least in the near surface (escape depth of photoelectrons is several lattice layers) of the catalysts prepared by galvanic displacement. The Pd and Ag peak intensities in Figure 4.8A and Figure 4.8B also indicate, as expected, that near surface Pd concentrations increase and Ag concentrations decrease when more Pd metal is galvanically-exchanged.

The assignment of Ag oxidation state by XPS is a matter of controversy. A large discrepancy and superposition of binding energy values of Ag 3d exists in the literatures [2,137-142]: Ag 3d<sub>5/2</sub> is reported to be from 366.4 to 369.2 eV for Ag<sup>0</sup>; from 367.5 to 368.8 eV for Ag<sub>2</sub>O; and from 367.4 to 368.4 eV for AgO. Therefore, some studies [137-139] report a negative shift for oxidized Ag <sup>$\delta^+$</sup>  versus Ag<sup>0</sup>, while others [2,140-142] observe a positive shift instead. Because of the uncertainty of Ag 3d binding energies of supported Ag catalysts, presumably due to the charging effects of the insulating silica support and possible Ag particle size effects, comparisons of Ag binding energies are valid only within a given study for similar Ag morphologies and particle size. To confirm the Ag 3d<sub>5/2</sub> binding energies for Ag<sup>0</sup> and Ag<sup>+</sup> (or Ag <sup>$\delta^+$</sup> ) species in this study, the XPS spectra for 2 wt% Ag/SiO<sub>2</sub> shown in Figure 4.9 were taken after *in situ* reduction in

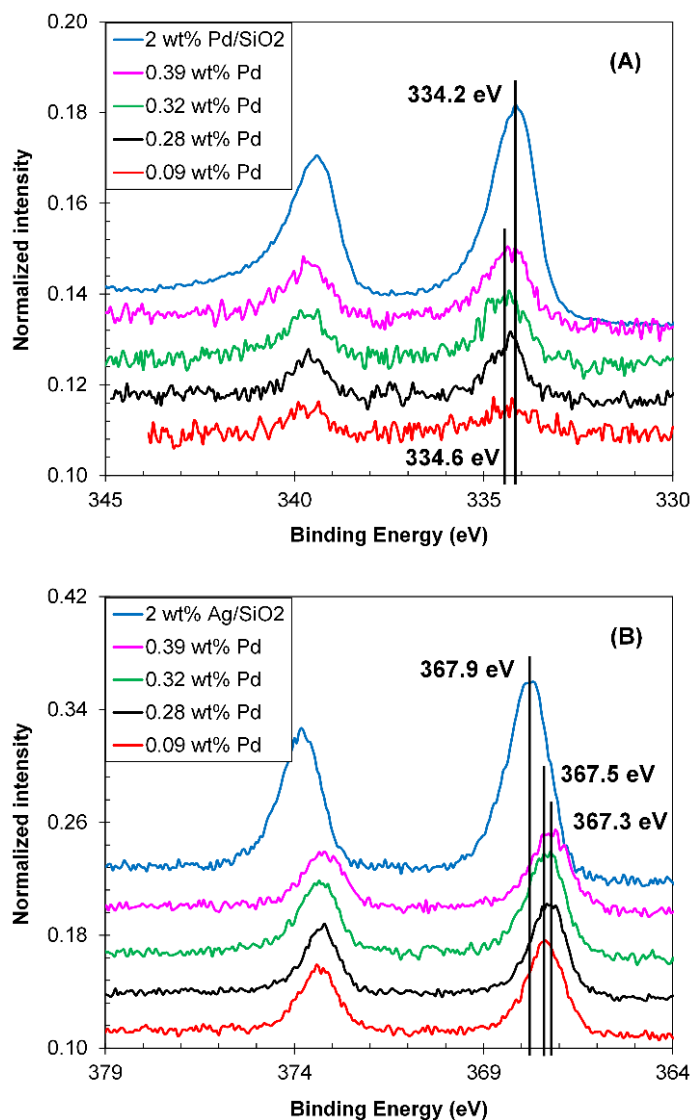


Figure 4.8 XPS spectra of (A) Pd 3d on 2 wt% Pd/SiO<sub>2</sub> and Pd-Ag/SiO<sub>2</sub> and (B) Ag 3d on 2 wt% Ag/SiO<sub>2</sub> and Pd-Ag/SiO<sub>2</sub>. All samples were reduced *in situ* at 200 °C in 100% H<sub>2</sub> for 2 h.

100% H<sub>2</sub> at 200 °C for 2 h and after *in situ* calcination in 100% O<sub>2</sub> at 200 °C for 2 h. The Ag 3d<sub>5/2</sub> values are 367.9 eV after reduction (red) and 368.7 eV after calcination (blue), corresponding to Ag<sup>0</sup> and Ag<sup>+</sup> respectively. Thus, the shift to higher Ag 3d<sub>5/2</sub> binding energy value in this study indicates electron transfer away from Ag. The similar trend on 12 wt% Ag/Al<sub>2</sub>O<sub>3</sub> sample was observed in a previous study from our group [2]. Besides, the XPS spectrum was also taken for the fresh prepared 2 wt% Ag/SiO<sub>2</sub> sample (black)

that was *ex situ* calcined and reduced before being loaded into XPS. It shows that the base Ag/SiO<sub>2</sub> was well reduced before the preparation of Pd-Ag/SiO<sub>2</sub> bimetallic catalysts. However, because of the complexity and controversy of binding energy shift for Ag systems, other reasonable explanations [140-142] for a positive shift due to factors other than an oxidation state change in Ag cannot be ruled out. For all bimetallic compositions in this study, shifts to higher binding energies were observed for the Pd 3d<sub>3/2</sub> and Pd 3d<sub>5/2</sub> peaks in comparison to 2 wt% Pd/SiO<sub>2</sub> catalyst. Conversely, the Ag 3d<sub>3/2</sub> and Ag 3d<sub>5/2</sub> peaks were shifted to lower binding energies compared to a 2 wt% Ag/SiO<sub>2</sub> catalyst. These shifts of Pd 3d and Ag 3d peaks indicate a net electron transfer from Pd to Ag, which is also consistent with previous work from our group<sup>12</sup> for Ag-Pd/SiO<sub>2</sub> catalysts prepared by ED of Ag on Pd.

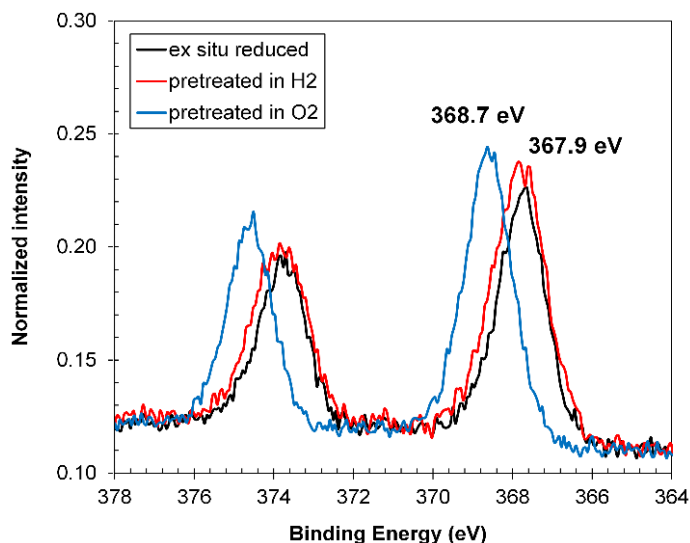


Figure 4.9 Ag 3d spectra of 2 wt% Ag/SiO<sub>2</sub> for (1) *ex situ* pretreatment in air at 300 °C for 2 h and in 10% H<sub>2</sub>/He at 300 °C for 2 h, (2) *in situ* pretreatment in 100% H<sub>2</sub> at 200 °C for 2 h, and (3) *in situ* pretreatment in 100% O<sub>2</sub> at 200 °C for 2 h.

As more Pd is deposited onto Ag, the binding energy shift to lower values for Ag in Figure 4.8B increases from 0.4 eV for 0.09 wt% Pd to 0.6 eV for 0.39 wt% Pd since there are more Pd atoms to interact with neighboring Ag atoms. Because Ag is the

majority component in these bimetallic particles, the magnitude of the BE shift is somewhat dampened by those Ag atoms that do not interact with Pd atoms. Higher Pd loadings increase the number of Pd-Ag interactions. The upshift in Pd 3d<sub>5/2</sub> BE values is approximately 0.4 eV for all Pd loadings since all Pd atoms are interactive with neighboring Ag atoms. The observed binding energy shifts for the Pd-Ag bimetallic catalysts as a function of Pd weight loading are consistent with the red shift of the CO-Pd vibrational band observed by FTIR spectroscopy and lend further credence to the supposition that there was a transfer of electrons from Pd to Ag.

Selective hydrogenation of acetylene in the presence of excess ethylene was carried out for the different compositions of Pd-Ag/SiO<sub>2</sub> catalysts at the same reaction conditions used for the Ag-Pd/SiO<sub>2</sub> bimetallic catalysts reported in our previous work<sup>7</sup>. The exception was that increased weights of catalysts were required to account for the lower number of accessible Pd sites with these catalysts.

Figure 4.10A shows conversion of acetylene and selectivity of acetylene hydrogenation towards ethylene as a function of Pd weight loading on Ag/SiO<sub>2</sub>. No data are shown for 0.09 wt% Pd-Ag/SiO<sub>2</sub> because activity was too low for accurate measurement. The base Ag/SiO<sub>2</sub> catalyst exhibited no reactivity for acetylene hydrogenation during a control experiment. The C<sub>2</sub>H<sub>2</sub> conversion increased from 2.0% to 17.5% with increasing Pd weight loadings, consistent with the FTIR results that showed more Pd on the Ag surface for higher levels of Pd deposited by GD. Selectivities for C<sub>2</sub>H<sub>4</sub> formation remained essentially constant at approximately 80% for the different Pd loadings; likewise, the selectivities for C<sub>2</sub>H<sub>6</sub> and C<sub>4</sub> hydrocarbons were also relatively constant for the different Pd loadings (Figure 4.10B). This indicates that the ensemble

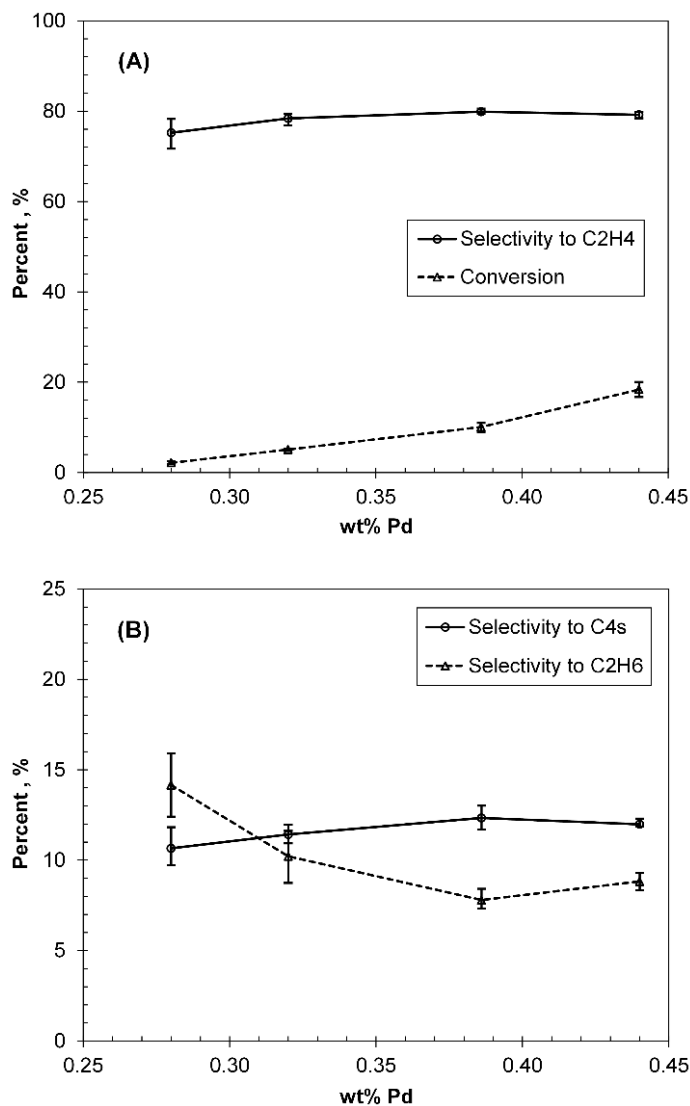


Figure 4.10 (A) Conversion of acetylene and selectivity of acetylene to ethylene and (B) selectivity of acetylene to ethane and C<sub>4</sub>s as a function of Pd weight loadings on Ag/SiO<sub>2</sub>. Reaction conditions: 65 °C and feed composition of 1% C<sub>2</sub>H<sub>2</sub>, 5% H<sub>2</sub>, 20% C<sub>2</sub>H<sub>4</sub>, and balance He at GHSV = 6.0 × 10<sup>5</sup> h<sup>-1</sup>. Error bars represent maximum and minimum values for each data point; data point is average value.

sizes and electronic charges of Pd sites were similar over this composition range, since changes in Pd ensemble sizes and/or changes in electronic charges of the Pd surface sites would be expected to change the selectivity for C<sub>2</sub>H<sub>4</sub> formation [98]. Atomic, or near atomic dispersion of surface Pd sites should favor  $\pi$ -bonded C<sub>2</sub>H<sub>2</sub> which favors C<sub>2</sub>H<sub>4</sub> formation [42]. Since FTIR and XPS analyses indicated that the Pd ensemble sizes and

electronic Pd 3d states were constant over this range of Pd weight loadings, catalyst selectivities should also remain the same.

In our previous work for the electroless deposition of Ag and Au on Pd catalysts, C<sub>2</sub>H<sub>2</sub> conversions decreased with increasing Group IB coverage (fewer surface Pd atoms were exposed) [42]. However, selectivity of C<sub>2</sub>H<sub>2</sub> to C<sub>2</sub>H<sub>4</sub> was enhanced at higher Ag and Au coverages, particularly for fractional coverages high than 0.80. The similar performance trends for both Ag-Pd and Au-Pd catalysts suggested the bimetallic effect was primarily geometric and not electronic in nature. That is, at high Group IB coverages with smaller ensembles of contiguous Pd sites, acetylene was weakly adsorbed as a  $\pi$ -bonded species, which favored the hydrogenation to ethylene which readily desorbed. On the other hand, acetylene was bonded in a multi- $\sigma$  mode on larger ensembles of Pd and desorbed only when fully hydrogenated to C<sub>2</sub>H<sub>6</sub>. However, the selectivity values for C<sub>2</sub>H<sub>4</sub> formation at high coverages of Ag and Au for the Ag-Pd and Au-Pd catalysts were as high as 86 – 90%, which is noticeably greater than 80% for this family of catalysts. Recent computational studies by Neurock [98] and Nørskov [106] for acetylene hydrogenation on Ag(111), Pd(111), Pd<sub>0.75</sub>Ag<sub>0.25</sub>/Pd(111), and Pd<sub>0.50</sub>Ag<sub>0.50</sub>/Pd(111) have shown that while the geometric effects of Pd surface dilution into small Pd ensembles by Ag are more important than electronic effects of Ag on Pd atoms, there are still observable electronic effects. Any electronic effect that lowers the adsorption energy of C<sub>2</sub>H<sub>2</sub> will increase selectivity of hydrogenation to form C<sub>2</sub>H<sub>4</sub>. Our XPS and FTIR data show e<sup>-</sup> transfer from Pd to Ag, leaving the Pd surface sites somewhat e<sup>-</sup> deficient. This results in stronger interaction between Pd and the e<sup>-</sup> rich  $\pi$ -bond system of C<sub>2</sub>H<sub>2</sub> to give higher adsorption energies of  $\pi$ -bonded C<sub>2</sub>H<sub>2</sub>. This higher adsorption energy increases the

extent of hydrogenation of  $C_2H_2$  to  $C_2H_6$  before desorption can occur. This is more pronounced in our current study because Pd is the minority component and more susceptible for  $e^-$  transfer to Ag; Table 4.1 confirms the minority compositions of the different bimetallic catalysts. In our earlier study [42] where Ag was confined to only the surface, Pd was by far the majority component with more limited Pd-Ag electronic interactions; hence the somewhat higher selectivities for  $C_2H_2$  hydrogenation to  $C_2H_4$ .

#### 4.4 Conclusions

A series of bimetallic Pd-Ag/SiO<sub>2</sub> catalysts were prepared by galvanic displacement with increasing loadings of Pd on Ag. The actually increased Pd deposition beyond the theoretical limit for galvanic displacement indicated that the large difference in surface free energy for Pd and Ag resulted in Pd diffusion into the bulk of Ag particles, or Ag diffusion to the surface to provide fresh Ag atoms for further galvanic displacement. Such migration led to the formation of a Pd-Ag alloy near the catalyst surface. FTIR results revealed that the Pd atoms on all prepared catalysts are distributed in very small ensembles or possibly even atomically on the Ag surface. Such geometric effects were further confirmed by evaluation studies revealing that the selectivities for  $C_2H_4$  formation remained high and constant for different Pd loadings. However, unlike for the case of Ag on Pd surfaces [42], the Pd sites here are significantly influenced by the electron transfer from Pd to Ag. This results in a competing electronic effect in these catalysts that limits the ability to obtain very high selectivity towards  $C_2H_4$ .

CHAPTER 5:

CONCLUSIONS

In this Dissertation, a series of Ag- and Au-Pd/SiO<sub>2</sub> bimetallic catalysts were prepared by electroless deposition with incremental and controlled coverages of Ag and Au on Pd. The catalysts were characterized by atomic absorption spectroscopy and selective chemisorption, and evaluated by selective hydrogenation of acetylene in excess ethylene followed by a corresponding kinetic study. Both Ag- and Au-Pd/SiO<sub>2</sub> catalysts showed increased selectivity of acetylene to ethylene and higher turnover frequencies of acetylene conversion at high Ag and Au coverages due to the transition of acetylene adsorption modes. That is, at low coverages where there was abundance of contiguous Pd surface sites on large Pd ensembles, acetylene was more likely to be strongly adsorbed as multi  $\sigma$ -bonded ethylidyne which was responsible for the formation of ethane. On the other hand, at high coverages when most of the Pd surface was covered by Ag or Au, the Pd ensembles were much smaller and acetylene was more likely adsorbed as a weaker  $\pi$ -bonded species which favored the conversion of acetylene to ethylene. Further kinetic studies on the Pd/SiO<sub>2</sub> and Ag-Pd/SiO<sub>2</sub> ( $\theta = 0.92$ , best catalyst performance) confirmed the above hypothesis. Results showed that acetylene reaction order increased from -0.67 to -0.20 for Pd and Ag-Pd, respectively. The negative reaction orders confirmed that acetylene was strongly adsorbed on the Pd surface of both catalysts, but the more negative reaction order for Pd than Ag-Pd implied that acetylene was more strongly adsorbed on the former catalyst. Finally, the similar performance trends for Ag- and Au-Pd/SiO<sub>2</sub> suggested that the bimetallic effect for these catalysts was likely geometric and not electronic in nature.

For comparison, a series of reverse Pd-Ag/SiO<sub>2</sub> bimetallic catalysts where variable theoretical coverages of Pd were deposited onto Ag surfaces was prepared using

galvanic displacement of  $\text{Ag}^0$  by  $\text{Pd}^{2+}$  to further explore the nature of bimetallic effects for selective acetylene hydrogenation. Characterization results from atomic absorption spectroscopy showed that the amount of actual Pd deposition was beyond the theoretical deposition limit, in contrast to the theory that galvanic displacement reaction should stop when the surface of the base material was completely displaced. Further results from Fourier transform infrared spectroscopy of CO adsorption indicated that the surface Pd concentrations were considerably lower than the amount of Pd deposited. The AA and FTIR results suggested that Pd diffused into the bulk of Ag particles or that Ag diffused to the surface to provide more fresh Ag atoms for further galvanic displacement. FTIR results also revealed that the Pd atoms left on the surface were distributed in very small ensembles or possibly even atomically on the surface for all catalysts, which resulted in high and constant selectivities for ethylene formation for different Pd loadings. Unlike the earlier case of Ag on Pd surfaces using ED, for the reverse Pd on Ag samples prepared by GD the diffusion of Pd into the Ag lattice led to greater electronic interactions between these two metals, which was confirmed from x-ray photoelectron spectroscopy results. These interactions resulted in a competing electronic effect in these catalysts that limited the selectivity of acetylene hydrogenation to form ethylene.

Both electroless deposition and galvanic displacement were proven to be viable methods to prepare Group IB-Pd bimetallic catalysts with proximal contact between two metals with controlled deposition of a secondary metal on the primary metal. Both methods permitted the design and preparation of bimetallic catalysts with surface compositions that greatly influenced the catalyst performance for selective acetylene hydrogenation.

## REFERENCES

- [1] W. Wittanadecha, N. Laosiripojana, A. Ketcong, N. Ningnuek, P. Praserttham, J.R. Monnier, S. Assabumrungrat, *Appl. Catal., A* 475 (2014) 292-296.
- [2] W. Diao, C.D. DiGiulio, M.T. Schaal, S. Ma, J.R. Monnier, *J. Catal.* 322 (2015) 14-23.
- [3] J.P. Hogan, R.L. Banks, US Patent 2,825,721 (1958).
- [4] R. Myers, *The Basics of Chemistry*, Greenwood Press: Westport, 2003, p.303.
- [5] W.R. True, *Oil Gas J.* 111 (2013) 90-94.
- [6] W.G. Augustyn, R.I. McCrindle, N.J. Coville, *Appl. Catal., A* 388 (2010) 1-6.
- [7] W. Huang, J.R. McCormick, R.F. Lobo, J.G. Chen, *J. Catal.* 246 (200) 40-51.
- [8] G.C. Bond, D.A. Dowden, N. Mackenzie, *Trans. Faraday. Soc.*, 54 (1958) 1537-1546.
- [9] D. Duca, F. Arena, A. Parmaliana, G. Deganello, *Appl. Catal., A* 172 (1998) 207-216.
- [10] Q. Zhang, J. Li, X. Liu, Q. Zhu, *Appl. Catal., A* 197 (2000) 221-228.
- [11] G.M. Schwab, *Disc. Faraday Soc.* 8 (1950) 166-171.
- [12] A. Couper, D.D. Eley, *Disc. Faraday Soc.* 8 (1950) 172-184.
- [13] D.A. Dowden, P. Reynolds, *Disc. Faraday Soc.* 8 (1950) 184-190.
- [14] J.A. Rodriguez, *Surf. Sci. Rep.* 24 (1996) 223-287.
- [15] J.R. Anderson, *Structure of Metallic Catalysts*, Academic Press, London, 1975.
- [16] D.C. Huang, K.H. Chang, W.F. Pong, P.K. Tseng, K.J. Hung, W.F. Huang, *Catal. Lett.* 53 (1998) 155-159.
- [17] M.W. Tew, H. Emerich, J. A. van Bokhoven, *J. Phys. Chem. C* 115 (2011) 8457–8465.

- [18] M. Armbrüster, K. Kovnir, M. Behrens, D. Teschner, Y. Grin, R. Schlögl, *J. Am. Chem. Soc.* 132 (2010) 14745-14747.
- [19] V.H. Sandoval, C.E. Gigola, *Appl. Catal., A* 148 (1996) 81-96.
- [20] W.-J. Kima, S.H. Moon, *Catal. Today* 185 (2012) 2-16.
- [21] A. Sárkány, A. Horváth, A. Beck, *Appl. Catal., A* 229 (2002) 117-125.
- [22] K.P. de Jong, *Curr. Opin. Solid State Mater. Sci.* 4 (1999) 55-62.
- [23] P. Munnik, P.E. de Jongh, K.P. de Jong, *Chem. Rev.* 115 (2015) 6687-6718.
- [24] J.W. Geus, in: J.R. Regalbuto (Ed.), *Catalyst Preparation: Science and Engineering*, CRC Press, Boca Raton, 2006, pp. 341-372.
- [25] S. S. Djokić, *Mod. Aspects Electrochem.* 35 (2002) 51-133.
- [26] E.J. O'Sullivan, in: R.C. Alkire, D.M. Kolb (Eds.), *Advances in Electrochemical Science and Engineering*, Wiley-VCH, Weinheim, 2001, pp. 225-273.
- [27] Y. Okinaka, T. Osaka, in: H. Gerischer, C.W. Tobias (Eds.), *Advances in Electrochemical Sciences and Engineering*, Wiley-VCH, Weinheim, 1994, pp. 55-116.
- [28] C. Carraro, R. Maboudian, L. Magagnin, *Surf. Sci. Rep.* 62 (2007) 499-525.
- [29] X. Xia, Y. Wang, A. Ruditskiy, Y. Xia, *Adv. Mater.* 25 (2013) 6313-6333.
- [30] S.M. Alia, Y.S. Yan, B.S. Pivovar, *Catal. Sci. Technol.* 4 (2014) 3589-3600.
- [31] M.T. Schaal, A.Y. Metcalf, J.H. Montoya, J.P. Wilkinson, C.C. Stork, C.T. Williams, J.R. Monnier, *Catal. Today* 123 (2007) 142-150.
- [32] M.T. Schaal, A.C. Pickerell, C.T. Williams, J.R. Monnier, *J. Catal.* 254 (2008) 131-143.
- [33] K.D. Beard, M. T. Schaal, J.W. Van Zee, J.R. Monnier, *Appl. Catal., B* 72 (2007) 262-271.
- [34] K.D. Beard, J.W. Van Zee, J.R. Monnier, *Appl. Catal., B* 88 (2009) 185-193.
- [35] K.D. Beard, D. Borrelli, A.M. Cramer, D. Blom, J.W. Van Zee, J.R. Monnier, *ACS Nano* 3 (2009) 2841-2853.

- [36] T.R. Garrick, W. Diao, J.M. Tengco, J. Monnier, J.W. Weidner, *ECS Trans.* 53 (2013) 79-84.
- [37] R.P. Galhenage, K. Xie, W. Diao, J.M.M. Tengco, G.S. Seuser, J.R. Monnier, D.A. Chen, *Phys. Chem. Chem. Phys.* (2015) DOI: 10.1039/C5CP00075K.
- [38] W. Diao, J.M.M. Tengco, J.R. Regalbuto, J.R. Monnier, *ACS Catal.* 5 (2015) 5123-5134.
- [39] J. Rebelli, M. Detwiler, S. Ma, C.T. Williams, J.R. Monnier, *J. Catal.* 270 (2010) 224-233.
- [40] A.A. Rodriguez, C.T. Williams, J.R. Monnier, *Appl. Catal., A* 475 (2014) 161-168.
- [41] Y.-J. Song, J.R. Monnier, P. T. Fanson, C.T. Williams, *J. Catal.* 315 (2014) 59-66.
- [42] Y. Zhang, W. Diao, C.T. Williams, J.R. Monnier, *Appl. Catal., A* 469 (2014) 419-426.
- [43] Y. Zhang, W. Diao, J.R. Monnier, C.T. Williams, *Catal. Sci. Technol.* 5 (2015) 4123-4132.
- [44] A. Borodziński, G.C. Bond, *Catal. Rev. Sci. Eng.* 48 (2006) 91-144.
- [45] A.J. McCue, J.A. Anderson, *Front. Chem. Sci. Eng.* 9 (2015) 142-153.
- [46] J.H. Kang, E. W. Shin, W.J. Kim, J.D. Park, S.H. Moon, *J. Catal.* 208 (2002) 310-320.
- [47] A.N.R. Bos, K.R. Westerterp, *Chem. Eng. Process.* 32 (1993) 1-7.
- [48] G.C. Bond, *Appl. Catal., A* 149 (1997) 3-25.
- [49] H.A. Aleksandrov, L.V. Moskaleva, Z.-J. Zhao, D. Basaran, Z.-X. Chen, D. Mei, N. Rösch, *J. Catal.* 285 (2012) 187-195.
- [50] J. Houzvicka, R. Pestman, V. Ponec, *Catal. Lett.* 30 (1994) 289-296.
- [51] A.J. Den Hartog, M. Deng, F. Jongorius, V. Ponec, *J. Mol. Catal.* 60 (1990) 99-108.
- [52] A. Borodziński, A. Cybulski, *Appl. Catal., A* 198 (2000) 51-66.
- [53] A. Borodziński, A. Gołębiowski, *Langmuir* 13 (1997) 883-887.
- [54] A. Borodziński, *Catal. Lett.* 63 (1999) 35-42.

- [55] M.A.G. Heviaa, B. Bridierb, J. Pérez-Ramírez, *Appl. Catal., A* 439-440 (2012) 163-170.
- [56] D.B. Tiedtke, T.T.P. Cheung, J. Leger, S.A. Zisman, J.J. Bergmeister, G.A. Delzer, *AIChE (13<sup>th</sup> EPC), Session 80, Volume 10, March 2001, Houston, TX.*
- [57] Y.H. Park, G.L. Price, *Ind. Eng. Chem. Res.* 30 (1991) 1700-1707.
- [58] S.S. Randhava, A. Rehmat, *Trans. Faraday Soc.* 66 (1970) 235-241.
- [59] Y.H. Park, G.L. Price, *Ind. Eng. Chem. Res.* 30 (1991) 1693-1699.
- [60] N.A. Khan, S. Shaikhutdinov, H.-J. Freund, *Catal. Lett.* 108 (2006) 159-164.
- [61] G.L. Price, in: J.R. Regalbuto (Ed.), *Catalyst Preparation: Science and Engineering*, CRC Press, Boca Raton, 2006, pp. 283-295.
- [62] J.R. Regalbuto, in: J.R. Regalbuto (Ed.), *Catalyst Preparation: Science and Engineering*, CRC Press, Boca Raton, 2006, pp. 297-318.
- [63] G. Ertl, H. Knözinger, J. Weitkamp, *Preparation of Solid Catalysts*; Wiley-VCH, Weinheim, 1999.
- [64] J.A. Schwarz, C. Contescu, A. Contescu, *Chem. Rev.* 95 (1995) 477-510.
- [65] M. Campanati, G. Fornasari, A. Vaccari, *Catal. Today* 77 (2003) 299-314.
- [66] E. Marceau, X. Carrier, M. Che, in: K.P. de Jong (Ed.), *Synthesis of Solid Catalysts*, Wiley-VCH, Weinheim, 2009, pp. 59-82.
- [67] C. Louis, in: J.R. Regalbuto (Ed.), *Catalyst Preparation: Science and Engineering*, CRC Press, Boca Raton, 2006, pp. 319-339.
- [68] K.P. de Jong, *Stud. Surf. Sci. Catal.* 63 (1991) 19-36.
- [69] K.P. de Jong, in: K.P. de Jong (Ed.), *Synthesis of Solid Catalysts*, Wiley-VCH, Weinheim, 2009, pp. 111-134.
- [70] J.P. Brunelle, *Pure Appl. Chem.* 50 (1978) 1211-1229.
- [71] J.R. Regalbuto, in: K.P. de Jong (Ed.), *Synthesis of Solid Catalysts*, Wiley-VCH, Weinheim, 2009, pp. 33-58.
- [72] S.S. Djokić, N.D. Nikolić, P.M. Živković, K.I. Popov, N.S. Djokić, *ECS Trans*, 33 (2011) 7-31.

- [73] M. Paunovic, M. Schlesinger, *Fundamentals of Electrochemical Deposition*, second ed., Wiley-VCH, Hoboken, 2006, pp. 169-176.
- [74] O. Deutschmann, H. Knözinger, K. Kochloefl, T. Turek, *Heterogeneous Catalysis and Solid Catalysts*, Wiley-VCH, Weinheim, 2009.
- [75] M. Paunovic, M. Schlesinger, *Fundamentals of Electrochemical Deposition*, second ed., Wiley-VCH, Hoboken, 2006, pp. 139-168.
- [76] B. Heinrichs, S. Lambert, N. Job, J.-P. Pirard, in: J.R. Regalbuto (Ed.), *Catalyst Preparation: Science and Engineering*, CRC Press, Boca Raton, 2006, pp. 163-208.
- [77] D.S. Deutsch, C.T. Williams, M.D. Amiridis, in: J.R. Regalbuto (Ed.), *Catalyst Preparation: Science and Engineering*, CRC Press, Boca Raton, 2006, pp. 209-236.
- [78] M. Schlesinger, in: M. Schlesinger, M. Paunovic (Eds.), *Modern Electroplating*, fifth ed., Wiley, New York, 2010, pp. 447-458.
- [79] A. Vakelis, in: A.A. Tracton (Ed.), *Coatings Technology Handbook*, third ed., CRC Press, Boca Raton, 2005, pp. 27(1)-27(12).
- [80] I. Ohno, O. Wakabayashi, S. Haruyama, *J. Electrochem. Soc.* 132 (1985) 2323-2330.
- [81] C.F. Baes, P.E. Mesmer, *The Hydrolysis of Cations*, Wiley, New York, 1976.
- [82] M. Paunovic, *Plating*, 55 (1968) 1161-1168.
- [83] M. Saito, *J. Met. Finish. Soc. Jpn.* 16 (1965) 300-305.
- [84] J.E.A.M. van der Meerakker, *J. Appl. Electrochem.* 11 (1981) 395-400.
- [85] A. Gutés, R. Maboudian, C. Carraro, *Langmuir* 28 (2012) 17846-17850.
- [86] L. Au, X. Lu, Y. Xia, *Adv. Mater.* 20 (2008) 2517-2522.
- [87] M. Liu, Y. Zheng, S. Xie, N. Li, N. Lu, J. Wang, M. J. Kim, L. Guo, Y. Xia, *Phys. Chem. Chem. Phys.* 15 (2013) 11822-11829.
- [88] H. Zhang, M. Jin, H. Liu, J. Wang, M. J. Kim, D. Yang, Z. Xie, J. Liu, Y. Xia, *ACS Nano* 5 (2011) 8212-8222.
- [89] S. M. Alia, K. Jensen, C. Contreras, F. Garzon, B. S. Pivovar, Y. Yan, *ACS Catal.* 3 (2013) 358-362.
- [90] Y. Sun, Y. Xia, *J. Am. Chem. Soc.* 126 (2004) 3892-3901.

- [91] C.M. Cobley, D.J. Campbell, Y. Xia, *Adv. Mater.* 20 (2008) 748-752.
- [92] S.R. Seyedmonir, D.E. Strohmayer, G.L. Geoffroy, M.A. Vannice, H.W. Young, J.W. Linowski, *J. Catal.* 87 (1984) 424-436.
- [93] H. Zea, K. Lester, A.K. Datye, E. Rightor, R. Gulotty, W. Waterman, *Appl. Catal., A* 282 (2005) 237-245.
- [94] C. Kemball, D.A. Dowden, G. Webb, *Catalysis*, 2 (1979) 145-175.
- [95] G.C. Bond, *Catalysis by Metals*, Academic Press, London, 1962.
- [96] J. Wood, M.J. Aldrick, J.M. Winterbottom, E.H. Stitt, S. Bailey, *Catal. Today* 128 (2007) 52-62.
- [97] J. Margitfalvi, L. Guzzi, A.H. Weiss, *React. Kinet. Catal. Lett.* 15 (1980) 475-479.
- [98] D. Mei, M. Neurock, C.M. Smith, *J. Catal.* 268 (2009) 181-195.
- [99] P. Miegge, J.L. Rousset, B. Tardy, J. Massardier, J.C. Bertolini, *J. Catal.* 149 (1994) 404-413.
- [100] S. Leviness, V. Nair, A.H. Weiss, *J. Mol. Catal.* 25 (1984) 131-140.
- [101] M.T. Schaal, M.P. Hyman, M. Rangan, S. Ma, C.T. Williams, J.R. Monnier, J.W. Medlin, *Surf. Sci.* 603 (2009) 690-696.
- [102] M.T. Schaal, J. Rebelli, H.M. McKerrow, C.T. Williams, J.R. Monnier, *Appl. Catal. A: Gen.* 382 (2010) 49-57.
- [103] J. Rebelli, A.A. Rodriguez, S. Ma, C.T. Williams, J.R. Monnier, *Catal. Today* 160 (2011) 170-178.
- [104] L.L. Kesmodel, L.H. Dubois, G.A. Somorjai, *J. Chem. Phys.* 70 (1979) 2180-2188.
- [105] J.W. Medlin, M.D. Allendorf, *J. Phys. Chem. B* 107 (2003) 217-223.
- [106] F. Studt, F. Abild-Pedersen, T. Bligaard, R.Z. Sørensen, C.H. Christensen, J.K. Nørskov, *Angew. Chem. Int. Ed.* 47 (2008) 9299-9302.
- [107] F. Studt, F. Abild-Pedersen, T. Bligaard, R.Z. Sørensen, C.H. Christensen, J.K. Nørskov, *Science* 320 (2008) 1320-1322.
- [108] S. Shaikhutdinov, M. Heemeier, M. Bäumer, T. Lear, D. Lennon, R.J. Oldman, S.D. Jackson, H.-J. Freund, *J. Catal.* 200 (2001) 330-339.

- [109] M. Li, J. Shen, *Mater. Chem. Phys.* 68 (2001) 204-209.
- [110] R. Van Hardeveld, F. Hartog, *Surf. Sci.* 15 (1969) 189-230.
- [111] P.S. Cremer, X. Su, Y.R. Shen, G.A. Somorjai, *J. Am. Chem. Soc.* 118 (1996) 2942-2949.
- [112] G.C. Bond, P.B. Wells, *J. Catal.* 5 (1965) 65-73.
- [113] H. Molero, B.F. Bartlett, W.T. Tysoe, *J. Catal.* 181 (1999) 49-56.
- [114] Y. Inoue, I. Yasumori, *J. Phys. Chem.* 75 (1971) 880-887.
- [115] L. Jiang, A. Hsu, D. Chu, R. Chen, *Electrochim. Acta* 55 (2010) 4506-4511.
- [116] C.-L, Lee, C.-M, Tseng, *J. Phys. Chem. C* 112 (2008) 13342-13345.
- [117] C.-L, Lee, C.-M, Tseng, R.-B Wu, C.-C, Wu, S.-C, Syu, *Electrochim. Acta* 54 (2009) 5544-5547.
- [118] C.-W, Chen, Y.-S, Hsieh, C.-C, Syu, H.-R, Chen, C.-L, Lee, *J. Alloys Compd.* 580 (2013) S359-S363.
- [119] S.M. Alia, K. Duong, T. Liu, K.O. Jensen, Y. Yan, *ChemSusChem* 7 (2014) 1739-1744.
- [120] S.M. Alia, B.S. Pivovarov, Y. Yan, *J. Am. Chem. Soc.* 135 (2013) 13473-13478.
- [121] S.M. Alia, K.O. Jensen, B.S. Pivovarov, Y. Yan, *ACS Catal.* 2 (2012) 858-863.
- [122] A. Gutes, I. Laboriante, C. Carraro, R. Maboudian, *J. Phys. Chem. C* 113 (2009) 16939-16944.
- [123] L. Magagnin, R. Maboudian, C. Carraro, *J. Phys. Chem. B* 106 (2002) 401-407.
- [124] M.B. Boucher, B. Zugic, G. Cladaras, J. Kammert, M.D. Marcinkowski, T.J. Lawton, E.C.H. Sykes, M. Flytzani-Stephanopoulos, *Phys. Chem. Chem. Phys.* 15 (2013) 12187-12196.
- [125] J. Ma, L. Xu, L. Xu, H. Wang, S. Xu, H. Li, S. Xie, and H. Li, *ACS Catal.*, 2013, 3, 985-992.
- [126] H. Li, H. Lin, Y. Hu, H. Li, P. Li, X. Zhou, *J. Mater. Chem.* 21 (2011) 18447-18453.
- [127] W.R. Tyson, W.A. Miller, *Surf. Sci.* 62 (1977) 267-276.

- [128] H.L. Skriver, N.M. Rosengaard, *Phys. Rev. B* 46 (1992) 7157-7168.
- [129] L.Z. Mezey, J. Giber, *Jpn. J. Appl. Phys.* 21 (1982) 1569-1571.
- [130] J. Tang, L. Deng, H. Deng, S. Xiao, X. Zhang, W. Hu, *J. Phys. Chem. C* 118 (2014) 27850-27860.
- [131] J. Chen, B. Wiley, J. McLellan, Y. Xiong, Z.-Y. Li, Y. Xia, *Nano Lett.* 5 (2005) 2058-2062.
- [132] H. Okamoto, *Desk Handbook: Phase Diagrams for Binary Alloys*, second ed., ASM International, Materials Park, 2010, pp. 2-24.
- [133] J.A. Rodriguez, C.M. Truong, D.W. Goodman, *Surf. Sci.* 271 (1992) L331-L337.
- [134] P. Gelin, A.R. Siedle, J.T. Yates Jr., *J. Phys. Chem.* 88 (1984) 2978-2985.
- [135] J.B. Giorgi, T. Schroeder, M. Bäumer, H. -J. Freund, *Surf. Sci.* 498 (2002) L71–L77.
- [136] D. Childers, A. Saha, N. Schweitzer, R.M. Rioux, J.T. Miller, *ACS Catal.* 3 (2013) 2487-2496.
- [137] Z. Qu, G. Ke, Y. Wang, M. Liu, T. Jiang, J. Gao, *Appl. Surf. Sci.* 277 (2013) 293-301.
- [138] M. Skaf, S. Aouad, S. Hany, R. Cousin, E. Abi-Aad, A. Aboukaïb, *J. Catal.* 320 (2014) 137-146.
- [139] V.I. Pârvulescu, B. Cojocaru, V. Pârvulescu, R. Richards, Z. Li, C. Cadigan, P. Granger, P. Miquel, C. Hardacre, *J. Catal.* 272 (2010) 92-100.
- [140] A.M. Venezia, L.F. Liotta, G. Deganello, Z. Schay, D. Horváth, L. Guczi, *Appl. Catal., A* 211 (2001) 167-174.
- [141] M. Al-Hada, S. Peters, S. Peredkov, M. Neeb, W. Eberhardt, *Surf. Sci.* 639 (2015) 43-47.
- [142] A.M. Ferraria, A.P. Carapeto, A.M. Botelho do Rego, *Vacuum* 86 (2012) 1988-1991.

## APPENDIX A:

### LIST OF PUBLICATIONS

1. **Y. Zhang**, W. Diao, J.R. Monnier, C.T. Williams, “Pd-Ag/SiO<sub>2</sub> bimetallic catalysts prepared by galvanic displacement for selective hydrogenation of acetylene in excess ethylene,” *Catal. Sci. Technol.* 5 (2015) 4123-4132.
2. **Y. Zhang**, W. Diao, C.T. Williams, J.R. Monnier, “Selective hydrogenation of acetylene in excess ethylene using Ag- and Au-Pd/SiO<sub>2</sub> bimetallic catalysts prepared by electroless deposition,” *Appl. Catal., A* 469 (2014) 419-426.
3. K. Punyawudho, N. Vorayos, **Y. Zhang**, S. Shimpalee, J.R. Monnier, “Identification and quantification of performance losses for PEM fuel cells as determined by selective chemisorption and ESA measurements,” *Int. J. Hydrogen Energy* 39 (2014) 11110-11119.
4. A. Wongkaew, **Y. Zhang**, J.M.M. Tengco, D.A. Blom, P. Sivasubramanian, P.T. Fanson, J.R. Regalbuto, J.R. Monnier, “Preparation using electroless deposition methods and subsequent characterization and evaluation of bimetallic Pt-Pd electrocatalysts,” *submitted to Appl. Catal., B*.
5. S. Riyapan, **Y. Zhang**, A. Wongkaew, J.R. Monnier, J. Panpranot, “Preparation of improved Ag-Pd/TiO<sub>2</sub> catalysts by strong electrostatic adsorption and electroless deposition methods for the selective hydrogenation of acetylene,” *submitted to Appl. Catal., A*.

APPENDIX B:

PERMISSION TO REPRINT

**ELSEVIER LICENSE  
TERMS AND CONDITIONS**

Oct 08, 2015

This is a License Agreement between Yunya Zhang ("You") and Elsevier ("Elsevier") provided by Copyright Clearance Center ("CCC"). The license consists of your order details, the terms and conditions provided by Elsevier, and the payment terms and conditions.

**All payments must be made in full to CCC. For payment instructions, please see information listed at the bottom of this form.**

Supplier	Elsevier Limited The Boulevard, Langford Lane Kidlington, Oxford, OX5 1GB, UK
Registered Company Number	1982084
Customer name	Yunya Zhang
Customer address	301 Main Street Columbia, SC 29208
License number	3724500585213
License date	Oct 08, 2015
Licensed content publisher	Elsevier
Licensed content publication	Applied Catalysis A: General
Licensed content title	Selective hydrogenation of acetylene in excess ethylene using Ag- and Au-Pd/SiO <sub>2</sub> bimetallic catalysts prepared by electroless deposition
Licensed content author	Yunya Zhang, Weijian Diao, Christopher T. Williams, John R. Monnier
Licensed content date	17 January 2014
Licensed content volume number	469
Licensed content issue number	n/a
Number of pages	8
Start Page	419
End Page	426
Type of Use	reuse in a thesis/dissertation
Portion	full article
Format	electronic
Are you the author of this Elsevier article?	Yes
Will you be translating?	No
Title of your thesis/dissertation	Supported Group IB-Pd Bimetallic Catalysts Prepared by Electroless Deposition and Galvanic Displacement for Selective Hydrogenation of Acetylene

Expected completion date	Nov 2015
Estimated size (number of pages)	120
Elsevier VAT number	GB 494 6272 12
Permissions price	0.00 USD
VAT/Local Sales Tax	0.00 USD / 0.00 GBP
Total	0.00 USD

Terms and Conditions

### INTRODUCTION

1. The publisher for this copyrighted material is Elsevier. By clicking "accept" in connection with completing this licensing transaction, you agree that the following terms and conditions apply to this transaction (along with the Billing and Payment terms and conditions established by Copyright Clearance Center, Inc. ("CCC"), at the time that you opened your Rightslink account and that are available at any time at <http://myaccount.copyright.com>).

### GENERAL TERMS

2. Elsevier hereby grants you permission to reproduce the aforementioned material subject to the terms and conditions indicated.

3. Acknowledgement: If any part of the material to be used (for example, figures) has appeared in our publication with credit or acknowledgement to another source, permission must also be sought from that source. If such permission is not obtained then that material may not be included in your publication/copies. Suitable acknowledgement to the source must be made, either as a footnote or in a reference list at the end of your publication, as follows:

"Reprinted from Publication title, Vol /edition number, Author(s), Title of article / title of chapter, Pages No., Copyright (Year), with permission from Elsevier [OR APPLICABLE SOCIETY COPYRIGHT OWNER]." Also Lancet special credit - "Reprinted from The Lancet, Vol. number, Author(s), Title of article, Pages No., Copyright (Year), with permission from Elsevier."

4. Reproduction of this material is confined to the purpose and/or media for which permission is hereby given.

5. Altering/Modifying Material: Not Permitted. However figures and illustrations may be altered/adapted minimally to serve your work. Any other abbreviations, additions, deletions and/or any other alterations shall be made only with prior written authorization of Elsevier Ltd. (Please contact Elsevier at [permissions@elsevier.com](mailto:permissions@elsevier.com))

6. If the permission fee for the requested use of our material is waived in this instance, please be advised that your future requests for Elsevier materials may attract a fee.

7. Reservation of Rights: Publisher reserves all rights not specifically granted in the combination of (i) the license details provided by you and accepted in the course of this licensing transaction, (ii) these terms and conditions and (iii) CCC's Billing and Payment terms and conditions.

8. License Contingent Upon Payment: While you may exercise the rights licensed immediately upon issuance of the license at the end of the licensing process for the transaction, provided that you have disclosed complete and accurate details of your proposed use, no license is finally effective unless and until full payment is received from you (either by publisher or by CCC) as provided in CCC's Billing and Payment terms and conditions. If full payment is not received on a timely basis, then any license preliminarily granted shall be deemed automatically revoked and shall be void as if never granted. Further, in the event

that you breach any of these terms and conditions or any of CCC's Billing and Payment terms and conditions, the license is automatically revoked and shall be void as if never granted. Use of materials as described in a revoked license, as well as any use of the materials beyond the scope of an unrevoked license, may constitute copyright infringement and publisher reserves the right to take any and all action to protect its copyright in the materials.

9. **Warranties:** Publisher makes no representations or warranties with respect to the licensed material.

10. **Indemnity:** You hereby indemnify and agree to hold harmless publisher and CCC, and their respective officers, directors, employees and agents, from and against any and all claims arising out of your use of the licensed material other than as specifically authorized pursuant to this license.

11. **No Transfer of License:** This license is personal to you and may not be sublicensed, assigned, or transferred by you to any other person without publisher's written permission.

12. **No Amendment Except in Writing:** This license may not be amended except in a writing signed by both parties (or, in the case of publisher, by CCC on publisher's behalf).

13. **Objection to Contrary Terms:** Publisher hereby objects to any terms contained in any purchase order, acknowledgment, check endorsement or other writing prepared by you, which terms are inconsistent with these terms and conditions or CCC's Billing and Payment terms and conditions. These terms and conditions, together with CCC's Billing and Payment terms and conditions (which are incorporated herein), comprise the entire agreement between you and publisher (and CCC) concerning this licensing transaction. In the event of any conflict between your obligations established by these terms and conditions and those established by CCC's Billing and Payment terms and conditions, these terms and conditions shall control.

14. **Revocation:** Elsevier or Copyright Clearance Center may deny the permissions described in this License at their sole discretion, for any reason or no reason, with a full refund payable to you. Notice of such denial will be made using the contact information provided by you. Failure to receive such notice will not alter or invalidate the denial. In no event will Elsevier or Copyright Clearance Center be responsible or liable for any costs, expenses or damage incurred by you as a result of a denial of your permission request, other than a refund of the amount(s) paid by you to Elsevier and/or Copyright Clearance Center for denied permissions.

#### LIMITED LICENSE

The following terms and conditions apply only to specific license types:

15. **Translation:** This permission is granted for non-exclusive world **English** rights only unless your license was granted for translation rights. If you licensed translation rights you may only translate this content into the languages you requested. A professional translator must perform all translations and reproduce the content word for word preserving the integrity of the article.

16. **Posting licensed content on any Website:** The following terms and conditions apply as follows: Licensing material from an Elsevier journal: All content posted to the web site must maintain the copyright information line on the bottom of each image; A hyper-text must be included to the Homepage of the journal from which you are licensing at <http://www.sciencedirect.com/science/journal/xxxxx> or the Elsevier homepage for books at <http://www.elsevier.com>; Central Storage: This license does not include permission for a scanned version of the material to be stored in a central repository such as that provided by Heron/XanEdu.

Licensing material from an Elsevier book: A hyper-text link must be included to the Elsevier homepage at <http://www.elsevier.com> . All content posted to the web site must maintain the

copyright information line on the bottom of each image.

**Posting licensed content on Electronic reserve:** In addition to the above the following clauses are applicable: The web site must be password-protected and made available only to bona fide students registered on a relevant course. This permission is granted for 1 year only. You may obtain a new license for future website posting.

17. **For journal authors:** the following clauses are applicable in addition to the above:

**Preprints:**

A preprint is an author's own write-up of research results and analysis, it has not been peer-reviewed, nor has it had any other value added to it by a publisher (such as formatting, copyright, technical enhancement etc.).

Authors can share their preprints anywhere at any time. Preprints should not be added to or enhanced in any way in order to appear more like, or to substitute for, the final versions of articles however authors can update their preprints on arXiv or RePEc with their Accepted Author Manuscript (see below).

If accepted for publication, we encourage authors to link from the preprint to their formal publication via its DOI. Millions of researchers have access to the formal publications on ScienceDirect, and so links will help users to find, access, cite and use the best available version. Please note that Cell Press, The Lancet and some society-owned have different preprint policies. Information on these policies is available on the journal homepage.

**Accepted Author Manuscripts:** An accepted author manuscript is the manuscript of an article that has been accepted for publication and which typically includes author-incorporated changes suggested during submission, peer review and editor-author communications.

Authors can share their accepted author manuscript:

- immediately
  - o via their non-commercial person homepage or blog
  - o by updating a preprint in arXiv or RePEc with the accepted manuscript
  - o via their research institute or institutional repository for internal institutional uses or as part of an invitation-only research collaboration work-group
  - o directly by providing copies to their students or to research collaborators for their personal use
  - o for private scholarly sharing as part of an invitation-only work group on commercial sites with which Elsevier has an agreement
- after the embargo period
  - o via non-commercial hosting platforms such as their institutional repository
  - o via commercial sites with which Elsevier has an agreement

In all cases accepted manuscripts should:

- link to the formal publication via its DOI
- bear a CC-BY-NC-ND license - this is easy to do
- if aggregated with other manuscripts, for example in a repository or other site, be shared in alignment with our hosting policy not be added to or enhanced in any way to appear more like, or to substitute for, the published journal article.

**Published journal article (JPA):** A published journal article (PJA) is the definitive final record of published research that appears or will appear in the journal and embodies all value-adding publishing activities including peer review co-ordination, copy-editing,

formatting, (if relevant) pagination and online enrichment.

Policies for sharing publishing journal articles differ for subscription and gold open access articles:

**Subscription Articles:** If you are an author, please share a link to your article rather than the full-text. Millions of researchers have access to the formal publications on ScienceDirect, and so links will help your users to find, access, cite, and use the best available version. Theses and dissertations which contain embedded PJAs as part of the formal submission can be posted publicly by the awarding institution with DOI links back to the formal publications on ScienceDirect.

If you are affiliated with a library that subscribes to ScienceDirect you have additional private sharing rights for others' research accessed under that agreement. This includes use for classroom teaching and internal training at the institution (including use in course packs and courseware programs), and inclusion of the article for grant funding purposes.

**Gold Open Access Articles:** May be shared according to the author-selected end-user license and should contain a [CrossMark logo](#), the end user license, and a DOI link to the formal publication on ScienceDirect.

Please refer to Elsevier's [posting policy](#) for further information.

18. **For book authors** the following clauses are applicable in addition to the above: Authors are permitted to place a brief summary of their work online only. You are not allowed to download and post the published electronic version of your chapter, nor may you scan the printed edition to create an electronic version. **Posting to a repository:** Authors are permitted to post a summary of their chapter only in their institution's repository.

19. **Thesis/Dissertation:** If your license is for use in a thesis/dissertation your thesis may be submitted to your institution in either print or electronic form. Should your thesis be published commercially, please reapply for permission. These requirements include permission for the Library and Archives of Canada to supply single copies, on demand, of the complete thesis and include permission for Proquest/UMI to supply single copies, on demand, of the complete thesis. Should your thesis be published commercially, please reapply for permission. Theses and dissertations which contain embedded PJAs as part of the formal submission can be posted publicly by the awarding institution with DOI links back to the formal publications on ScienceDirect.

### **Elsevier Open Access Terms and Conditions**

You can publish open access with Elsevier in hundreds of open access journals or in nearly 2000 established subscription journals that support open access publishing. Permitted third party re-use of these open access articles is defined by the author's choice of Creative Commons user license. See our [open access license policy](#) for more information.

#### **Terms & Conditions applicable to all Open Access articles published with Elsevier:**

Any reuse of the article must not represent the author as endorsing the adaptation of the article nor should the article be modified in such a way as to damage the author's honour or reputation. If any changes have been made, such changes must be clearly indicated.

The author(s) must be appropriately credited and we ask that you include the end user license and a DOI link to the formal publication on ScienceDirect.

If any part of the material to be used (for example, figures) has appeared in our publication with credit or acknowledgement to another source it is the responsibility of the user to ensure their reuse complies with the terms and conditions determined by the rights holder.

#### **Additional Terms & Conditions applicable to each Creative Commons user license:**

**CC BY:** The CC-BY license allows users to copy, to create extracts, abstracts and new works from the Article, to alter and revise the Article and to make commercial use of the Article (including reuse and/or resale of the Article by commercial entities), provided the

user gives appropriate credit (with a link to the formal publication through the relevant DOI), provides a link to the license, indicates if changes were made and the licensor is not represented as endorsing the use made of the work. The full details of the license are available at <http://creativecommons.org/licenses/by/4.0>.

**CC BY NC SA:** The CC BY-NC-SA license allows users to copy, to create extracts, abstracts and new works from the Article, to alter and revise the Article, provided this is not done for commercial purposes, and that the user gives appropriate credit (with a link to the formal publication through the relevant DOI), provides a link to the license, indicates if changes were made and the licensor is not represented as endorsing the use made of the work. Further, any new works must be made available on the same conditions. The full details of the license are available at <http://creativecommons.org/licenses/by-nc-sa/4.0>.

**CC BY NC ND:** The CC BY-NC-ND license allows users to copy and distribute the Article, provided this is not done for commercial purposes and further does not permit distribution of the Article if it is changed or edited in any way, and provided the user gives appropriate credit (with a link to the formal publication through the relevant DOI), provides a link to the license, and that the licensor is not represented as endorsing the use made of the work. The full details of the license are available at <http://creativecommons.org/licenses/by-nc-nd/4.0>. Any commercial reuse of Open Access articles published with a CC BY NC SA or CC BY NC ND license requires permission from Elsevier and will be subject to a fee.

Commercial reuse includes:

- Associating advertising with the full text of the Article
- Charging fees for document delivery or access
- Article aggregation
- Systematic distribution via e-mail lists or share buttons

Posting or linking by commercial companies for use by customers of those companies.

## 20. Other Conditions:

v1.8

**Questions? [customercare@copyright.com](mailto:customercare@copyright.com) or +1-855-239-3415 (toll free in the US) or +1-978-646-2777.**

## Permission to Reproduce Chapter 4

Dear Yunya

The Royal Society of Chemistry (RSC) hereby grants permission for the use of your paper(s) specified below in the printed and microfilm version of your thesis. You may also make available the PDF version of your paper(s) that the RSC sent to the corresponding author(s) of your paper(s) upon publication of the paper(s) in the following ways: in your thesis via any website that your university may have for the deposition of theses, via your university's Intranet or via your own personal website. We are however unable to grant you permission to include the PDF version of the paper(s) on its own in your institutional repository. The Royal Society of Chemistry is a signatory to the STM Guidelines on Permissions (available on request).

Please note that if the material specified below or any part of it appears with credit or acknowledgement to a third party then you must also secure permission from that third party before reproducing that material.

Paper title

“Pd–Ag/SiO<sub>2</sub> bimetallic catalysts prepared by galvanic displacement for selective hydrogenation of acetylene in excess ethylene”

Please ensure that the thesis states the following:

Reproduced by permission of The Royal Society of Chemistry

and include a link to the paper on the Royal Society of Chemistry's website.

Please ensure that your co-authors are aware that you are including the paper in your thesis.

Regards

Gill Cockhead

Publishing Contracts & Copyright Executive

**Gill Cockhead**

Publishing Contracts & Copyright Executive

Royal Society of Chemistry,

Thomas Graham House,

Science Park, Milton Road,

Cambridge, CB4 0WF, UK

Tel +44 (0) 1223 432134